Project Deliverable D-2.1

WP2: Pharmacodynamics and transmission models

Responsible Partner: Anses

Contributing partners:

GENERAL INFORMATION

European Joint Programme full title	**Promoting One Health in Europe through joint actions on foodborne zoonoses, antimicrobial resistance and emerging microbiological hazards**
European Joint Programme acronym	**One Health EJP – RaDAR: Risk and Disease burden of Antimicrobial Resistance**
Funding	**This project has received funding from the European Union's Horizon 2020 research and innovation programme under Grant Agreement No 773830.**
Grant Agreement	**Grant agreement n° 773830**
Start Date	**01/01/2018**
Duration	**24 Months**

DOCUMENT MANAGEMENT

Project deliverable	D-2.1
Project Acronym	
Author	Alexis Viel - Anses
Other contributors	Pascal Sanders - Anses
Due month of the report	November 2020
Actual submission month	November 2020
Type *R: Document, report DEC: Websites, patent filings, videos, etc.; OTHER*	R
Dissemination level *PU: Public (default) CO: confidential, only for members of the consortium (including the Commission Services)*	CO If this project deliverable should be confidential, please add justification here (may be assessed by PMT): Publication currently under writing combining tasks 2.1 and 2.2
Dissemination *Author's suggestion to inform the following possible interested parties.*	OHEJP WP 1 ☐ OHEJP WP 2 ☐ OHEJP WP 3 ☐ OHEJP WP 4 ☐ OHEJP WP 5 ☐ OHEJP WP 6 ☐ OHEJP WP 7 ☐ Project Management Team ☐ Communication Team ☐ Scientific Steering Board ☐ National Stakeholders/Program Owners Committee ☐ EFSA ☐ ECDC ☐ EEA ☐ EMA ☐ FAO ☐ WHO ☐ OIE ☐ Other international stakeholder(s): …… Social Media: ……

REPORT ON GENERIC PKPD MODEL

Table of contents

List of figures

List of tables

1. General introduction:

In the agricultural sector, antimicrobial drugs are widely used as curative or metaphylactic treatment in food producing animals. One side effect of these usages concerns the development of resistance among the commensal bacteria of animals, mainly within guts, and their potential spread between animals. Then, the resistant bacteria could spread in all the food chain, from the animal towards the food and finally towards the consumers intestines. The risk could be worrying when looking at the plasmid-mediated resistance, like Extended-spectrum β-lactamases (ESBL) for beta-lactamin/cephalosporin or *mcr* for colistin, due to the possibility that a resistant bacteria originating from animals could transmit its plasmid to human commensal bacteria or pathogen bacteria that are present within guts (Madec*, et al.*, 2017; Nordmann, Poirel, 2016).

The link between antimicrobial drug (AMD) use and the development of antimicrobial resistance (AMR) in bacterial strains has been mainly studied *in vitro* experiments and sometimes modelled thanks to pharmacokinetics-pharmacodynamics (PKPD) approaches. Many within-host models of antibiotic resistance are based on this pharmacokinetics/pharmacodynamics (PK/PD) approach as opposite to the between-host models, which are mainly epidemiological models. Within-host models are useful for understanding bacteria dynamics and response to an AMD treatment, within a single individual (Tetteh*, et al.*, 2020). PKPD models are a good basis to explore mechanistically the relationship between drug concentrations and the development/selection of resistant bacteria and may be extrapolated to *in vivo* situations (Nielsen, Friberg, 2013). However, there are only few PKPD models that describe the impact of AMD within the gut for several reasons: (i) these mechanisms occur in a complex environment (intestinal microbiota) with various interactions and external factors (ii) we face a lack of observed data to inform the PKPD model (need of longitudinal data); (iii) this could be time and computer-intensive.

Hence, the goal of this work was to refine and develop a "within-host PKPD model" (hereafter simplified as PKPD model) to assess and predict the impact of an AMD treatment (as an input of the model) on the emergence/selection of resistant bacteria within guts and excretion towards faeces (output of the model) for pig, at the individual level and population level (taking into account the inter-individual variability).

2. Objectives:

- Develop a "generic" PKPD model to assess the impact of targeted AMD on the development of AMR in the intestinal microbiota of pigs (especially in *E. coli*) that will be linked with an epidemiological model at a farm level (APHA).
- Use different case scenario with 2 drugs having different properties, amoxicillin (bacteriostatic, absorbable) and colistin (bactericidal, non-absorbable) to illustrate the predictive ability of the PKPD model
- Explore the impact of clone properties in the clonal dissemination

3. PKPD model to assess relationship between animal exposure and change in antimicrobial resistance:

3.1. PKPD model development

3.1.1. Literature review

The Scopus research databased was used with the following keywords to get a general overview :

((((TITLE-ABS-KEY (model)) OR (TITLE-ABS-KEY (mathematic*))) AND (TITLE-ABS-KEY (antimicrobial* OR antibiotic*)) AND (TITLE-ABS-KEY (resistance))) OR (((TITLE-ABS-KEY (model)) OR (TITLE-ABS-KEY (mathematic*))) AND((TITLE-ABS-KEY (pharmacolog*)) OR ((TITLE-ABS-KEY ("pharmacokinetic/pharmacodynamic*" OR pharmacokinetic* OR pharmacodynamic* OR kinetic*)) OR (TITLE-ABS-KEY (pk/pd)))) AND (TITLE-ABS-KEY (antimicrobial* OR antibiotic*)))) AND ORIG-LOAD-DATE AFT 1605501975 AND ORIG-LOAD-DATE BEF 1606107181 AND PUBYEAR AFT 2018

Relevant articles selection was made based on the title, then the abstracts. By adding the term "swine" OR "pig* OR "porcine", we focused the search to find PKPD models relevant to our target specie. We found only 5 PKPD models focusing on the intestinal microbiota that have been published but 4 of them being developed by the same team (ANNEXE 1). In all these models, only *E.coli* strains were considered as it will be the case in this work. However, they are somehow biased because they use the plasma concentrations of antimicrobials as a surrogate for PK part of the model instead of a more mechanistic modelling of the antibiotic PK within guts. Only one study used the faecal data of antibiotic as the PK surrogate (Nguyen*, et al.*, 2014) and this was this only study with a full data-driven PKPD model, but an empirical one. The others studies used more mechanistic PKPD model but did not assess the predictive ability of their model by comparison with observed data.

Due to the lack of mechanistic PKPD model in pigs, the previous works from Volkova *et al* (Cazer, *et al.*, 2014; Volkova, *et al.*, 2016; Volkova, *et al.*, 2017; Volkova, *et al.*, 2012) that were done with cattle were also considered as important references. These models are based on a semi-mechanistic PK model: a compartmental approach to describe plasma/tissues and physiological compartment for the digestive tract with physiological volume/rate of digesta flow. Regarding the PD model, it often involves one or several sensitive (S) and resistant (R) strains (from the same species, mainly *E. coli*) located within the large intestine compartment.

3.1.2. Model construction

The model should be balanced between complexity and willing of reality. Different levels were considered as shown in Figure 1 and detailed below:

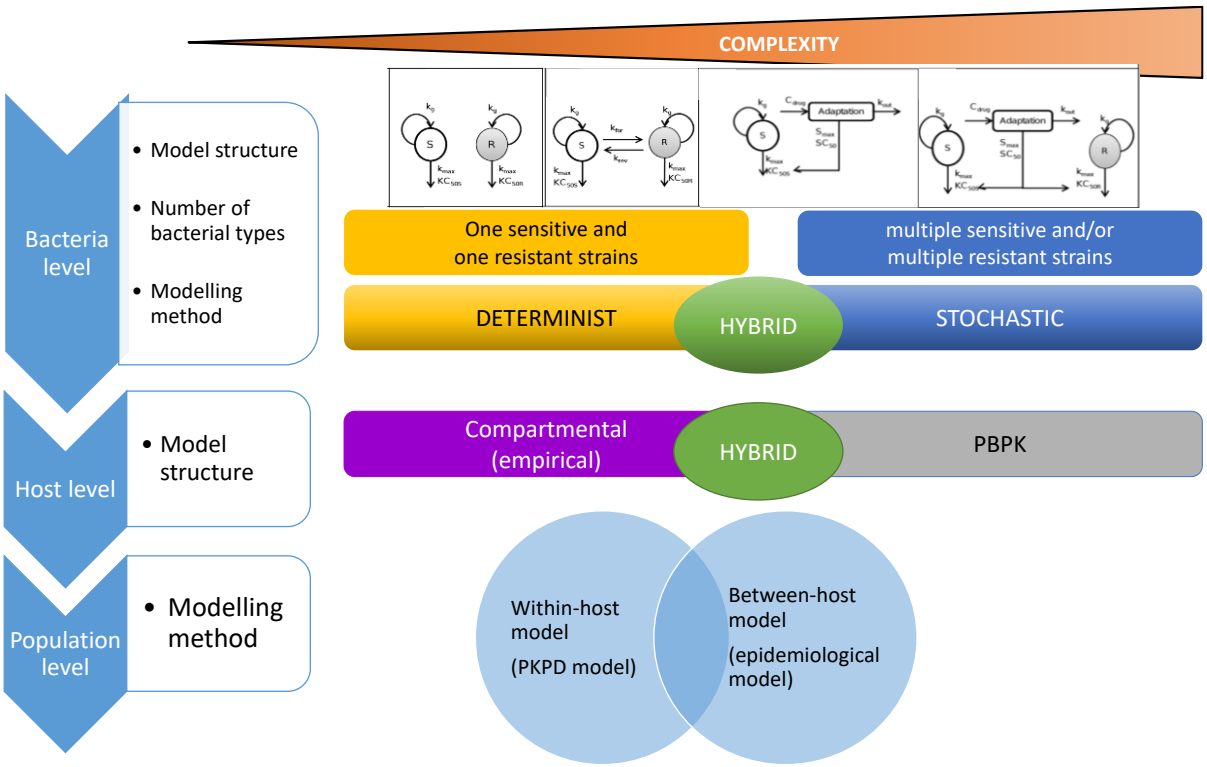

- ***Bacteria level***: Only *E. coli* will be considered in this work, as a sentinel of the resistant spread. Concerning the structural model, different mechanisms could be used with different level of complexity, with the presence of several sub-populations (persisters, for instance (Nielsen, Friberg, 2013). Some PKPD models may include intermediary sensitive strains (Cazer, *et al.*, 2017) or resting/persisters sub-populations (Nielsen, Friberg, 2013).

Resistance mechanism: We considered *the* plasmid-mediated resistance mechanism as the main driver of resistance spread and therefore neglect the chromosomal mutations. We also didn't take into account the transduction and transformation due to the lack of data/model exploring these possible mechanisms (Leclerc*, et al.*, 2019).

Modelling method: Usually for PKPD models, a determinist approach is used and the model is described by ordinary differential equations (ODE). However, some events occurs randomly when we consider a microbial population therefore a stochastic approach could also be a suitable approach (Coates*, et al.*, 2018). A mix between both method seems a good balance, as we could define some events to be a probability of occurrence, e.g. the disappearance of the R strain when its population decreases under a defined threshold, and the other mechanisms (drug effect,…) to be deterministic. Moreover, it was shown that deterministic approach could be similar to stochastic one when the number of simulated individuals is sufficiently large for SIR models dealing with antimicrobial resistance (Boëlle, Thomas, 2016).

- ***Host level***: This deals with the description of the PK of the antibiotic after administration. Different structural models could be used, typically divided in empirical ones (compartmental approach) or (semi) mechanistic ones, based on real physiology (with realists volumes and transit rates). As the PK of the drug within the digestive tract is of great importance in our PKPD model, a hybrid model between compartmental (for plasma and tissue) and PBPK approach may be the best choice. PKPD model usually used ODE, considering the environment space as homogenous. For the digestive tract, partial differential equations (PDE) should be more suitable; however the modelling of several compartments of the digestive tract (e.g. stomach/small intestines/large intestines) with their own ODE somewhat mimic the PDE (ref). Moreover there is also a lack of data to describe properly the space dimension within guts of pigs.

- ***Population level:*** At the population level, we must take into account the population variabilities. We can consider either the between-host model to study the transmission of AMR or the within-host model, *i.e.* PKPD models, that describe the individual outcome of AMR. In this work, we only focused on PKPD models and used Monte Carlo simulations, based on the probability distributions of each parameters to simulate a virtual pig population and its associated biological variabilities. The epidemiological model was developed by other partners from this WP.

The choice for each level depends on the existing data in literature. Therefore, a review of literature has been done (see below for construction of the generic model).

3.1.3. Structure of the *PKPD model*

The generic structural model is presented in Figure 2.

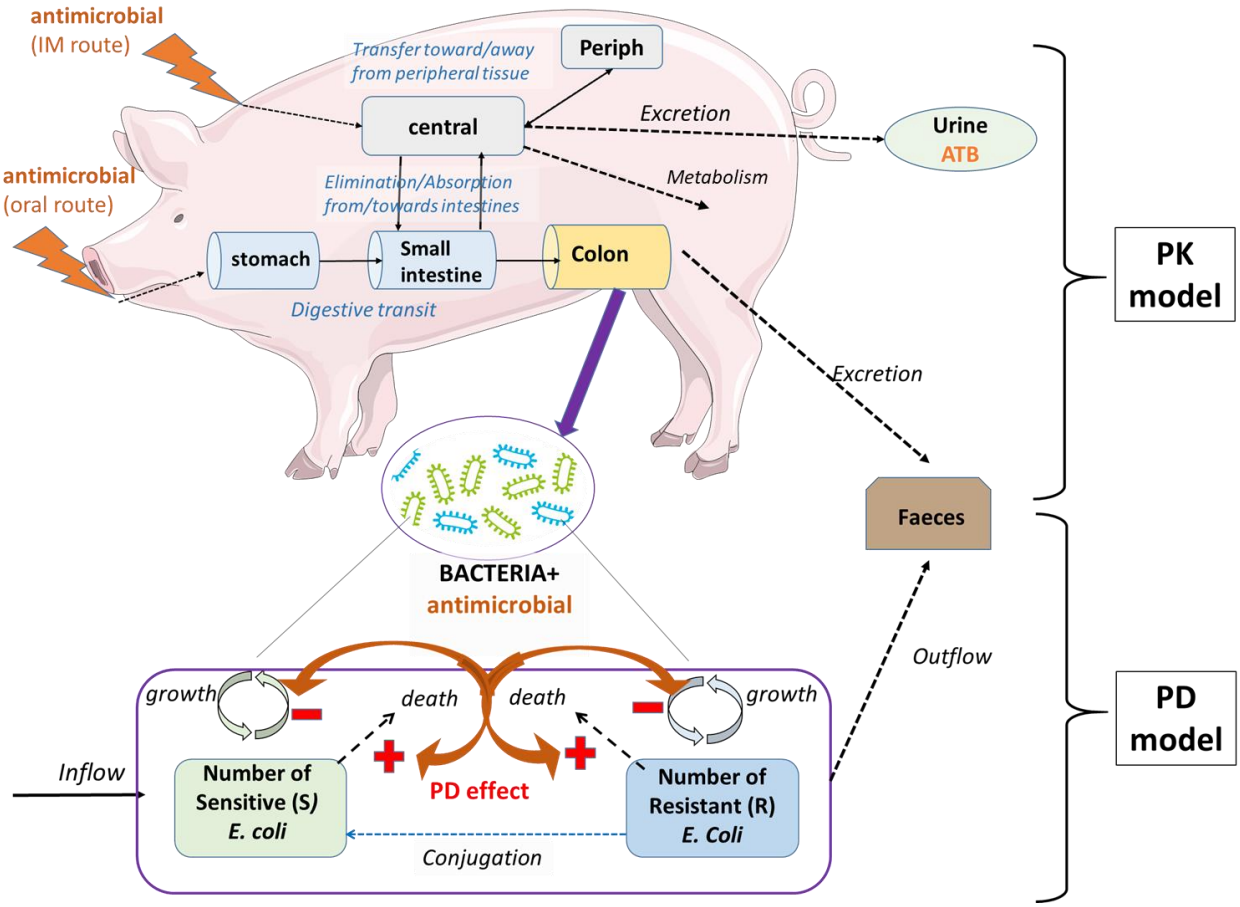

Figure 2: diagram of the PKPD model of any antimicrobial administered either orally or via intra muscular route to pigs.
ATB : antibiotic drug; PK : pharmacokinetics; PD ; pharmacodynamic

3.1.3.1. Concerning the PK model:

- Oral treatment was considered as it represents the main route of antibiotic administration for metaphylactic antimicrobial treatment for piglets. We only considered the water medication in this work because it is easier to model as a (temporary) infusion process compared to food medication; moreover EMA strongly advised to use water medication compared to treatment via feed when other routes of administration are not possible (EMA, 2019) . As an alternative to oral treatment, the IM route was also modelled. Depending on the PK properties of the drug, the drug can: (i) be absorbed and distributed within the body (represented by central and peripheral compartments) before being

excreted through urine and/or through faeces via the bile and/or eliminated through metabolism processes(ii) or only transits within the digestive tract without being absorbed and be only excreted through faeces. In the digestive tract, the drug may be degraded by biological process (e.g., Beta-lactamase) or abiotic process (chemical hydrolysis, pH, etc…).

3.1.3.2. Concerning the PD model:

This model involves one Sensitive (S) and one Resistant (R) sub-population of E.coli within the colon, the latter harbouring resistance genes within a plasmid. Each bacteria population grows following a logistic model until they reach the (shared) maximal capacity of bacteria load within intestines, meaning that they compete for the same ecological niche (nutrients, space, etc…). This competition process has been shown to be a key factor that should be included within models of antibiotic resistance (Blanquart, 2019; Davies*, et al.*, 2019). Bacteria are also affected by a natural death constant. Moreover, there is an income of bacteria from the environment (via feeding/coprophagia) and an outcome by fecal excretion. The AMD concentrations within colon impacts the bacteria with either a decrease of the growth rate or an increase of the death of bacteria (or both). This effect is assessed by the variation of concentrations of each bacterial sub-population. Finally, a transmission of plasmid from R to S by conjugation process is also considered.

For parameters distributions; log-Normal distribution was preferentially chosen for physiological parameters (transit rates, clearance,…). When the literature values were heterogeneous, a uniform distribution was considered with the minimal and maximal value found. For PD parameters, only uniform distribution was considered due to the wide range of values that were usually found in literature.

3.2. Case scenario: use of amoxicillin

Amoxicillin was chosen to illustrate the PKPD approach for several reasons : (i) it is widely used in pig production, especially against several systemic (e.g. *Streptococcus suis*), respiratory (*Pasteurella multocida*) and enteric bacterial infections (*E.coli*) (Burch, Sperling, 2018) ; (ii) there are a lot of literature data about beta-lactamin ; (iii) ESBL *E.coli* are a major public health concern and amoxicillin (and overall beta-lactamin drug) contribute to the selection of ESBL in pig production (Bergšpica*, et al.*, 2020).

3.2.1. Simulated dosing regimens

Piglets of 17kg at post-weaning phase were considered for simulation purposes and they received either an IM treatment of 15 mg/kg/day of AMOX for 5 days or a water treatment also based on 15mg/kg/day but associated a variability of exposure. It was assumed that the IM treatment was correctly given, meaning that all pigs received the same correct dose. For the oral treatment, we simulated the drinking pattern behaviour of weaned piglets (Rousseliere*, et al.*, 2016; Rousselière*, et al.*) that showed 2 peaks of consumption over 24h. We thus simulated 2 periods of drinking as a 6h-infusion process. The total quantity of water consumed per day was also variable, and followed a normal distribution (mean = 10.7% of BW, sd = 31% x mean) (Rousseliere*, et al.*, 2016)

A population of 5000 virtual piglets was simulated thanks to Monte Carlo simulations based on the probability distribution of each parameter (*Tableau 2*,*Tableau 2: Values and probability distribution of PK parameters from the AMOX modelTableau 4*)

3.2.2. Parametrization of the PK model

All equations related to the PK model are presented in *Tableau 1* and parameters values in *Tableau 2*. Two case-study were considered for AMOX treatment: either IM treatment (referred as IMexp) or via water medication (referred as POexp). It is anticipated that the oral treatment will lead to higher exposure variability for pigs compared to IM treatment, as already seen with other drugs in pigs (Soraci*, et al.*, 2014) and sheep (Ferran*, et al.*, 2020) .

Concerning the administered dose, we considered no variability for the IM treatment, i.e. 100% of the nominal dose was effectively injected within the pig body. However, an IM bioavailability was considered that would reduce the amount of drug reaching the plasma.

As the main interest was the intestinal AMOX concentrations, the digestive tract was mechanistically described. We also modelled the unbound fraction of AMOX within colon, *i.e.* the pharmacological active fraction of this antibiotic which acts on the bacteria. Values were found based on experiments with human faecal solutions (fu=0.3-0.5) (Jansen*, et al.*, 1992) but due to the paucity of these data, we extend the range of the upper bound limit to the plasma protein binding found in pigs (fu=0.75) (Agersø, Friis, 1998a). The AMOX unbound fraction and could be degraded by beta-lactamase enzyme (BL) produced by the resistant bacteria (see 3.1.3.2) whereas we assumed that the bound fraction was still subject to abiotic degradation (chemical hydrolysis) (Hirte*, et al.*, 2016; Kaeseberg*, et al.*, 2018).

Equation number	Equation	Description
1	$\frac{\mathrm{d}A_{dep\_im}}{\mathrm{dt}} = -(K_{im1} \times Frac_{kim1} + K_{im2} \times (1 - Frac_{kim1})) \times A_{dep\_im}$	Change in IM depot AMOX amount due to 2 different absorption rate constants (Kim1, Kim2)
2	a) $\frac{\mathrm{dAc}}{\mathrm{dt}} = \left(K_{im1} \times Frac_{kim1} + K_{im2} \times (1 - Frac_{kim1})\right) \times A_{dep_{im}} + ka \times A_{int} - kel \times Ac$ b) $Cc = \frac{Ac}{Vc}$	a) Change in plasma AMOX amount due to the absorption through either IM route (Kim1, Kim2) or oral route (ka) and the elimination process (kel); b) Plasma AMOX concentration
3	$\frac{\mathrm{d}A_{sto}}{\mathrm{dt}} = -K_{sto} \times A_{sto}$	Change in stomach AMOX amount due to outflow transit rate (Ksto) Degradation considered as negligible (Erah*, et al.*, 1997)
4	$\frac{\mathrm{d}A_{int}}{\mathrm{dt}} = K_{sto} \times A_{sto} - \left(K_{int} + ka + K_{deg}\right) \times A_{int} + F_{bile} \times kel \times Ac$	Change in intestines AMOX amount due to inflow transit rate from stomach (Ksto), oral absorption (ka), non-specific degradation (Kdeg) and outflow transit rate from small intestines, as well as inflow from bile of the excreted AMOX (Fbile * kel).
5	a) $A_{col} = A_{col\_ub} + A_{col\_b} = fu \times A_{col} + (1 - fu) \times A_{col}$ b) $\frac{\mathrm{d}A_{col\_ub}}{\mathrm{dt}} = fu \times K_{int} \times A_{int} - (K_{col} + DEG_{BL}) \times A_{col\_ub}$	a) Amount of AMOX within colon as the sum of unbound and bound fractions of AMOX quantities

This meeting is part of the European Joint Programme One Health EJP.
This project has received funding from the European Union's Horizon 2020 research and innovation programme under Grant Agreement No 773830.

	c) $\frac{\mathrm{d}A_{col\_b}}{\mathrm{dt}} = (1-fu) \times K_{int} \times A_{int} - (K_{col} + K_{deg}) \times A_{col\_b}$ d) $C_{col\_ub} = A_{col\_ub}/Vcol$	b) Change in colon unbound AMOX amount due to inflow transit rate from small intestines (Kint), degradation by beta-lactamase enzymes produced by the Resistant E.coli population (DEG_{BL}, see *Tableau 4*) and outflow transit rate from colon c) Change in colon bound AMOX amount due to inflow transit rate from small intestines (Kint), non-specific degradation (Kdeg) and outflow transit rate from colon d) Unbound AMOX concentration within colon

Tableau 1: Pharmacokinetic model equations for AMOX model

Parameter (unit)	signification	Values and distribution type	Reference
CL/F_im (L/h/kg)	Apparent plasma clearance	LogNormal (0.39, 0.14)	(Rey, *et al.*, 2014)
Vc/F_im (L/kg)	Apparent central volume	LogNormal (0.25, 0.32)	(Rey, *et al.*, 2014)
Vp (L/kg)	Peripheral volume	LogNormal (1.05, 0.36)	(Rey, *et al.*, 2014)
Q (L/h/kg)	Inter-compartmental clearance	LogNormal (0.089, 0.088)	(Rey, *et al.*, 2014)
Ka (h^{-1})	Absorption constant for oral route	LogNormal (0.15, 0.5)	(Agersø, Friis, 1998b)
F_im	Intra-muscular bioavailibility	LogNormal (0.82, 0.1)	(Agersø, Friis, 1998b)
Kim1 (h^{-1})	Fast absorption constant for IM route	LogNormal (0.34, 0.29)	(Rey, *et al.*, 2014)
Frac_kim1 (%)	Fraction of the dose absorbed following kim1	LogNormal (0.16, 0.59)	(Rey, *et al.*, 2014)
Kim2 (h^{-1})	Low absorption constant for IM route	LogNormal (0.04, 0.52)	(Rey, *et al.*, 2014)
Fbile (%)	Fraction of plasma clearance linked to the excretion biliary system	Uniform (0.14,0.30)	(Bernier, 2010; Martinez-Larranaga, *et al.*, 2004)

This meeting is part of the European Joint Programme One Health EJP.
This project has received funding from the European Union's Horizon 2020 research and innovation programme under Grant Agreement No 773830.

Ksto (h^{-1})	Transit constant through stomach	Uniform (0.49, 1.76)	(Anderson, *et al.*, 2002; Davis, *et al.*, 2001; Freire, *et al.*, 2000; Gregory, *et al.*, 1990; 1995; Snoeck, *et al.*, 2004; Suenderhauf, Parrott, 2013; Wilfart, *et al.*, 2007)
Kint (h^{-1})	Transit constant through intestines	LogNormal (0.22, 0.2)	
Kcol (h^{-1})	Transit constant through colon	LogNormal (0.04, 0.2)	
Vcol (L/kg)	Volume of digesta content within colon	LogNormal (0.018, 0.25)	(Merchant, *et al.*, 2011; Suenderhauf, Parrott, 2013)
Kdeg (h^{-1})	Unspecific degradation rate constant of amoxicillin within digestive tract	Uniform (0.048,0.02)	(Hirte, *et al.*, 2016; Kaeseberg, *et al.*, 2018) (Chesa-Jiménez, *et al.*, 1994)
Fu_dig	Available fraction of amoxicillin within colon	Uniform (0.3, 0.75)	(Agersø, Friis, 1998a; Jansen, *et al.*, 1992)
Qtity_fec (g)	Quantity of faeces produced per day	Normal (753, 50)	Ref Catherine for weaned piglets

Tableau 2: Values and probability distribution of PK parameters from the AMOX model

3.2.3. Parametrization of the PD model

All equations describing the PD part and the associated parameters values are presented in *Tableau 3* and *Tableau 4*, respectively.

The growth rate was obtained from experiments with *E.coli* in anaerobic conditions in an *in vitro* gut model (de Muinck*, et al.*, 2013). Concerning the fitness cost of R linked to the plasmid, very heterogeneous results are given in the literature for beta-lactamase carrier-plasmid. Indeed, from no fitness cost (or even an increase growth rate) to about 10% of reduced growth were observed, depending on the plasmid, the BL enzyme and the E.coli strains (Fischer*, et al.*, 2014; Humphrey*, et al.*, 2012; Santiago*, et al.*, 2020; Shin, Ko, 2015). Therefore, we assumed an uniform distribution of fitness cost from 0 to a 10% decrease in the R bacteria growth rate. The maximal carrying capacity of E.coli within intestines (Nmax) is also associated to high variability between studies, therefore we used a uniform distribution from 10^8 to 10^10 CFU (Hansen*, et al.*, 2013; Herrero-Fresno*, et al.*, 2016; Jensen-Waern*, et al.*, 1998; Jensen, 1998; Luise*, et al.*, 2019; Nadeau*, et al.*, 2017; Nguyen*, et al.*, 2014; Rhouma*, et al.*, 2016; Trckova*, et al.*, 2015; Viel*, et al.*, 2018; Zhou*, et al.*, 2015). For the inflow of bacteria ($\mathrm{IN}_S/\mathrm{IN}_R$), the rate is poorly studied and was obtained from the PKPD cattle model (Volkova*, et al.*, 2012) and assumed to be constant over time. The associated bacterial load of incoming sensitive E.coli was kept constant (10^6 CFU), considering the microbiological load within food (Royer*, et al.*, 2004; 2005) but we simulate different scenario of the incoming resistant bacterial load ranging from 10^2 to 10^8 CFU/g. The outflow of bacteria was obtained from previous studies but was also associated to high uncertainty (Cazer*, et al.*, 2017; Graesboll*, et al.*, 2014). Parameters values of inflow and outflow of bacteria were chosen to avoid an extreme loss of bacteria and thus an extinction of any *E.coli* strains, event without antimicrobial treatment. A threshold of 10 CFU/g was considered as the minimum value for each strain to multiply. Under this value, the strain does not grow any more.

Killing of bacteria was modelled as an Emax function but Emax parameter was depending linearly on the growth rate of each strain (Lee*, et al.*, 2018b). The EC50 were fixed to the MIC values of each strain, as it was shown to be linearly correlated in a study with ampicillin and E.coli (Ahmad*, et al.*, 2016b). For the MIC, the values of ½*ECOFF for S and 16*ECOFF for R (EUCAST, 2020) were taken and an uncertainty factor was applied (Range_{CMI}), taking into account the acceptable double-dilution precision of the MIC method measurement. The plasmid transfer by conjugation and plasmid loss by segregation were obtained from several studies focusing on beta-lactamases but we found values differing by several order of magnitude, therefore a uniform distribution was chosen (Fischer*, et al.*, 2014; Lopatkin*, et al.*, 2017; Zwanzig*, et al.*, 2019). Finally, the degradation rate of unbound amoxicillin by BL-enzyme was obtained from parameter estimations coming from recent PKPD models (Chauzy*, et al.*, 2019; Kristoffersson*, et al.*, 2020), that were also heterogeneous.

Equation number	Equation	Description
6	a) $G_S = K_{growth} \times \left(1 - \frac{N}{Nmax}\right)$ $G_R = K_{growth} \times (1 - FIT_R) \times \left(1 - \frac{N}{Nmax}\right)$ b) $N = S + R$	a) Logistic growth of S (G_S) and R (G_R) populations, limited by the colon carrying capacity (Nmax), with a plasmid fitness cost (FIT_R) resulting in decrease growth rate for R. b) N is the total number of E.coli within colon
7	$\mathrm{IN}_S = \mathrm{Inflow}_S \times \mathrm{IN}_{EC}$ $\mathrm{IN}_R = \mathrm{Inflow}_R \times \mathrm{IN}_{EC}$	Inflow of S (IN_S) and R (IN_R) from ingestion (water,food)/environment with a rate IN_{EC}
8	$\mathrm{OUT}_S = \mathrm{OUT}_{EC}$ $\mathrm{OUT}_R = \mathrm{OUT}_{EC}$	Outflow of S (OUT_S) and R (OUT_R) from toward faeces with a rate OUT_{EC}
9	a) $\mathrm{Kill}_S = \mathrm{Emax}_S \times \left(\frac{C_{col\_ub}}{\mathrm{EC50}_S + C_{col\_ub}}\right)$ $\mathrm{Kill}_R = \mathrm{Emax}_R \times \left(\frac{C_{col\_ub}}{\mathrm{EC50}_R + C_{col\_ub}}\right)$ b) $\mathrm{Emax}_S = (Coeff_{Emax} + 0.18) \times K_{growth}$ $\mathrm{Emax}_R = (Coeff_{Emax} + 0.18) \times K_{growth} \times (1 - FIT_R)$ c) $\mathrm{EC50}_S = \mathrm{Range}_{CMI} \times \mathrm{CMI}_S$ $\mathrm{EC50}_R = \mathrm{Range}_{CMI} \times \mathrm{CMI}_R$	a) Pharmacodynamic effect of AMOX on S (Kill_S) and R (Kill_R), with the maximum pharmacodynamic effect (Emax_S, Emax_R) and the concentration of unbound AMOX producing 50% of Emax ($\mathrm{EC50}_S$, $\mathrm{EC50}_R$) b) Emax is defined as a linear function ($Coeff_{Emax}$) of the growth of Ecoli (K_{growth}) (Lee, *et al.*, 2018b) d) The EC50 were fixed to the values of ½*ECOFF for S and 16*ECOFF for R (EUCAST, 2020) and corrected by a uncertainty factor (Range_{CMI})
10	a) $PT = \gamma \times \left(\frac{S}{N}\right)$ b) $SEG = \beta \times K_{growth} \times (1 - FIT_R)$	a) The plasmid transfer from R to S, by conjugative process with a rate γ b) There is a density-dependent plasmid loss, which a plasmid loss constant (β) proportional to the growth rate of the R population ($K_{growth} \times (1 - FIT_R)$) (Fischer, *et al.*, 2014)

This meeting is part of the European Joint Programme One Health EJP.
This project has received funding from the European Union's Horizon 2020 research and innovation programme under Grant Agreement No 773830.

11	$DEG_{BL} = K_{\deg\_BL} \times \left(\frac{\mathrm{R}}{\mathrm{R50} + \mathrm{R}}\right)$	AMOX degradation by beta-lactamases produced by R, expressed as a sigmoidal function with maximal degradation rate ($K_{\deg\_BL}$) and R50 the bacterial density at 50% of $K_{\deg\_BL}$
12	a) $\frac{\mathrm{dS}}{\mathrm{dt}} = \mathrm{IN}_S + (G_S - \mathrm{Kill}_S - \mathrm{OUT}_S) \times \mathrm{S} + (SEG - PT) \times R$ $S0 = \mathrm{Nmax} - (\mathrm{R0} \times \mathrm{Nmax})$ b) $\frac{\mathrm{d}R}{\mathrm{dt}} = \mathrm{IN}_R + (G_R - \mathrm{Kill}_R - SEG - \mathrm{OUT}_R + PT) \times R$ $R0 = \mathrm{R0} \times \mathrm{Nmax}$	Change in the number of (a) susceptible and (b) resistant E. coli over time due to the population growth, plasmid transfer and loss, killing effect of AMOX and inflow and outflow. Initial condition are given for each subpopulation (S0 and R0)

Tableau 3: Pharmacodynamics model equations of the AMOX model

Parameter (unit)	signification	Values and distribution type	Reference
Kgrowth (h^{-1})	Net growth rate of E.coli	Uniform (0.69,0.92)	(de Muinck, *et al.*, 2013)
FITr (%)	Fitness cost for Resistant population	Uniform (0, 0.1)	(Fischer, *et al.*, 2014; Humphrey, *et al.*, 2012; Santiago, *et al.*, 2020; Shin, Ko, 2015).
Nmax (CFU/g)	Maximal E.coli carriage within colon	Uniform (10^8,10^10)	(Hansen, *et al.*, 2013; Herrero-Fresno, *et al.*, 2016; Jensen-Waern, *et al.*, 1998; Jensen, 1998; Luise, *et al.*, 2019; Nadeau, *et al.*, 2017; Nguyen, *et al.*, 2014; Rhouma, *et al.*, 2016; Trckova, *et al.*, 2015; Viel, *et al.*, 2018; Zhou, *et al.*, 2015)
EC50_s (µg/mL) **EC50_r (µg/mL)**	AMX concentration leading to 50% of Emax effect, for S and R respectively	S : Range_MIC x CMI_S R : Range_MIC x CMI_R With CMI_S = 4 and CMI_R= 128	(Ahmad, *et al.*, 2016b) (EUCAST, 2020)
Range_MIC	Correcting factor for EC50, considering the imprecision of the MIC measurement method	Uniform (0.5,2)	(EUCAST, 2020)
Coeff_Emax (h^{-1})	Maximal amoxicillin effect on E.coli growth, expressed as multiples of Kgrowth	Uniform (1.5, 2.5)	(Lee, *et al.*, 2018a; Tuomanen, *et al.*, 1986)
INec (h^{-1})	Inflow rate of E.coli within colon	0.01	(Volkova, *et al.*, 2012)
Inflow_S (CFU) **Inflow_R (CFU)**	Amount of incoming S and R bacteria	S : 1000000 R : From 400 to 400000000, with a 10 fold-increment depending on the tested scenario	(Royer, *et al.*, 2005)

OUTec (h^{-1})	Outflow rate of E.coli from colon	Uniform (0.015, 0.055)	(Cazer, *et al.*, 2017; Graesboll, *et al.*, 2014)
Kdeg_BL	Degradation rate constant of amoxicillin by beta-lactamase enzymes	Uniform (0.0042, 1.5)	(Chauzy, *et al.*, 2019; Kristoffersson, *et al.*, 2020)
BL50 (CFU)	half density for max Beta lactamase effect	Uniform (10^3.8–10^5.1)	(Kristoffersson, *et al.*, 2020)
γ (h^{-1})	Beta-lactamase carrying-plasmid transfer rate	Uniform (0.0000093, 0.093)	(Fischer, *et al.*, 2014; Lopatkin, *et al.*, 2017; Zwanzig, *et al.*, 2019)
β(h^{-1})	Plasmid loss by segregation rate	Uniform (0.0001, 0.005)	(Fischer, *et al.*, 2014; Lopatkin, *et al.*, 2017)

Tableau 4: Values and probability distribution of PD parameters from the AMOX model

3.2.4. Sensitivity analysis

Global Sensitivity Analysis (GSA) was carried-out to find the most influential parameters of the PKPD model. The fast99 Method was used to get the Sobol indices for each parameters. The GSA was applied to the AUC over a time period from start of treatment to 30 days after end of treatment, for three different outputs : OUTs, OUTr and OUTcol which are the quantity of sensitive, resistant and amoxicillin excreted within faeces. The range of parameters values for the GSA was 5^{th}-95^{th} percentiles of their distribution(McNally*, et al.*, 2011), except for INCr which was over 8 order of magnitude and for the MIC of the S and R strain which could respectively varied from 1 to 8 and 64 to 512 mg/L, reflecting the range of sensitive and resistant E.coli strains in the EUCAST database. This methods allow the quantification of the first order effects which represent the variation caused by the parameter alone and the total effects for the overall effect of varying the remaining parameters, including variance caused by parameter interactions.

3.2.5. Software

Rstudio (Rstudio, 2018) was used for all simulations. The package mlxR from Lixoft (Lavielle, 2020) was used with the simulX function to performe the monte carlo simulation. Several packages from the tidyverse set (Wickham, 2019) were used to clean, format and plot the data.

3.2.6. Results for the amoxicillin case scenario

3.2.6.1. Case scenario 1: permanent contamination with high level of resistance

For this case scenario, a resistant strain with a MIC equals to 128 mg/L (associated to the EC50 in our model, see *Tableau 4*) was considered as a circulating strain in a pig farm. The incoming inoculum load of R bacteria was supposed to be constant all over the simulation period (due to environmental contamination), and being present in a subdominant level within pig guts.

The treatment is given from T=50h for 5 consecutive days. The corresponding plasma concentrations are shown in *Figure 3*. Due to the lowest bioavailability of the oral route, the concentrations are below those of IM route, with Cmax approximatively twice lower with water treatment.

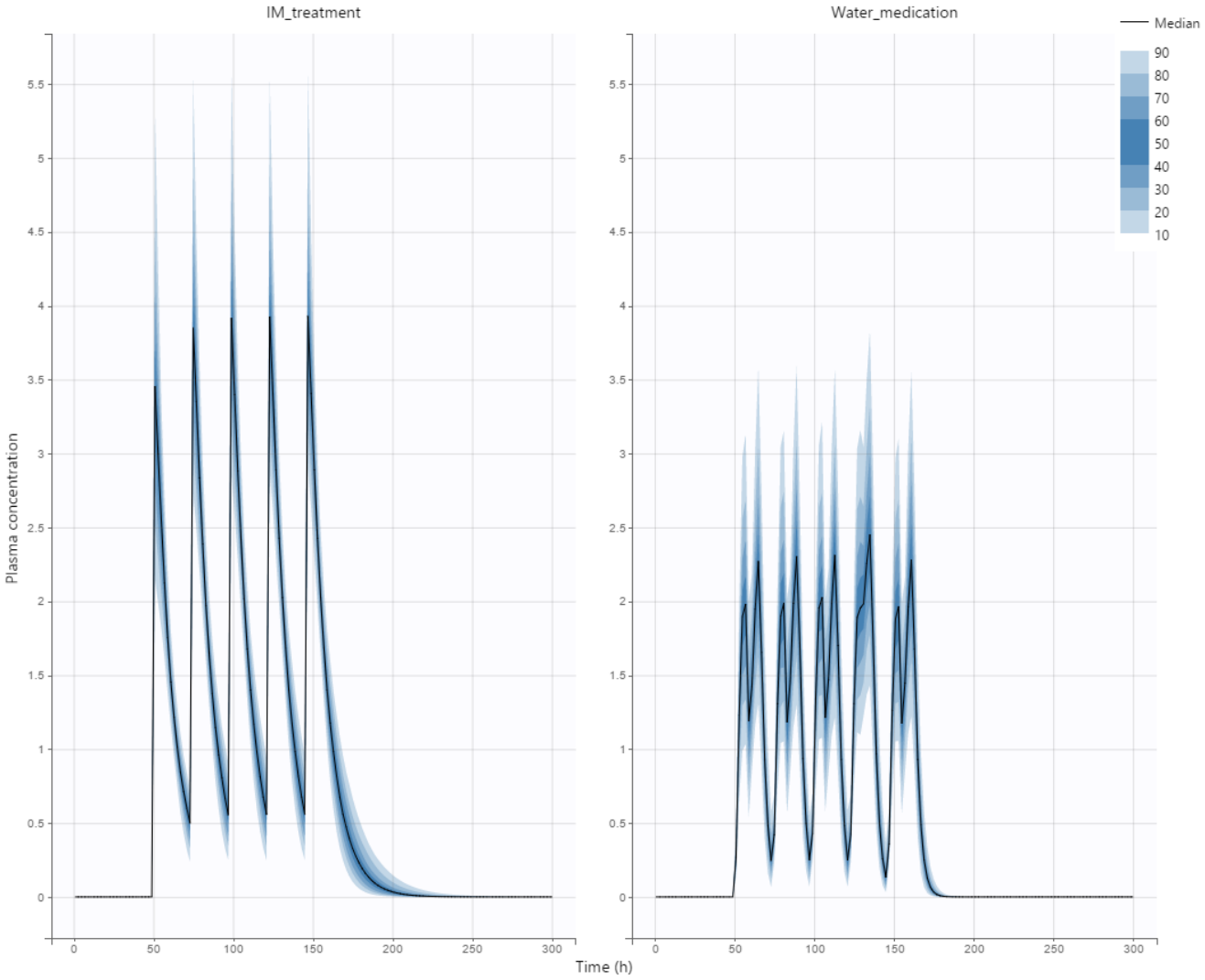

Figure 3 : Plasma concentration of AMOX either after IM injection or water medication in case scenario 1

Regarding the unbound concentration within colon, i.e the active fraction of AMOX, they are presented in *Figure 4*. It is clear that colon is greater exposed to AMOX with the oral treatment compared to the IM treatment (around 8 to 10 times higher).

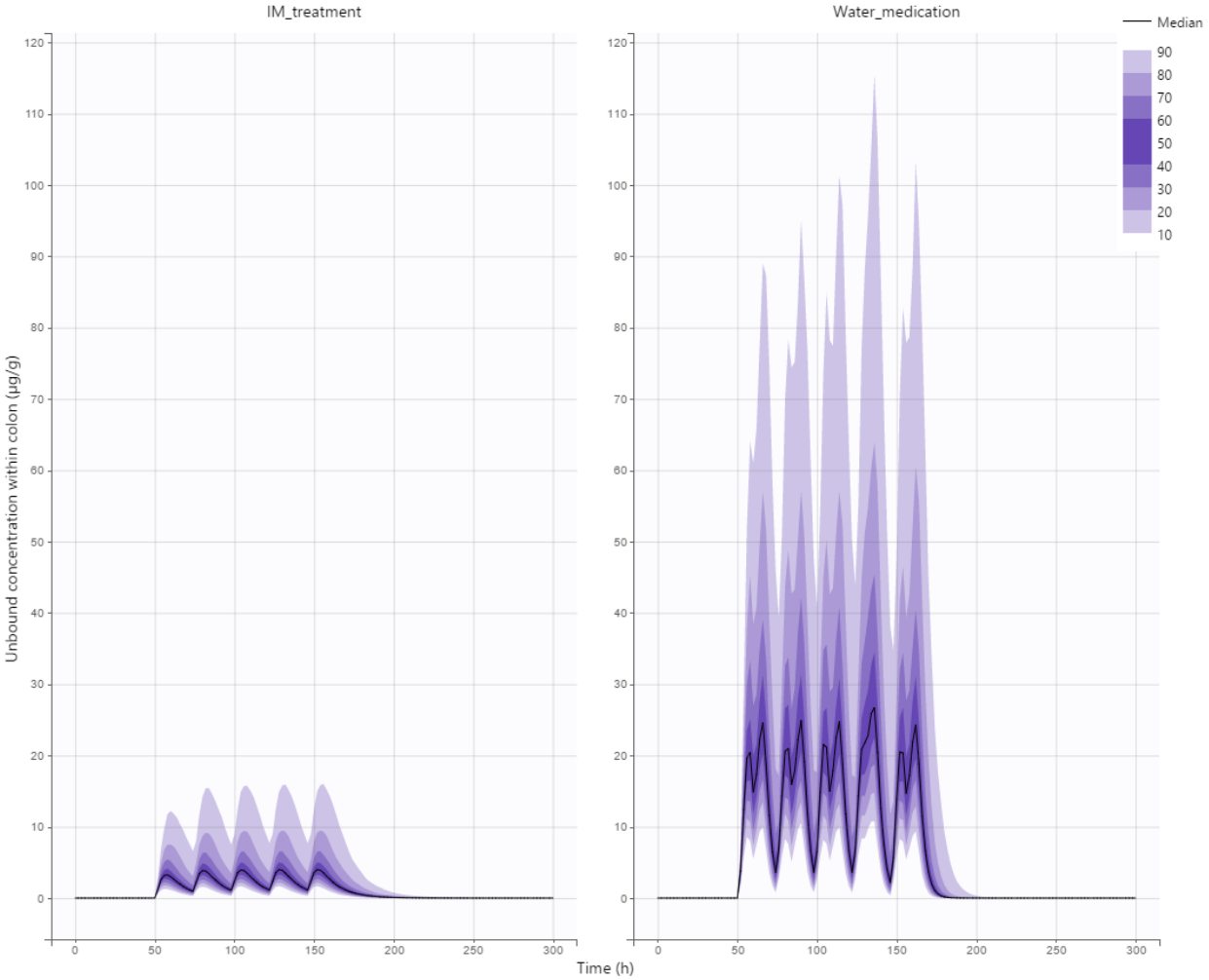

Figure 4 : Unbound colon concentration of AMOX after either IM injection or water medication in case scenario 1

The corresponding impact on the sensitive and resistance bacteria is presented in *Figure 5*. Despite a greater impact on the sensitive bacteria during treatment, the initial level is nearly achieved at the end of the simulation time, i.e around 25 days after the end of treatment. For the resistant bacteria level, despite more variability within treatment period, the impact was closed between both modalities. This is clearly observed with , where we can see that the level of resistance achieved is 100% before a decrease but the initial state is not achieved at the end of the simulation. Worst, for 10% of pigs, the level of resistance is still 70% at the end.

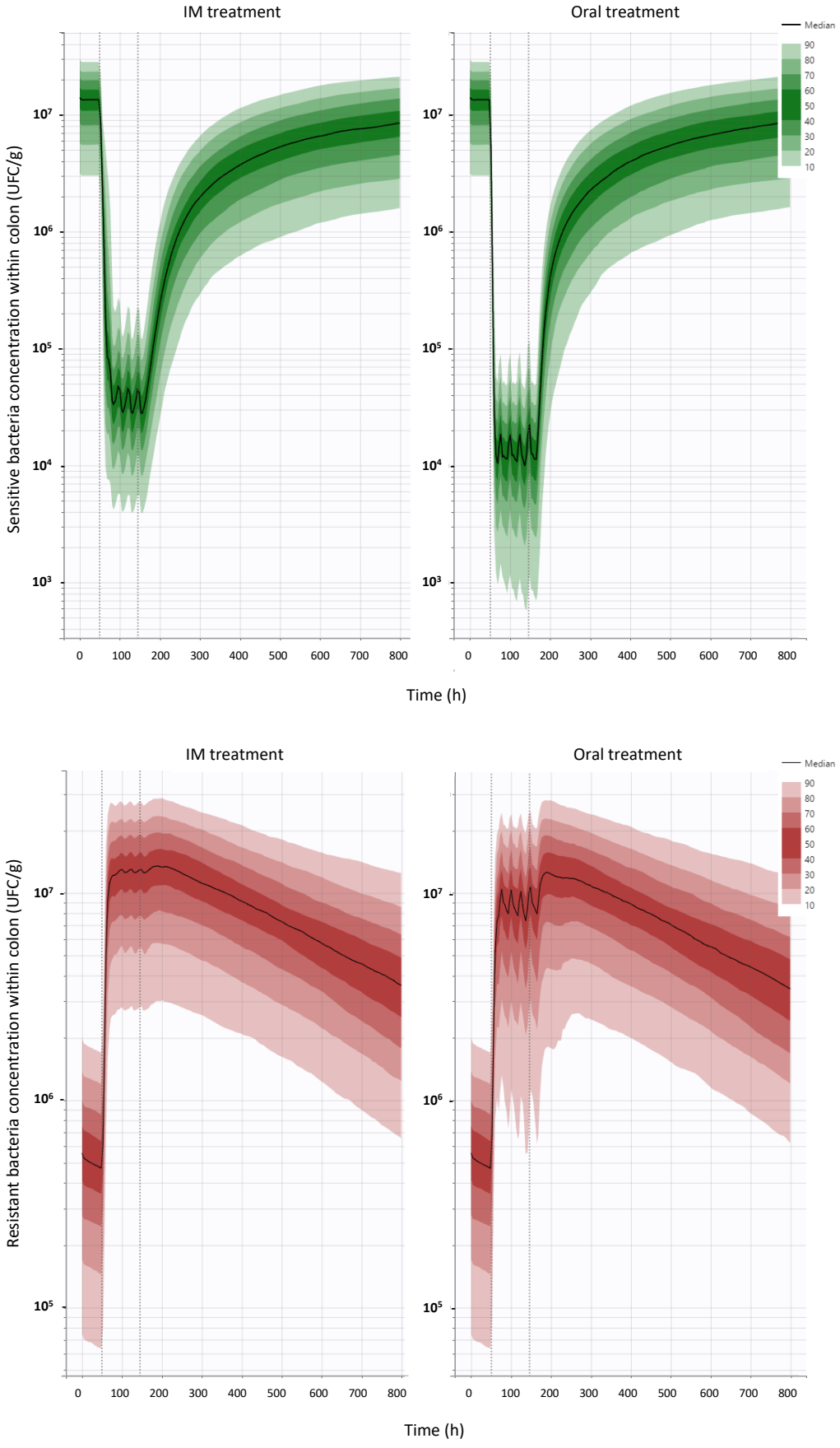

Figure 5 : Concentration of sensitive (top) and resistant (bottom) bacteria within colon after either IM injection or water medication in case scenario 1

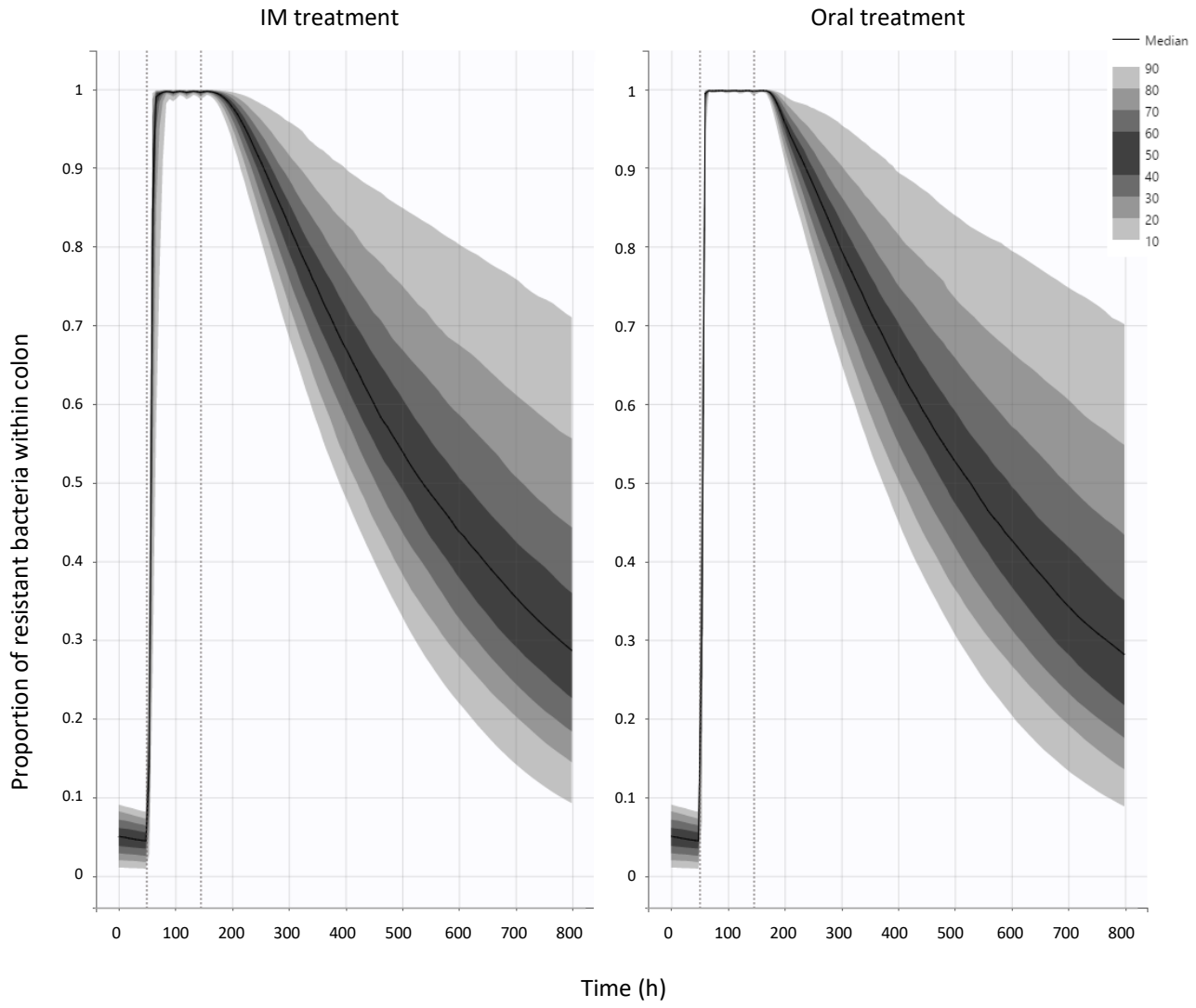

Figure 6 : Proportion of Resistance after either IM injection or water medication in case scenario 1

3.2.6.2. Case scenario 2: permanent contamination with low level of resistance

In this other scenario, the MIC of the resistant strain is about 16 mg/L, so closer to the MIC of the sensitive strain. The dosing regimens were the same (see *Figure 3*). Concerning the unbound AMOX concentration within colon, we can observed a huge variability associated to the water treatment, with some pigs presenting very high level of concentrations over 300 µg/g.

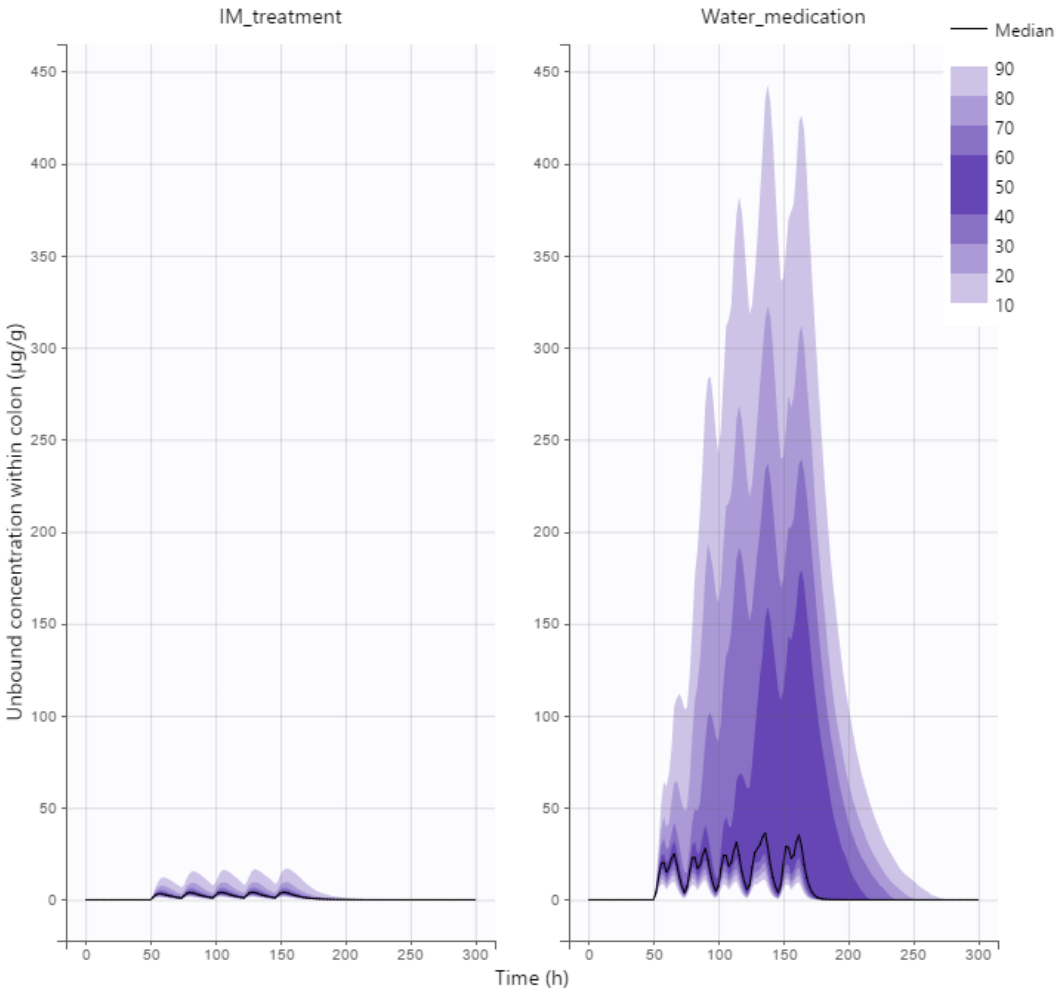

Figure 7 : Unbound colon concentration of AMOX after either IM injection or water medication in case scenario 2

As a consequence, the sensitive and resistant bacteria equilibrium is much more disturbed in the water treatment (see *Figure 8*). Hence, compared to the first case scenario, a large proportion of pigs present a huge decrease of the sensitive and the resistant bacteria and the proportion of resistance stayed low for these pig (*Figure 9*).

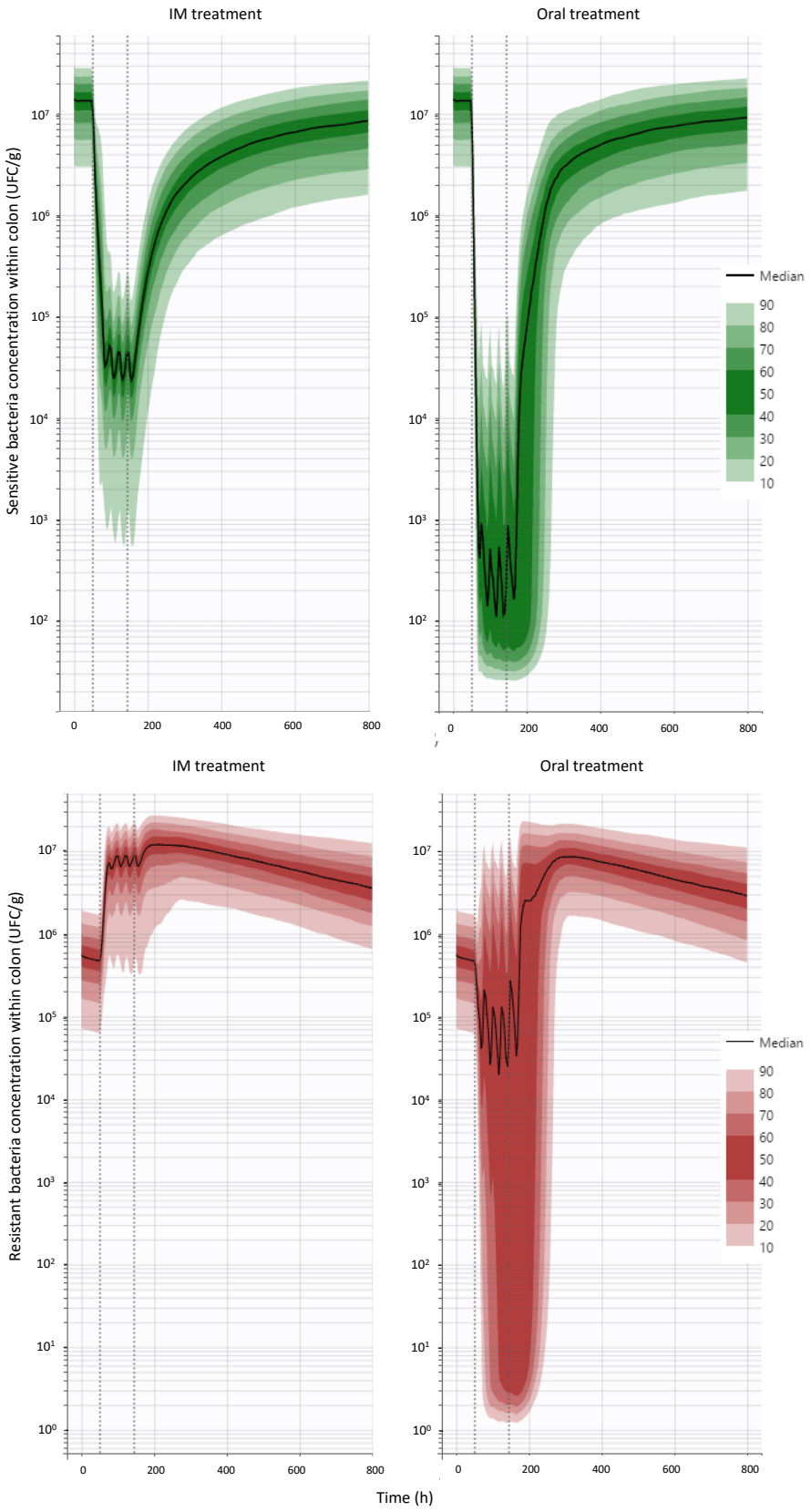

Figure 8 : Concentration of sensitive (top) and resistant (bottom) bacteria within colon after either IM injection or water medication in case scenario 2

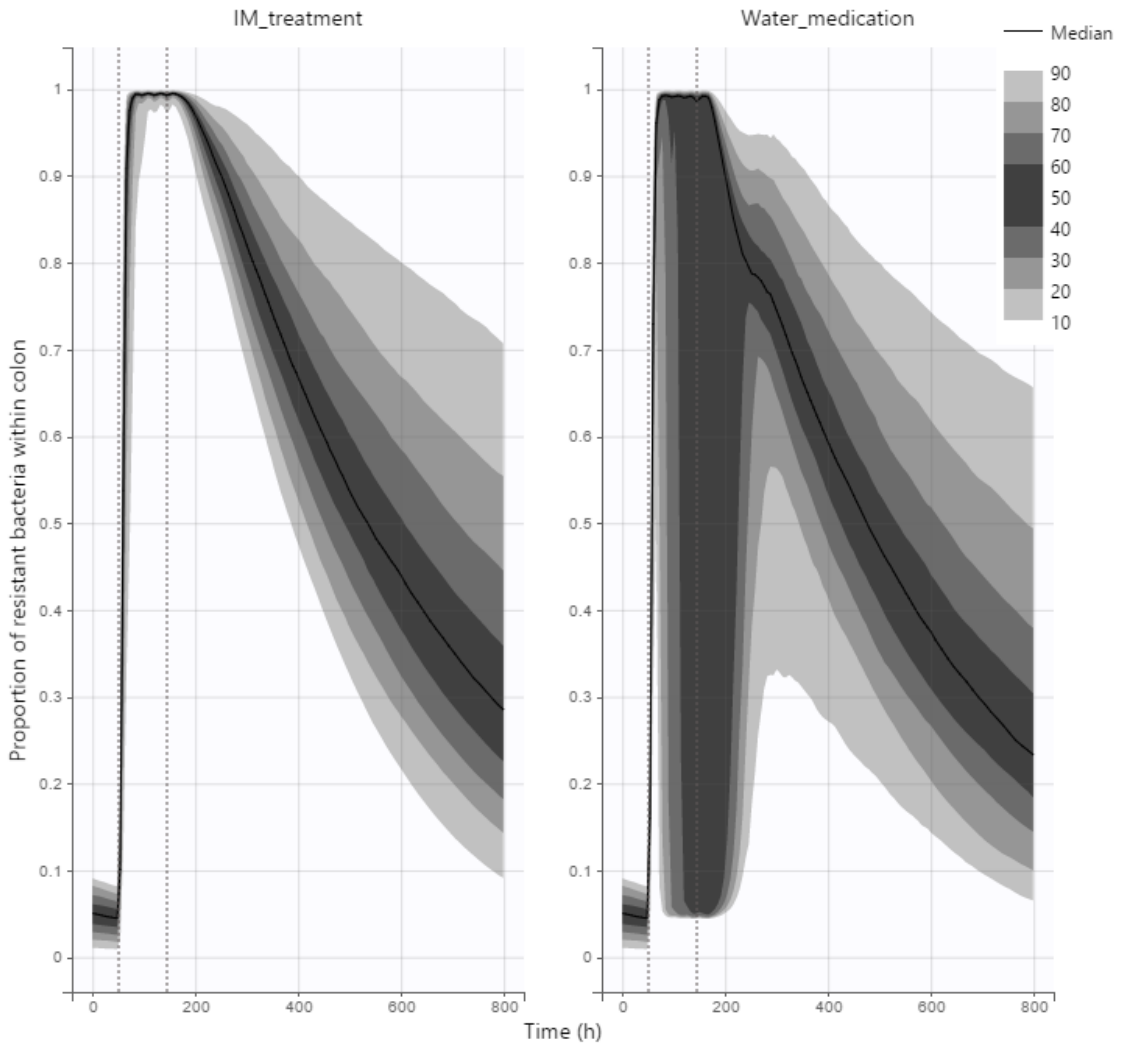

Figure 9 : Proportion of Resistance after either IM injection or water medication in case scenario 2

3.2.6.3. Case scenario 3: no income of resistant bacteria and low level of resistance

In this scenario, we still considered a MIC of 16 µg/mL and simulate the (impossible) absence of new contamination of pigs with resistant bacteria, meaning that the income of resistant bacteria is null. However, the pigs harbour a resistant strain at a subdominant level within the gut at the beginning of treatment. Compared to the previous case study, the absence of incoming bacteria and the high level of concentration within gut are sufficient to eradicate the resistant bacteria in a high proportion of pigs (*Figure 10*,*Figure 11*). However, looking at the median profile, it should be noted that 50% of the simulated pigs will keep the resistance strain at a level of 15% or higher at the end of the simulation period.

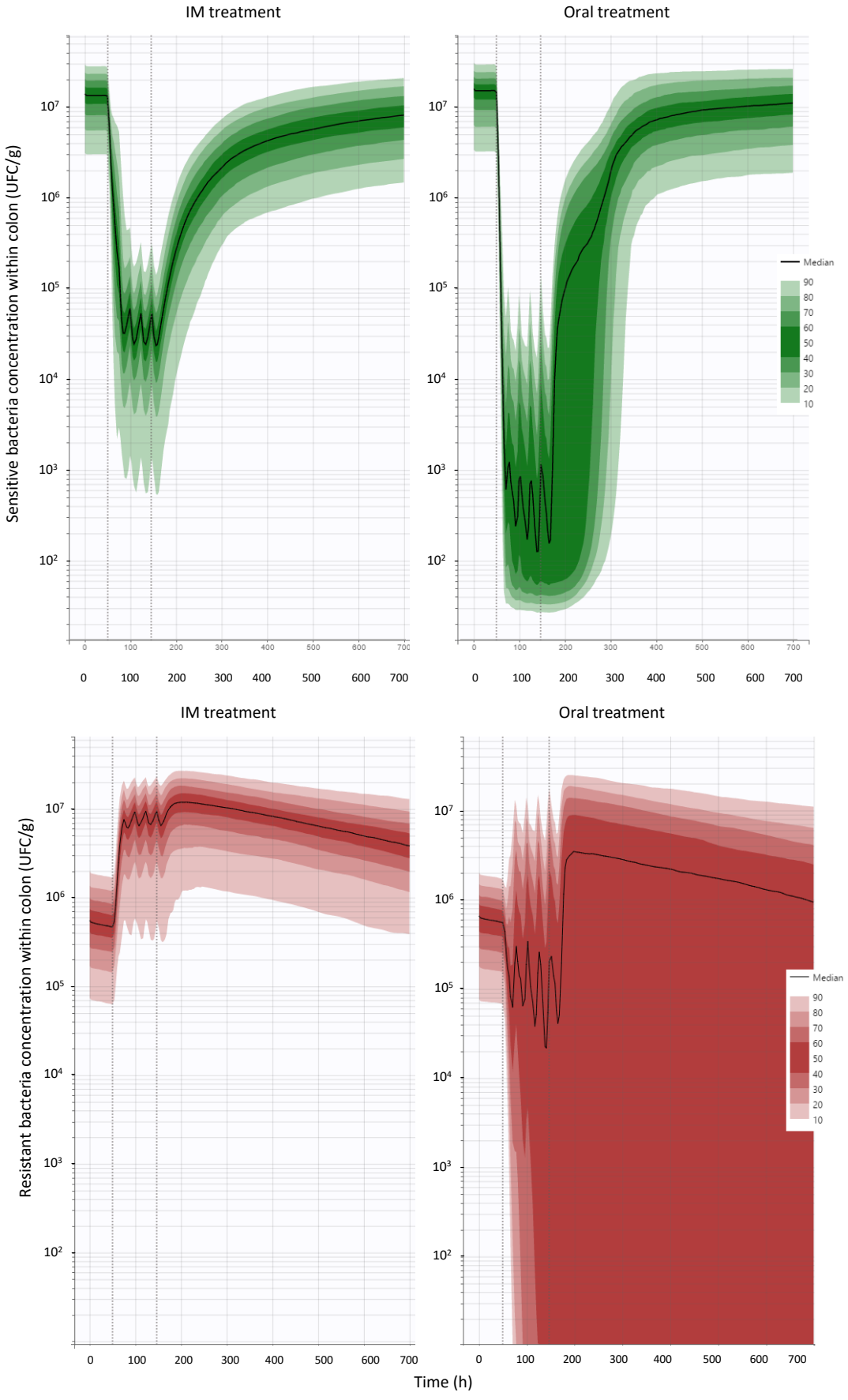

Figure 10 : Concentration of sensitive (left) and resistant (right) bacteria within colon after either IM injection or water medication in case scenario 3

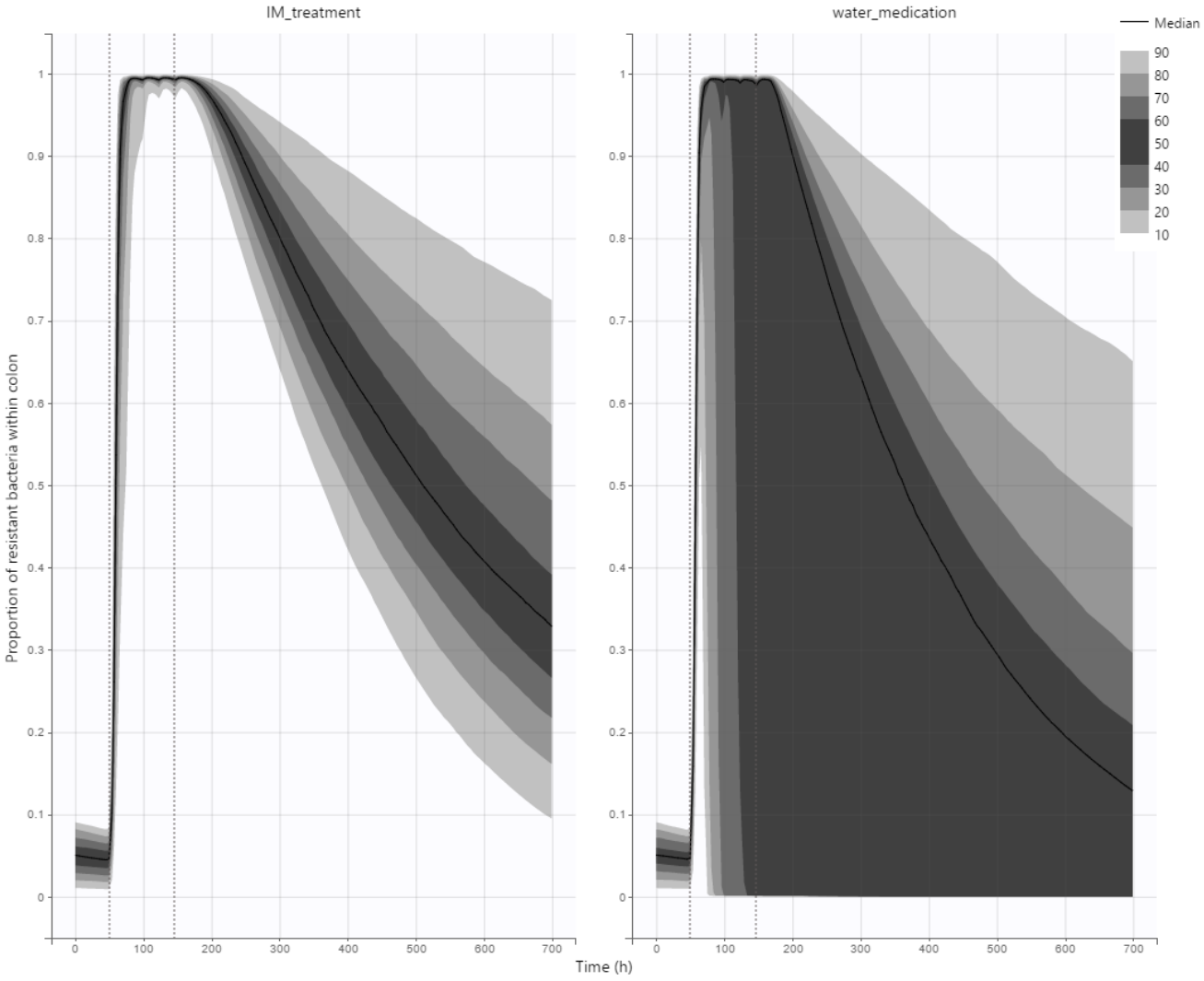

Figure 11 : Proportion of Resistance after either IM injection or water medication in case scenario 3

3.2.6.4. Global sensitivity analysis

Results from the GSA are presented in the *Figure 12*. For the quantity of excreted AMOX, 2 major influential parameters were observed : Kcol and kdeg, meaning that the excretion flow and the abiotic degradation of AMOX (*Figure 12*) contribute exclusively to the variability of this outputs. The other parameters contributed to less than 10% of the total variance and could therefore be considered as non-influential.

For the resistant bacteria, parameters linked to the increase of their number (Inc_R and Ks) were obviously found to be very influential. At a lower level, the parameters associated to the plasmid loss (Tr_plas) and spread (Beta_seg) were observed. The other parameters contributed to less than 10% of the total variance and could therefore be considered as non-influential.

Finally, for the quantity of excreted sensitive bacteria, the maximal carrying capacity and the excretion flow were the only major influential parameters.

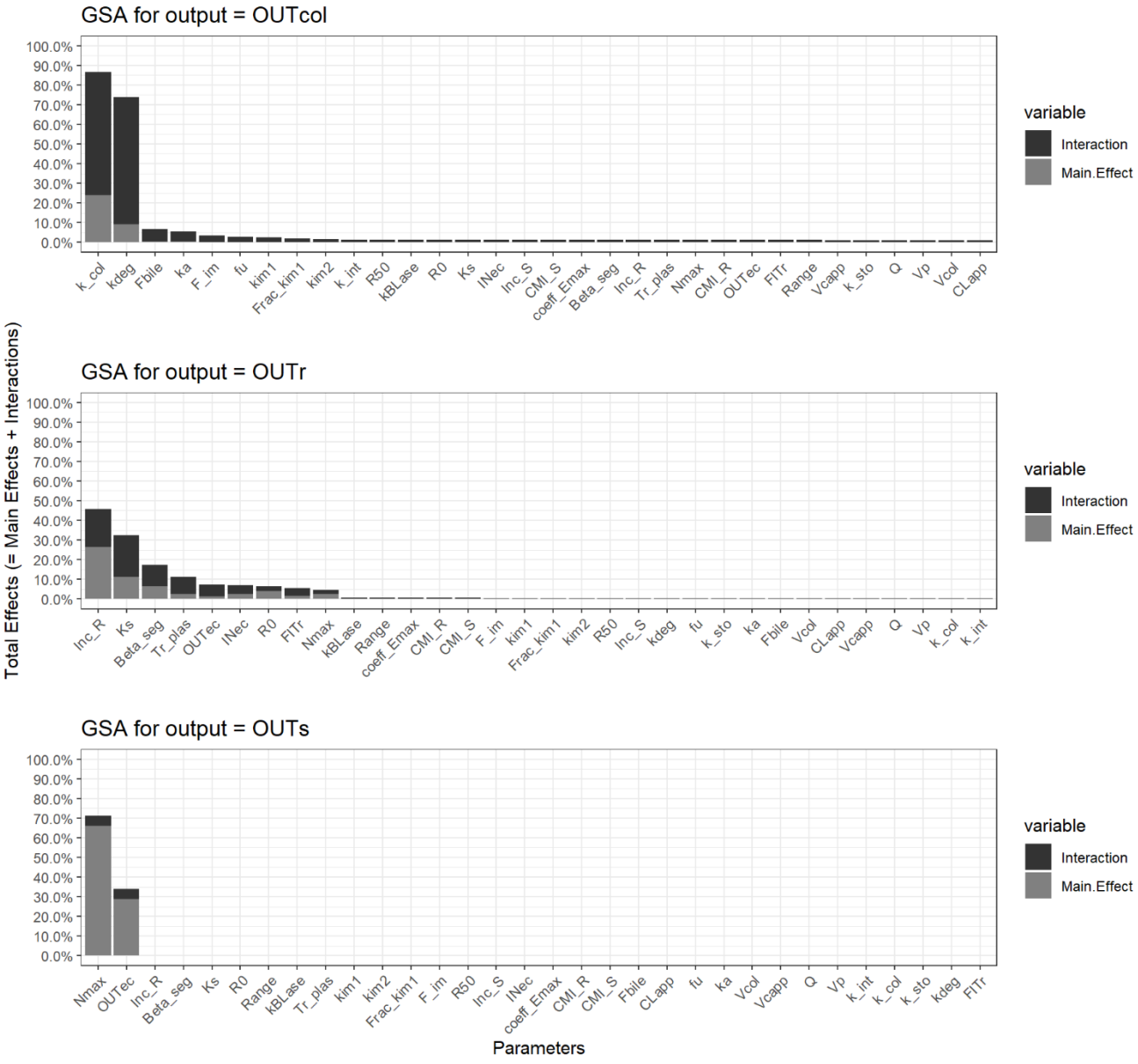

Figure 12 : Global sensitivity analysis for IM treatment.
The 3 main outputs are the quantity of resistant (OUTr) and sensitive (OUTs) bacteria and amoxicillin (OUTcol) excreted trough faeces, for the whole period of simulation (800h)

For the oral treatment, the GSA gave similar results as for IM treatment concerning the most influential parameters (*Figure 13*). The main differences, for minor influential factors, concerned the excreted amount of AMOX within faeces (OUTcol): for IM treatment, PK parameter related to excretion through

bile (Fbile) was the 3rd most influential parameter whereas for the oral route, it was a PD parameter linked to the action of BL enzyme (R50).

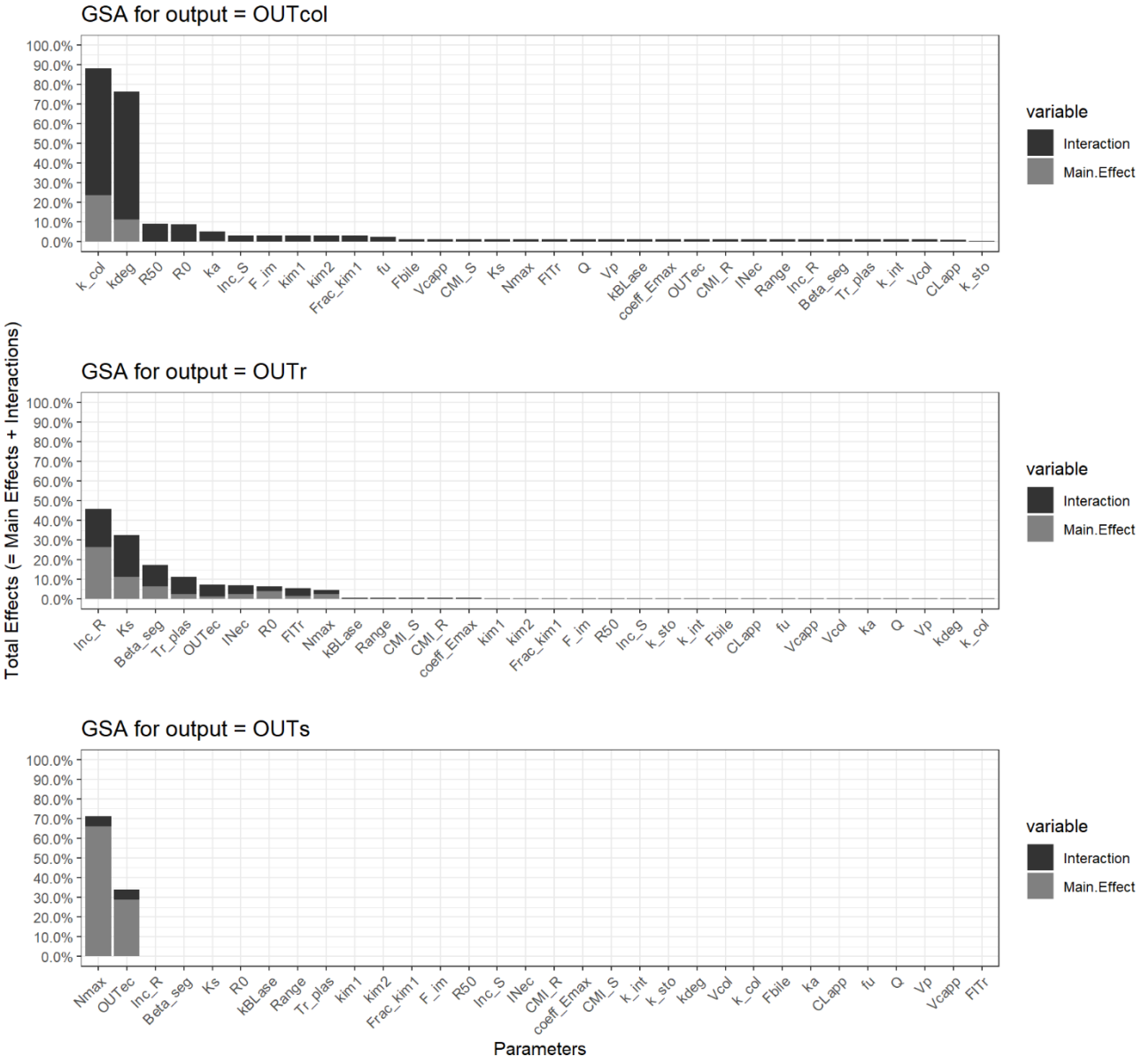

Figure 13: Global sensitivity analysis for oral treatment.
The 3 main outputs are the quantity of resistant (OUTr) and sensitive (OUTs) bacteria and amoxicillin (OUTcol) excreted trough faeces, for the whole period of simulation (800h)

3.2.6.5. External validation of the PK model

Unfortunately, to our knowledge there is no published data about the intestinal or faecal concentrations of amoxicillin in pigs. Therefore it is not possible to assess the predictive ability of our PKPD model with observed data concerning the digestive part.

However, we assessed the relevance of the PK model with published data of 10 pigs treated with amoxicillin in water(Agersø, *et al.*, 1998). We simulated the treatment design as described in the paper but the information were scarce (no individual weight, …) and did not took into account the potential variability of the input doses. Therefore we used the observed pattern drinking of pigs (Rousseliere, *et al.*, 2016; Rousselière, *et al.*) and simulate a variability of 30% of the input dose. Results of the simulation and comparison with the published data(Agersø, *et al.*, 1998) are presented in Figure 14.

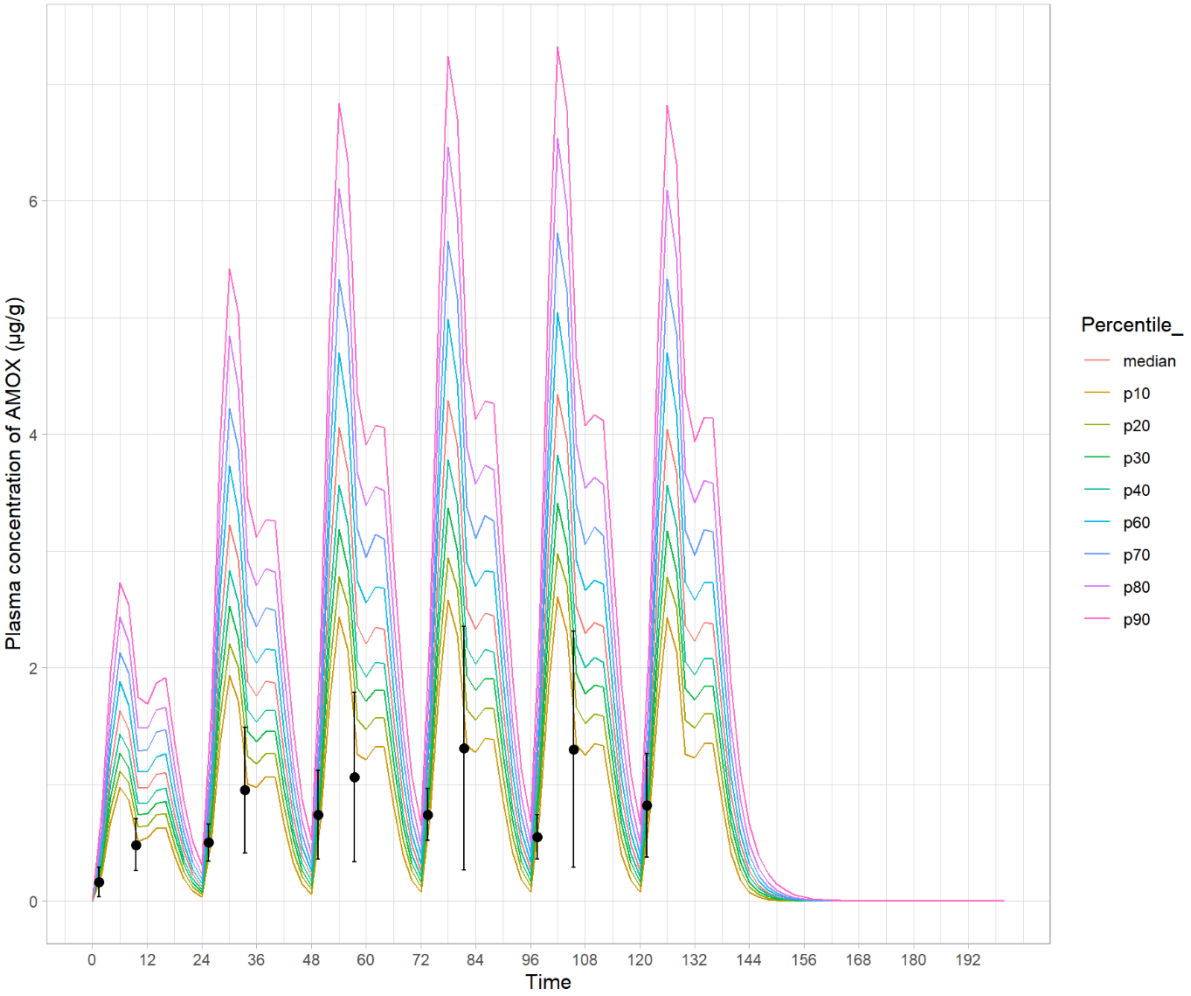

Figure 14 : Comparison between Simulated and observed plasma amoxicllin concentration based on the publication of Agerso
Black dots represent the mean and black bars the SD, recalculated from the SEM, of observed data from(Agersø, et al., 1998). The colored lines are the simulations.

The model slightly over-predicted the observed data but was overall in good agreement with the data considering the lack of detailed information about the treatment design from the original paper.

3.2.6.6. Connexion with the epidemiological "on farm" model

To connect with the farm model, a fixed dosing regimen of IM treatment of 15 mg/kg/day for 5 days were simulated. Amount of R and S bacteria as well as amount of AMOX excreted by pigs over a 24h interval were extracted and divided by the quantity of faeces excreted over a 24h interval. The MIC of S and R were fixed, however, different incoming loads of Resistant bacteria were considered (from 10^2 to 10^8 CFU). These data were used to inform the farm model (WP 2.2)

3.3. Case scenario: use of colistin

Colistin is an old polypeptidic drug used in pig production, especially against digestive infection due to E.coli after weaning. It has been extensively used during decades but with the recent discovery of a plasmid-mediated resistance mechanism (*mcr*) (Liu*, et al.*, 2015), a great concern has been raised concerning the risk of transmission of resistant strain towards human. Indeed, in human medicine, colistin is used as a last-resort treatment {Nordmann, 2016 #333}.

3.3.1. Simulated dosing regimens

Colistin is essentially used through the oral route. Therefore we only considered the oral treatment. In contrast to AMOX, there are published longitudinal data about the faecal concentrations of colistin in pigs (Viel*, et al.*, 2018), thus we used the dosing regimen from this paper for our simulation (oral dosing by gavage).

3.3.2. Parametrization of the PK model

We used the same equations as for the AMOX model with some modifications. Colistin is a non-absorbable molecule (Rhouma*, et al.*, 2015), therefore the systemic compartments were not considered (eq 1-2). Moreover, a high and rapid degradation of colistin has been observed in gastric fluid leading to 50% of degradation (Rhouma*, et al.*, 2015). Therefore the degradation rate was set equal to the stomach flow. It was assumed no other degradation within intestines.
The remaining equations are a simplification of those concerning AMOX because with colistin there is no intestinal absorption thus no possible biliary excretion.

All parameters were kept at the same value as for AMOX (*Tableau 2*), except concerning the unbound fraction which is supposed to be as low as 1% to 10% in media supplemented with faeces (Hazenberg*, et al.*, 1986; Van Saene*, et al.*, 1985).

Equation number	Equation	Description
1	$\frac{\mathrm{d}A_{sto}}{\mathrm{dt}} = -(Kdeg_{sto} + K_{sto}) \times A_{sto}$	Change in stomach colistin amount due to outflow transit rate (Ksto) Degradation up to 50% within stomach (Rhouma, *et al.*, 2015), with $Kdeg_{sto}$ equal to Ksto
2	$\frac{\mathrm{d}A_{int}}{\mathrm{dt}} = K_{sto} \times A_{sto} - (K_{int}) \times A_{int}$	Change in intestines colistin amount due to inflow transit rate from stomach (Ksto) and outflow transit rate from small intestines
3	a) $A_{col} = A_{col\_ub} + A_{col\_b} = fu \times A_{col} + (1 - fu) \times A_{col}$ b) $\frac{\mathrm{d}A_{col\_ub}}{\mathrm{dt}} = fu \times K_{int} \times A_{int} - (K_{col}) \times A_{col\_ub}$ c) $\frac{\mathrm{d}A_{col\_b}}{\mathrm{dt}} = (1 - fu) \times K_{int} \times A_{int} - (K_{col}) \times A_{col\_b}$ d) $C_{col\_ub} = A_{col\_ub}/Vcol$	a) Amount of colistin within colon as the sum of unbound and bound fractions of colistin quantities b) Change in colon unbound colistin amount due to inflow transit rate from small intestines (Kint), and outflow transit rate from colon c) Change in colon bound colistin amount due to inflow transit rate from small intestines (Kint) and outflow transit rate from colon d) Unbound colistin concentration within colon

Tableau 5 : Equations for the PK model of colistin

3.3.3. Parametrization of the PD model

For the PD, it was not possible to find enough relevant data to inform the mechanistic model, especially concerning the killing mechanism (Emax, EC50). Indeed, the published data with colistin mainly concern bacterial species that are a concern for human medicine (*e.g., P. aeruginosa, A. baumanii* …). Moreover, we have previously published an experimental study with pigs harbouring mcr-1-positive E.coli that were treated with colistin (Viel*, et al.*, 2018) and surprisingly didn't observe a selective effect of colistin on the resistant strains. In order to explore in a mechanistic way these results, we carried-out several time-kill experiments in order to estimate some of the PD parameters.

3.3.3.1. Time-kill experiments

Two intestinal porcine E.coli strains, a resistant one harbouring *mcr-1* (named EC-R) and a sensitive one (named EC-S, with a MIC 32 times lower) were used in the Time-kill studies (TKS). A fresh inoculum of 10^5 UFC/mL of each strain was prepared in MHB liquid media (separated tubes), and strains were exposed to different concentrations of colistin as multiples of their respective MIC over 24H. Regular sampling was performed and bacteria were counted on agar plate with serial dilutions.

Results of these experiments are presented in

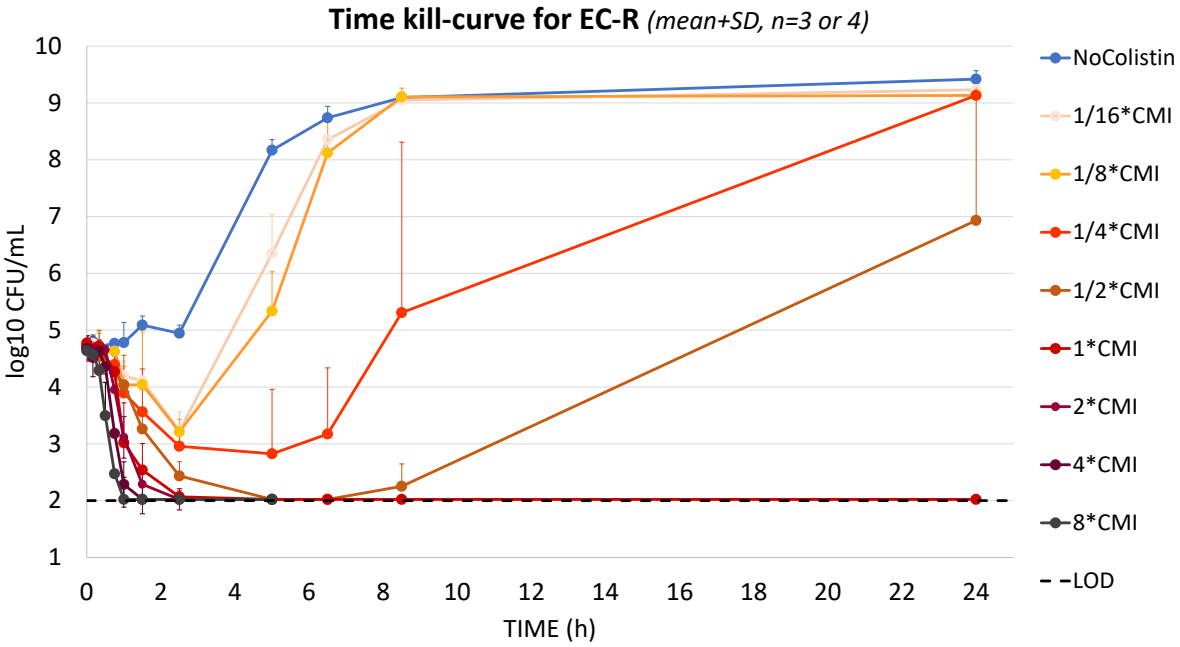

Figure 15 : time kill curve of EC-R with colistin

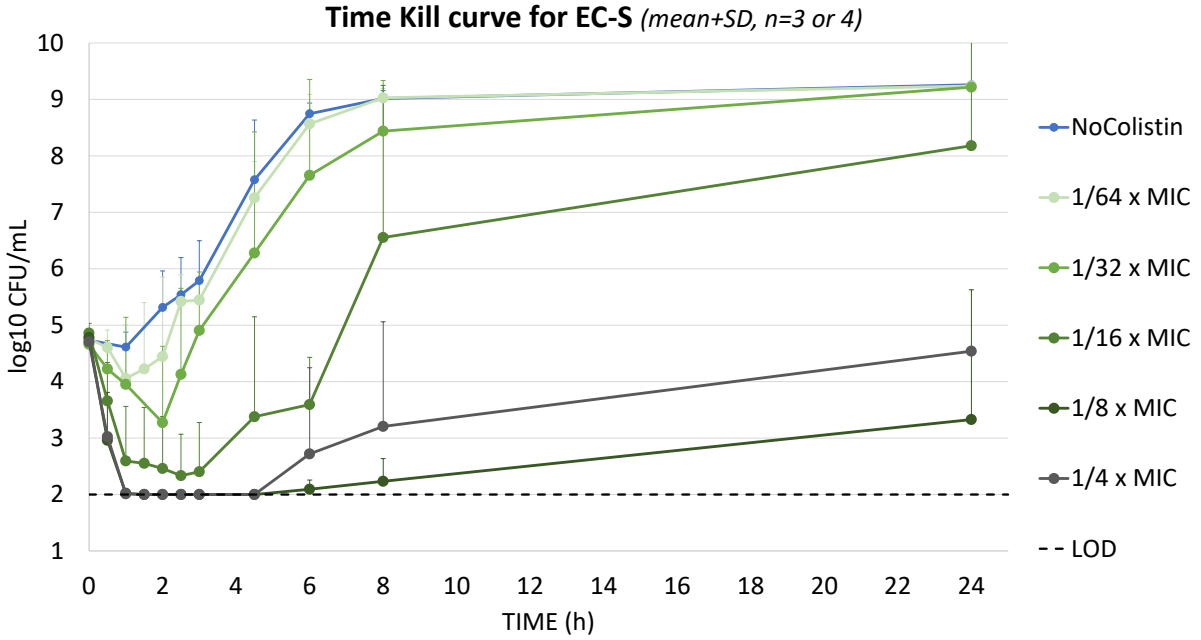

Figure 16 : time kill curve of EC-S with colistin

A rapid and concentration-dependant killing of colistin was observed for each strain. However, a re-growth was noted for all colistin concentrations < MIC even for the EC-S despite no change in the MIC values between t=0 and t=24h. These TKC are necessary to assess the response of each strain to colistin separately but in *in vivo* conditions, both resistant and sensitive strains are present within guts.

Threfore, the TKS were performed over 30h in co-culture condition that would mimic the *in vivo* situation of intestinal E.coli of our study (Viel*, et al.*, 2018) with a dominant EC-S population (starting inoculum: 10^6 CFU/mL) and EC-R at a sub-dominant level (starting inoculum: 10^3 CFU/mL). Regular sampling was performed and total and EC-R bacteria were counted on agar plates (selective agar with antibiotic for the resistant strain) with serial dilutions.

Results are presented on the

Figure 17.

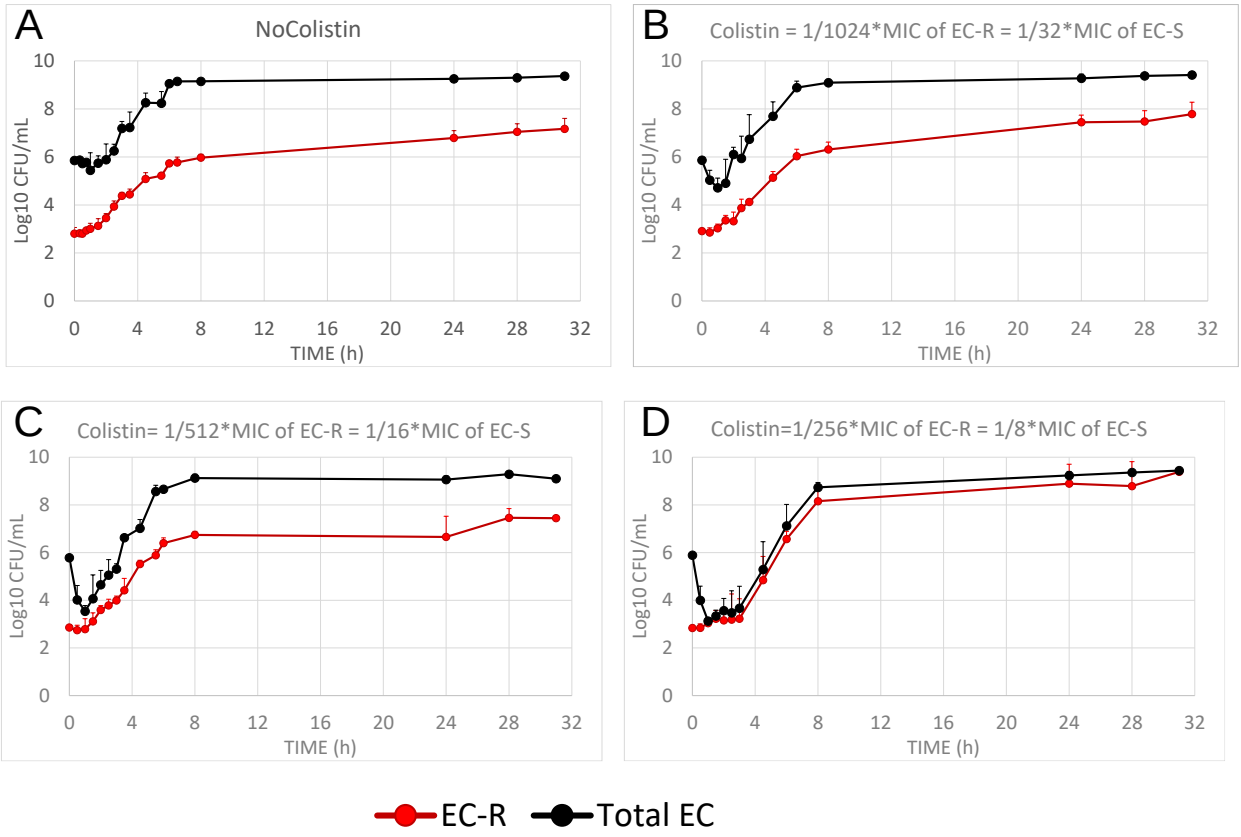

Figure 17 : time kill curve of EC-S and EC-R in co-culture with colistin

After 24h, EC-R stayed at a subdominant level (~2 log10 under total E.coli *level) in*

*Figure 17*A-C, even when total *E.coli* (and therefore EC-S) concentrations decreased sharply between 0 and 4h (C). However, for the highest concentration (D), EC-R became dominant*, i.e.* equal to the total *E.coli* population.

3.3.3.2. Modified mechanistic PKPD model (under development)

In order to describe mechanistically the results of TKS, a previous semi-mechanistic PKPD model with colistin was adapted (Mohamed*, et al.*, 2014) (*Figure 18*). As a regrowth is observed, even for the sensitive strain, an adaptive resistance mechanism and the presence of persisters was considered (Nielsen, Friberg, 2013).

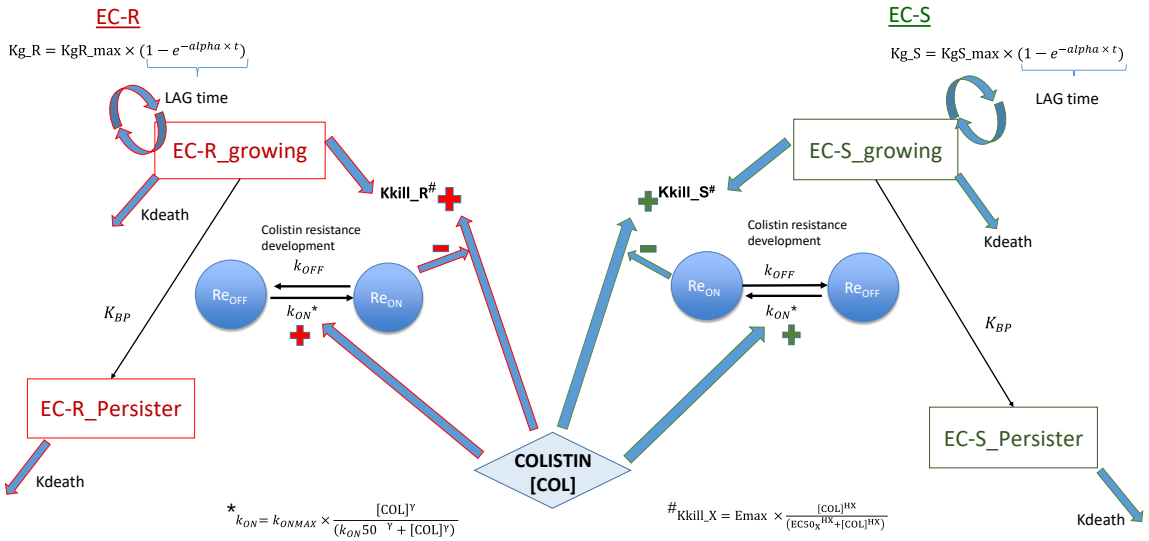

Figure 18 : Semi mechanistic PKPD model of colistin with EC-S and EC-R

This model is still under current development at the time of this report because this model adequately fitted the separated TKS but failed to capture properly the co-culture TKS, especially the data observed in *Figure 17* D (data not shown). An interaction term between EC-R and EC-S may be needed to characterize the inhibition of the EC-R even when the EC-S are sharply decreasing (Lenhard*, et al.*, 2019).

3.3.4. External validation of the PK model

As for the AMOX case scenario, we only assessed the predictive ability of the PK part of the PKPD model with observed data. We simulated the conditions of the study from our lab (Viel*, et al.*, 2018), with 2 groups of 5 pigs receiving 2 different doses (simple dose : 50 000 UI/kg or double dose: 100 000 UI/kg twice a day for 5 days) and taking into account the individual dosages. The observed fecal concentrations reported in the publication were considered as representative of the concentration within colon and were thus compared with the corresponding simulated concentrations from the PK model. The results are shown in *Figure 19*.

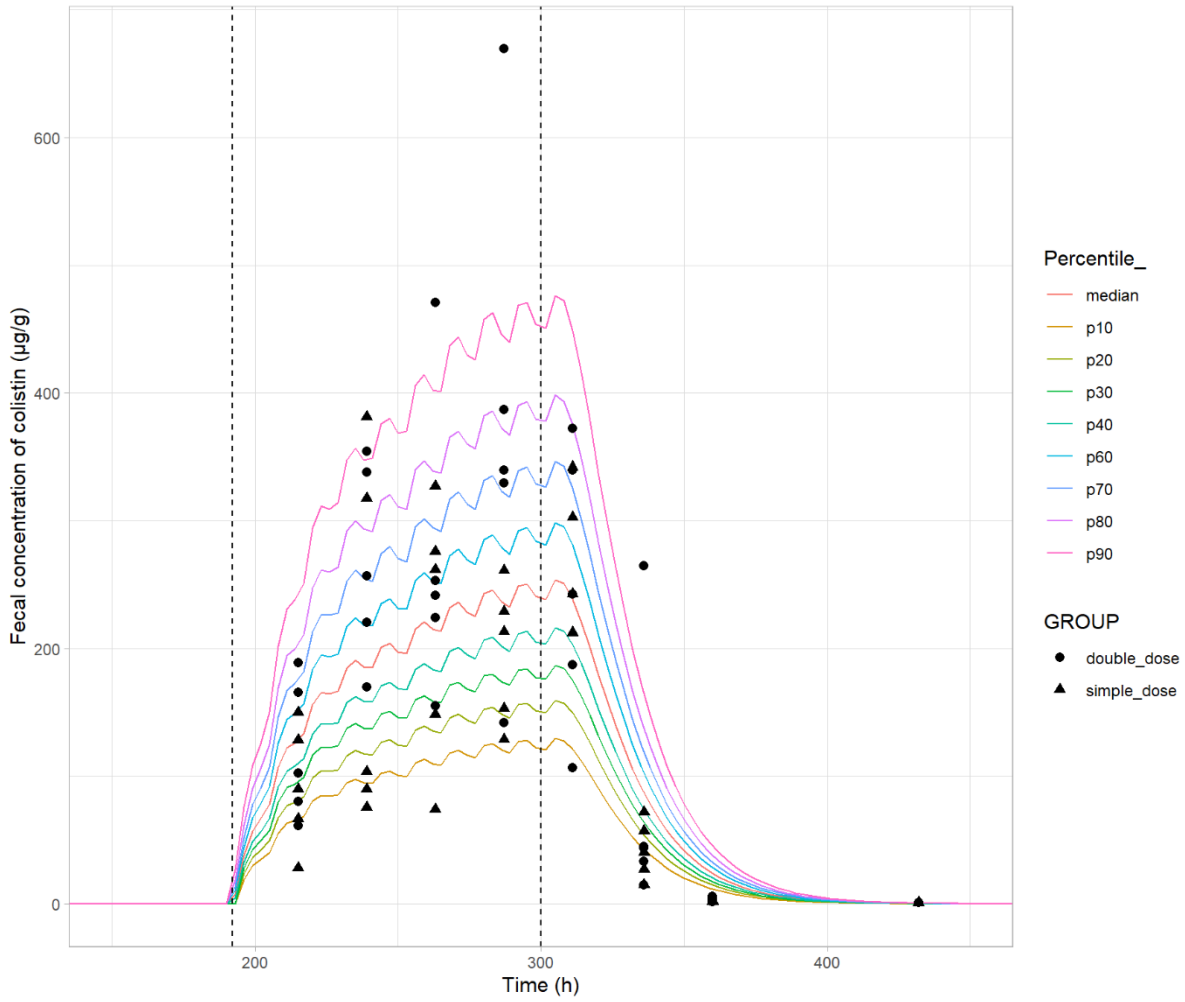

Figure 19 : Comparison between simulated and observed fecal colistin concentrations based on the publication of Viel
Black dots represent the observed data from (Viel, *et al.*, 2018) and colored lines the simulations by the PK model

The model was in very good agreement with the observed data despite a higher variability of the latter. These results gave confidence in the relevance of the PK model of the digestive tract.

3.4. Discussion about the PKPD model

With the AMOX case scenario, the PKPD model clearly highlighted the importance on the administration route on the evolution of resistance *E.coli* within guts. Looking at the IM treatment, we can observe that the AMOX concentration within colon are sufficient to allow the amplification of the R strain, meaning that the concentrations are within the mutant selection window. These results are in accordance with experiments in pigs and ampicillin, which is close to AMOX, showing a strong increase of the resistant population of ESBL E.coli (that was already present within gut) after IM treatment (Bibbal, *et al.*, 2007). However, others author has not observed a selective effect of

amoxicillin on an inoculated ESBL strain within gut, i.e. that was not present "naturally" within pig guts (Cavaco*, et al.*, 2008). The limiting factor of this last study may be the inadequacy of the strain to colonize efficiently the gut (as seen in their control group) compared to a strain which would be already well established. To avoid an over-parametrisation of our model, we chose to represent only Resistant (R) and Sensitive (S) strains, both of them being represented by one compartment. We could have used more complex models (as for the colistin case) but it was shown that it hard to find the most relevant mechanistic model (*i.e*. the best mathematical description of the data) based solely on the count of resistant/sensitive data without an exploration in deep of the resistant mechanisms that are involved (Jacobs*, et al.*, 2016).

Concerning the intestinal concentrations of AMOX, there are no studies within literature that have measured this. Our predictions are in accordance with the predictions made earlier by Burch (Burch, 2007). However, it should be necessary to check the accuracy of the predictions by comparing them with observed data. Nerveless, we were able to validate the predictability of the model concerning the plasma concentrations following an oral treatment trough water (Agersø*, et al.*, 1998).
For the colistin case, the digestive PK model was able to predict with a good agreement the observed fecal data from pigs treated with colistin (Viel*, et al.*, 2018) giving good confidence in our digestive PK model. Some recent studies have followed the intestinal concentration of several antimicrobials, and these data should be used to further assess the predicting ability of the PKPD model (De Smet*, et al.*, 2017; De Smet*, et al.*, 2018).

Despite the importance of BL enzyme in the resistance phenomena and interaction between R and S, the degradation of AMOX by BL did not seem to be an influential factor concerning the excreted quantity of AMOX. This is confirmed by other authors looking at the inactivation of amoxicillin by biological and non-biological processes (Jensen*, et al.*, 2006). However, other studies have shown a significant impact of these BL on the protection of other bacteria species against ampicillin (Gjonbalaj*, et al.*, 2020). The importance of the gut microbiota (especially within caecum) an the metabolism of antimicrobial drug is an ongoing subject (Zimmermann*, et al.*, 2019) and new data may help to refine the PKPD model

The GSA highlighted the importance of knowing some key parameters values with high precision. For the amount of excreted antibiotic drug, the outflow rate and the abiotic degradation rate are the most influencing parameters and therefore their values should be known with good precision. However, these are maybe the most difficult parameters to measure.

Concerning the colistin case, unfortunately the PD values for colistin and *E.coli in* pigs are very scarce in literature and due to the regrowth phenomena that is observed in time-kill studies (*Figure 16*), the

PD model from the AMOX model with only S and R subpopulations will not be sufficient to describe adequately the data. Hence, a more mechanistic model is currently under development and once finalized, it could be included within the generic PKPD model. This reveals the impossibility to develop a real generic, meaning universal, PKPD model that would be predictive for all couple bacteria/AMD.

As seen in our results, the oral treatment leads to an increase of the inter-individual variability concerning the pig exposure to antibiotic (either in plasma and in guts) and hence the impact on the gut *E.coli*. As outlined by a recent review, this kind of antibiotic delivery could result in under-dosing or over-dosing of many pigs (Little*, et al.*, 2019). The impact of social rank has been highlighted as a main covariate explaining these results (Soraci*, et al.*, 2014). Treatments via feed could also have been considered and other authors explored (quite empirically) the impact of such route on the variability of plasma exposure (Li*, et al.*, 2008). However, EMA recently discouraged the use of feed medication due to the high risk of AMR selection (EMA, 2019).

The difficulty of such model is to be able to adapt to the physiological status/disease condition of the animal and their impact on the parameters values (especially the physiological values). Hence for amoxicillin, it was shown that pigs with diarrhoea will absorb less drug than healthy animals (Burch, Sperling, 2018) and this will also probably increase the excretion of bacteria. Therefore an adaptation of the model, especially the outflow rate, could be made. This has already been explored in a previous PKPD model of pigs (Ahmad*, et al.*, 2016b) but in a rather theoretical was without proper data validation.

4. Assess relative importance of clonal dissemination for resistance occurrence

4.1. Introduction

Antimicrobial treatment creates a selection window for antimicrobial resistance strains. Mechanistic Pharmacokinetic/Pharmacodynamic (PK/PD) models were developed to describe the antimicrobial effect on bacterial growth (Nielsen and Friberg 2013). Several of them takes into account different sub-populations with different antimicrobial susceptibility to be kill. Horizontal gene transfer (HGT) of resistance is a major mechanism of acquisition of antimicrobial resistance by bacteria. It is assume that antibiotics promote HGT but this notion lacks of conclusive evidence in the literature (Lopatkin, Sysoeva, and You 2016). If bacterial models of HGT were described, we lack of rigorous data

interpretation (Lopatkin, Sysoeva, and You 2016) to interpret the role of selection dynamics (Lopatkin, Sysoeva, and You 2016).

Considering the importance of the phenomenon, a part of the project was dedicated to study the variability of these processes in function of the bacterial capacity to disseminate resistance by combining a microbial model associated with the PK/PD model and to discuss if the structural adaptation of the generic model is necessary.

4.2. Objectives

The main objectives of this part were: (i) Review of the literature to determine the range of value for the pharmacodynamic parameters; (ii) Develop a process to simulate the model in fixed PK conditions and analyse the pattern of evolution of resistance along time to determine the combination of PD parameters value leading to a success of the resistance; (iii) Simulate different antimicrobial dosage regimens.

4.3. Literature review

Horizontal gene transfer is the transfer of DNA from one organism to another independently from reproduction, and facilitates genetic recombination in bacteria and other single celled organisms. Of the three main mechanisms of HGT (transformation, conjugation and transduction), conjugation is often cited as the most significant in the spread of antibiotic resistance. A recent meta-analysis of plasmid transfer rates from laboratory experiments was reported and reviewed theoretical models (Sheppard, Beddis, and Barraclough 2020). The main parameters of the theoretical models are plasmid transfer and loss rates (segregation), the cost or benefit of plasmid carriage on the host (Carroll and Wong, 2018), and the population size (N). In theory, a plasmid can persist when its transfer rate is greater than the combination of the rate of loss and the cost of the plasmid, within a large population size (Lopatkin et al. 2017).

The model proposed by Levin et al, is used to described the transfer of plasmids from a donor and a receptor population. (Levin, Stewart, and Rice 1979). Different methods (endpoint measurements, endpoint model) are used to determine the transfer rates. Several factors (type of cells, culture conditions, bacterial species, donor and receptor density, size of plasmids) has to be taken into account for the analysis. A recent systematic review demonstrated that the transfer rates varied over 13 orders of magnitude, ranging from 1.6×10^{-20} to $4.8\ 10^{-7}$ ml $cell^{-1}h^{-1}$ (Sheppard, Beddis, and Barraclough 2020).

While plasmid confer a benefit to their hosts under particular conditions (e.g. antimicrobial resistance), a fitness cost of plasmid carriage is expected (Carroll and Wong 2018). Many studies have suggested that carriage of antimicrobial resistance is generally costly to the host, although this cost can be reduced over time. According a recent systematic review, the fitness reductions is low ranging from 1% to 28 % (Carroll and Wong 2018). The host genetic background may be an important determinant of plasmid fitness and can be dependant of the carriage of several plasmids with different fitness costs.

Plasmids are expected to slowly be lost from a population due to segregational loss where a plasmid is lost by chance during cell division. Estimates of the rate of segregational loss vary from 10^{-3} per cell per generation to 0.05 per cell per generation according to a recent review (Carroll and Wong 2018).

4.4. Modelling

Different PKPD modelling of antimicrobial effects were described in the literature but few contains the plasmid dynamics, focusing mainly on the horizontal gene transfer (Leclerc, Lindsay, and Knight 2019). The combination of a PKPD model with a model of HGT is explored in a limited set of papers (Volkova et al. 2013)(Volkova, Cazer, and Gröhn 2017).

The PK model used in this part is represented by a single central compartment with an extravascular administration associated to 3 PK parameters: V, volume of distribution, ka, rate of absorption and k, rate of elimination to described concentration (C) along time for different dosage regimen.

For the purpose of our study, we establish a set of ordinary differential equations to describe the growth of bacteria and describing the transfer rate of plasmids, the segregation rate of them during replication and their fitness cost (

Table 1, Equations 1-5). These equations take into account a logistic growth in the compartment. For the simulation of the effect of the drug on the growth rate of bacteria, we use pharmacodynamic model based on a hill function for the effect of the antimicrobial on the 2 bacterial populations (

Table 1, Equations, 6 and 7). The multiplicative effect on the growth is adapted to antimicrobials active only on growing bacteria such as beta-lactams.

#	Equation	Description
1	$\frac{dB_s}{dt} = G_s \times B_S \times K_S - tr \times B_R \times B_s + sg * G_R * B_r$	Growth of susceptible population B_S with loss due to transfer of plasmid (tr), gain of segregated resistant cells (sg) and antimicrobial effect (K_S)
2	$\frac{dB_R}{dt} = G_R \times B_R \times K_R + tr \times B_R \times B_s - sg * G_R * B_r$	Growth of resistant population B_R with gain due to transfer of plasmid (tr), loss of segregated resistant cells (sg) and antimicrobial effect (K_R)
3	$G_s = g \times \left(1 - \frac{B}{Bmax}\right)$	Logistic growth of B_S, limited by the carrying capacity in the compartment Bmax
4	$G_R = g \times (1 - FC) * \left(1 - \frac{B}{Bmax}\right)$	Logistic growth of B_R, limited by the carrying capacity in the compartment Bmax and a plasmid fitness cost (FC)
5	$B = B_S + B_R$	Total bacterial population
6	$K_S = \left(1 - KK_S \times \left(\frac{C^\gamma}{CS50^\gamma + C^\gamma}\right)\right)$	Antimicrobial effect on growth rate according antimicrobial concentration C, CS50 (concentration to obtain 50 % of the maximal killing effect KK_S on susceptible population)
7	$K_R = \left(1 - KK_R \times \left(\frac{C^\gamma}{CR50^\gamma + C^\gamma}\right)\right)$	Antimicrobial effect on growth rate according antimicrobial concentration C, CR50 (concentration to obtain 50 % of the maximal killing effect KK_R on resistant population)

Table 1 : Equations of the PD part of the PKPD model of clonal dissemination

The model can be used to investigate the effect of different dosage regimens on the selection of resistance in function of the bacterial parameters of HGT. Different conditions have been fixed such as the initial proportion of bacteria at the start of treatment, dosage regimen (dose, number and interval), pharmacokinetic and pharmacodynamic parameters (*Table 2*). Rmarkdown reports were generated to investigate the influence of parameters on the development of resistance (see annexes for some examples).

Parameter Class	Parameter	Definition	Value	Unit
PK	F	Fraction absorbed	1	Unitless
PK	Ka	Absorption rate	1, 0.1	h^{-1}
PK	K	Elimination rate	0.1, 0.01	h^{-1}
PK	V	Volume of distribution	1	L/Kg
Bacteria	Bo	Initial Bacterial population without plasmid	10^6	Bacteria/ml
Bacteria	Bop	Initial Bacterial population with plasmid of resistance	10^4	Bacteria/ml
Bacteria	BM	Maximal population	10^6	Bacteria/ml
PD	CS50	concentration to obtain 50 % of the maximal killing effect KK_S on susceptible population	1	mg/L
PD	CR50	concentration to obtain 50 % of the maximal killing effect KK_R on resistant population	8	mg/L
PD	Gamma	Gamma	1	Unitless
PD	KKs	Killing rate for susceptible population	2 X Growth rate	h^{-1}
PD	KKr	Killing rate for susceptible population	2 X Growth rate	h^{-1}

Table 2 : Fixed conditions tested in the PKPD model of clonal dissemination

4.5. Pattern analysis and software

To study the relationship between bacteriological parameters and the development of resistance in fixed condition of exposure, we performed Monte Carlo Simulations only for the 4 following microbial parameters: growth, plasmid transfer, segregation rate and fitness cost *Table 3*.

Parameter	Definition	Unit	Range	Distribution
g	growth rate	h-1	0.5 - 1	Uniform
Tr	transfer rate	ml $cell^{-1}h^{-1}$	10^{-20} – 10^{-7}	Log Uniform
Sg	segregation rate	h^{-1}	0.01 – 0.3	Log Uniform
FC	Fitness cost	Unitless	0-0.1	Uniform

Table 3 : Microbial parameters and their probability distribution for Monte Carlo simulation

To analyse the different patterns, we developed a Rmarkdown (Allaire, 2020) process using R with different packages as detailed below

The processing contains the simulation of different randomized bacteriological parameters using Simulx (Lavielle, 2020). The sets of parameter values, leading to a correct simulation, were collected for analysis. The outputs were the size of the two bacterial populations and the percentage of resistance observed over time.

During the development of the processing, problems in simulation were identified for a part of the generated parameters. After a filtering of the outputs, we performed the statistical analysis on the valid simulation outputs.

Pattern analysis and clustering of the time series of resistance along time were performed using the package dtwclust (Sardá-Espinosa 2019) and the function tclust. The type of clustering is 'partitional'. The number of pattern cluster is set at 9. The different classes of patterns were graphically reported. The distribution of the different parameters and the values of resistance at different time according to the pattern were analysed.

A factorial analysis (Partial Component Analysis) using the package FactomineR (Sebastien, 2008) studies the correlation between resistance and bacteriological parameters.

4.6. Results

4.6.1. No antibiotic

The clusters (*Figure 20*A) lead to 100 % of resistance (1, 5, 9), high level of resistance (3), intermediate (7) and low level of resistance with slow increase (4), negligible with slow increase (2, 8) or decrease (6).

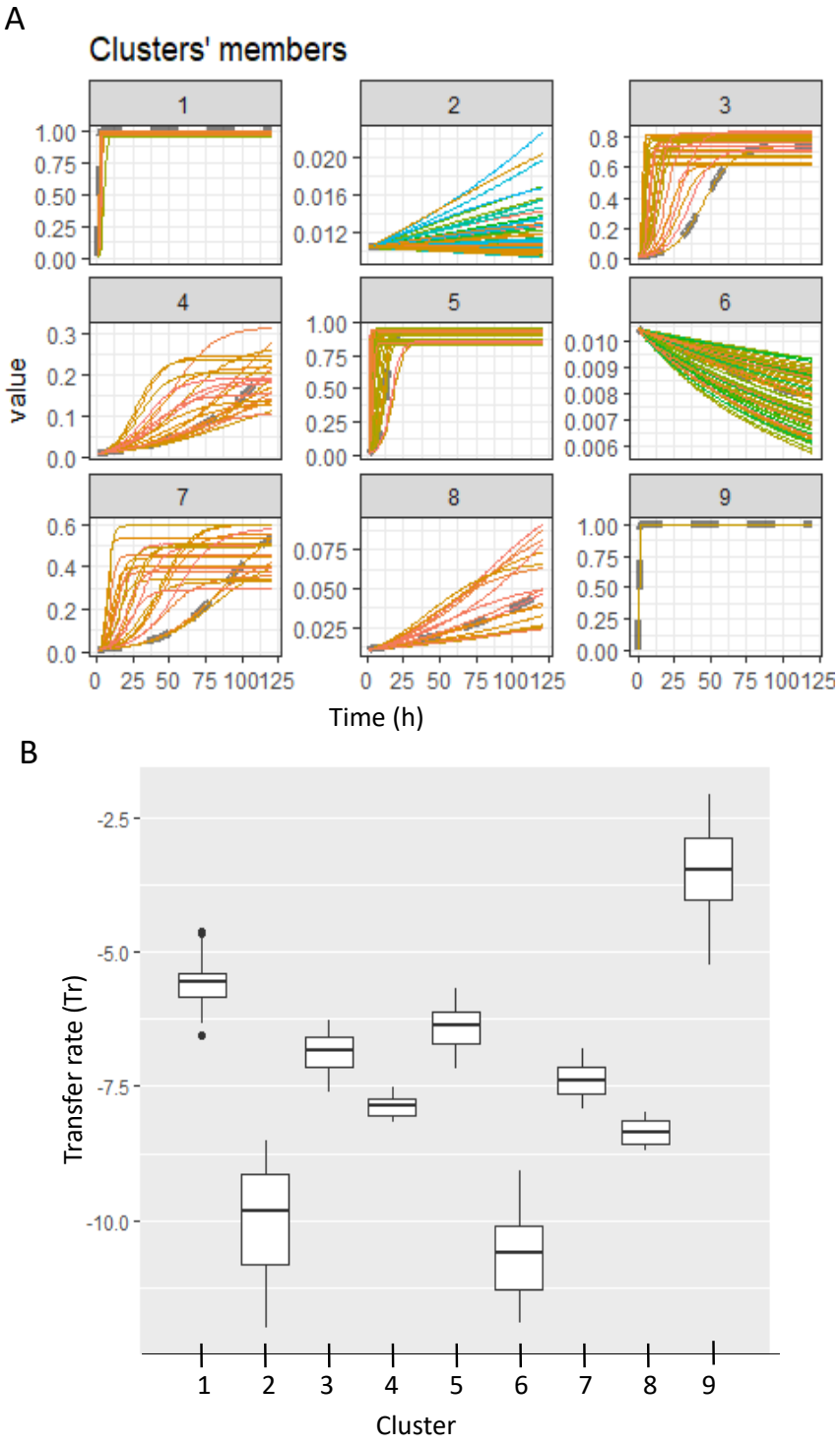

Figure 20 : Clusters' members of antimicrobial resistance evolution (A) and the associated distribution of transfer rate values (B)

A: The cluster were simulated over time (by step of 4 h) in case of no treatment. B : Boxplot of log of transfer rates for the 9 clusters observed in absence of antibiotic.

The pattern are clearly associated to the plasmid transfer rates (expressed as decimal log) (*Figure 20*B). However, fitness cost, growth and segregation rates are not correlated with the development of resistance in absence of antimicrobials as shown by the PCA graph (*Figure 21*).

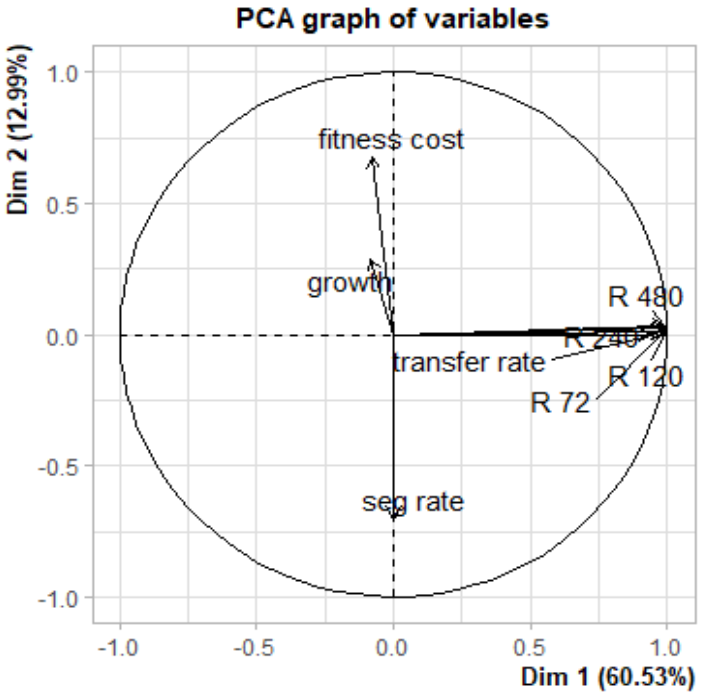

Figure 21 : Partial component analysis of relation between variances and bacterial parameters as explicative variables.
Resistance ratio at 72, 120, 240 and 480 h are reported as observed variables.

4.7. PK and Dosage regimen

The model was then applied with fixed pharmacokinetic parameters (no variability) and different dosage regimens to analyse the influence of bacterial parameters on development of antimicrobial resistance.

4.7.1. Dosing regimen n°1

The first dosing regimen was based on three doses of 10 mg/kg at 24 h interval were simulated to show the effect of a selective pressure on the evolution of the susceptible and resistant populations and development of resistance.

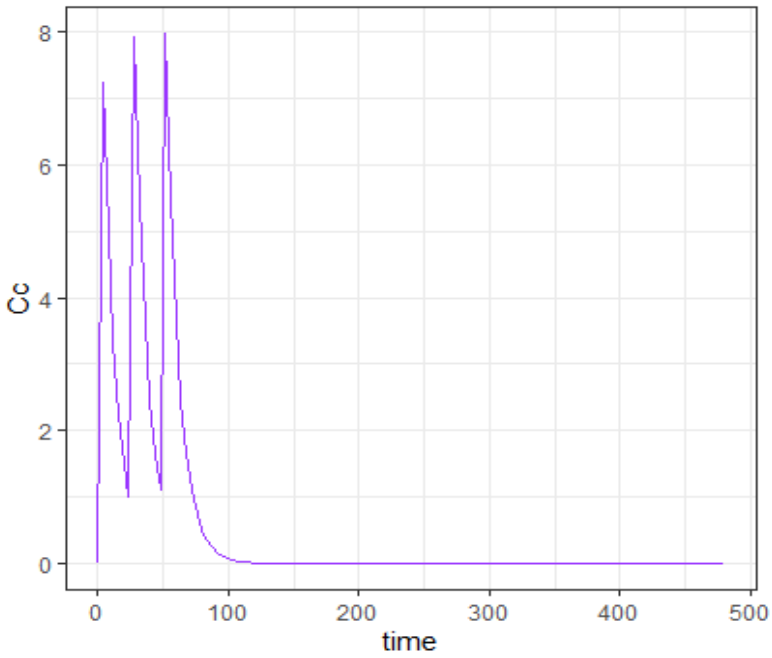

Figure 22 : Antibiotic time-concentration profile with the dosing regimen n°1
Conditions: 3 doses of 10 mg/kg/24h, Ka=1, k=0.1, V=1, F=1 mono-compartmental model with absorption.

The impact of such dosing regimen on the number of resistant and sensitive bacteria is given in *Figure 23*. The impact of the antibiotic treatment is clear with a median resistance ratio close to 100% during the whole treatment period. After the end of treatment, the level of each bacteria greatly varied.

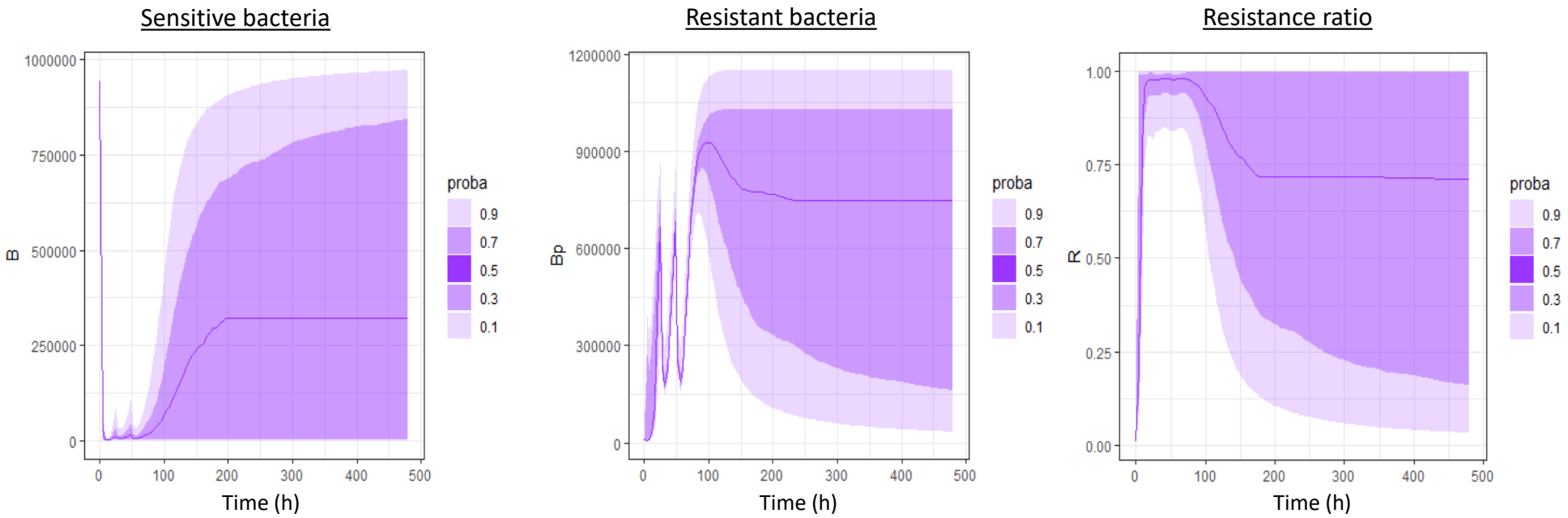

Figure 23 : Percentiles distribution for the Sensitive, Resistant bacteria number and resistance ratio over time with the dosing regimen N°1
Conditions: 3 doses of 10 mg/kg/24h, Ka=1, k=0.1, V=1, F=1 mono-compartmental model with absorption.

The evolution of resistance follows different patterns, as illustrated in the *Figure 24*A. The clusters lead to 100 % of resistance at 48 h that persisted to a value close to 100% until 480h (2, 4, 5, 6), high level of resistance (1,8), medium level (1,7) and low level of resistance (3,9). Again, the patterns were clearly associated to the plasmid transfer rates (expressed as decimal log, *Figure 24*B) with high value associated to high level of resistance. On the contrary, high value of segregation rate were associated to the loss of resistance along time (9) (*Figure 24*C). These relations were confirmed by the PCA analysis (*Figure 25*).

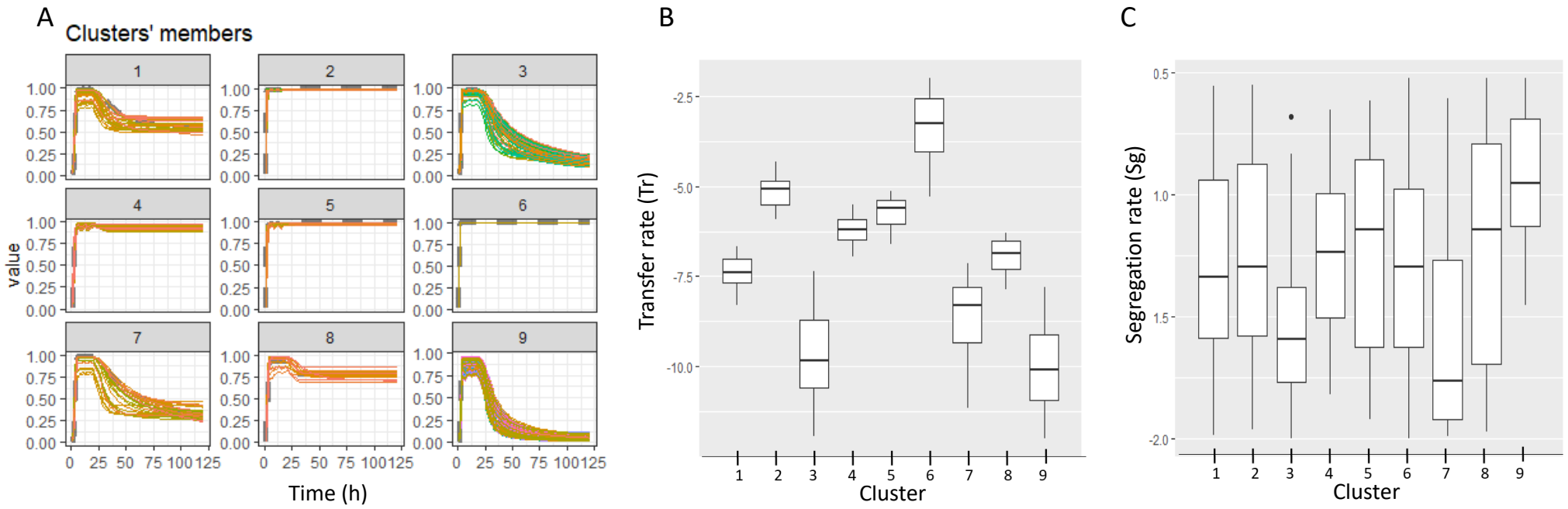

Figure 24 : Clusters' members of antimicrobial resistance evolution (A) and the associated distribution of transfer rate values (B) and segregation rate (C).
A: The cluster were simulated over time (by step of 4 h) with the following treatment: 3 doses of 10 mg/kg/24h, Ka=1, k=0.1, V=1, F=1 mono-compartmental model with absorption. B and C : Boxplot of log of transfer rates and segregation rate (respectively) for the 9 clusters;

According to this PCA analysis, the fitness cost and growth were also partially correlated with the percentage of resistance at different time points as shown in *Figure 25*.

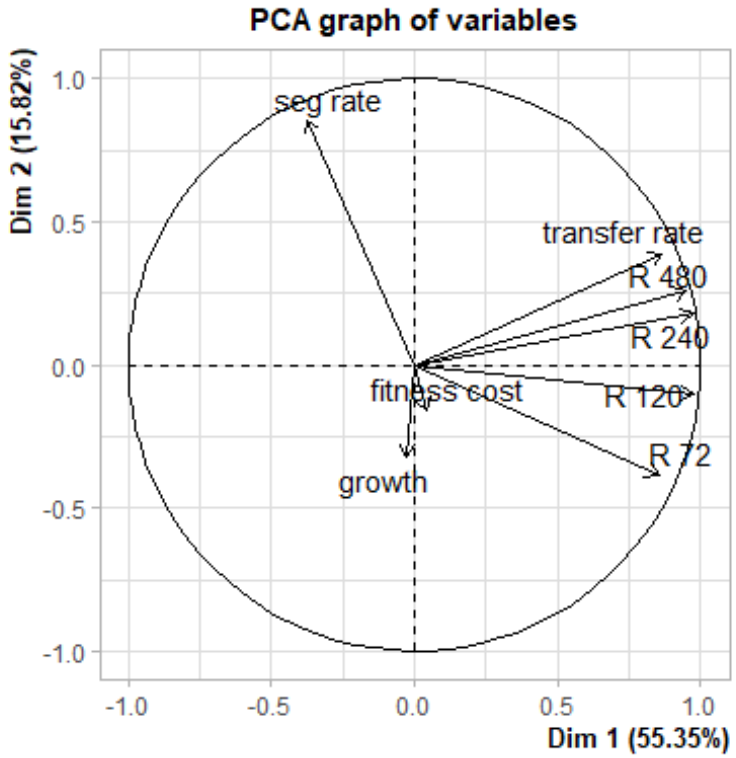

Figure 25 : Partial component analysis of relation between variances and bacterial parameters as explicative variables for the design regimen n°1.
Resistance ratio at 72, 120, 240 and 480 h are reported as observed variables.

4.7.2. Dosing regimen n°2

The second dosing regimen included five doses of 10 mg/kg at 24 h interval (*Figure 26*) to simulate the effect of a longer treatment on the selective pressure of the susceptible and resistant populations and development of resistance (*Figure 27*)

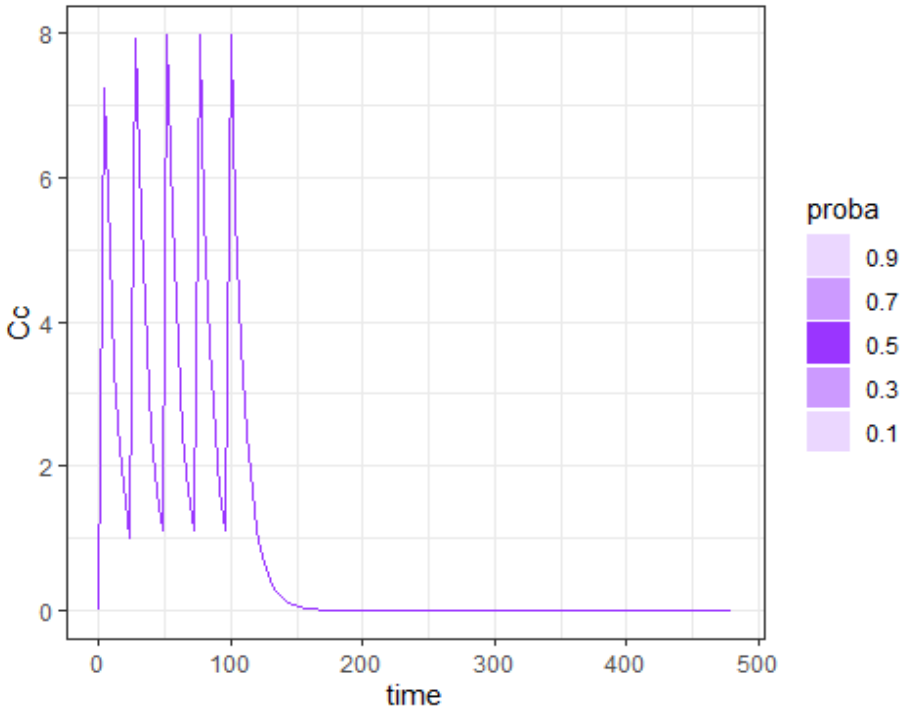

Figure 26 : Antibiotic time-concentration profile with the dosing regimen n°2

Conditions: 5 doses of 10 mg/kg/24h, Ka=1, k=0.1, V=1, F=1 mono-compartmental model with absorption)

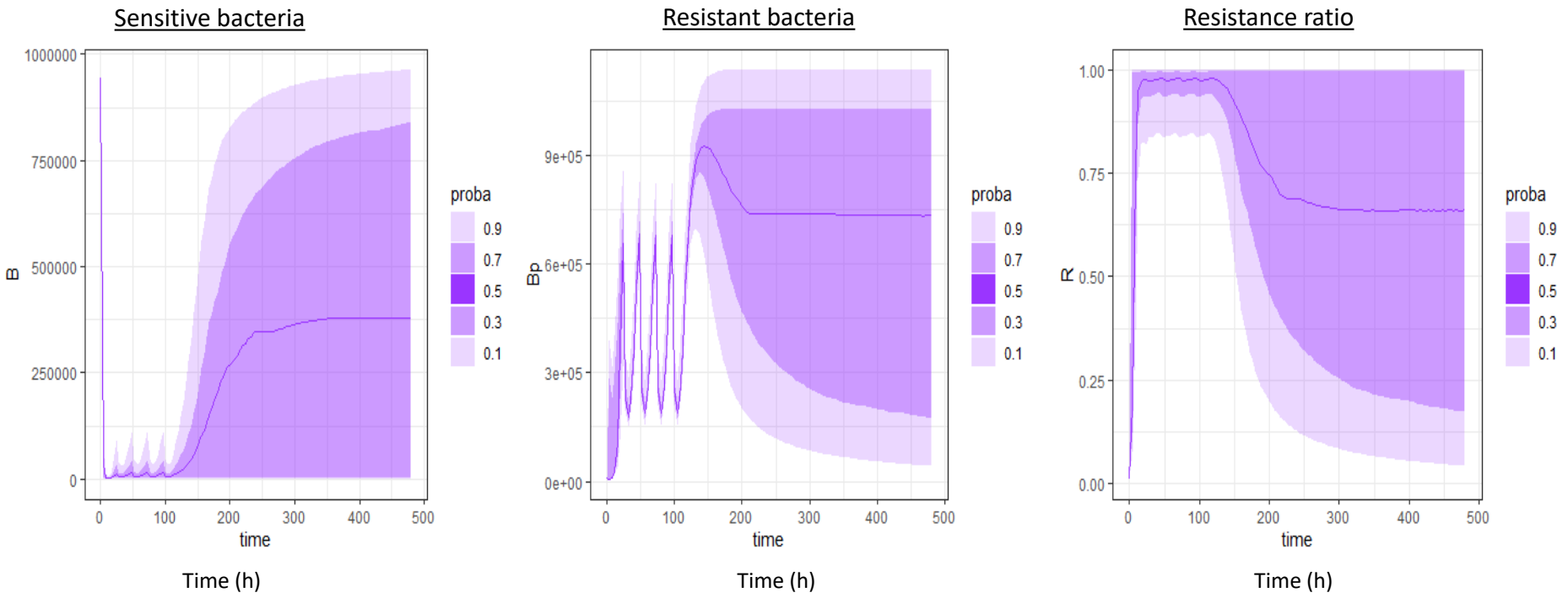

Figure 27 : Percentiles distribution for the Sensitive, Resistant bacteria number and resistance ratio over time with the dosing regimen N°2
Conditions: 5 doses of 10 mg/kg/24h, Ka=1, k=0.1, V=1, F=1 mono-compartmental model with absorption.

As for the first dosing regimen, the evolution of resistance follows different patterns. The clusters lead to 100 % of resistance at 48 h followed by high levels of resistance until 480h (1, 2, 3), high level of resistance (4, 6), medium level (7) and low levels of resistance (5,8,9). The patterns were still clearly associated to the plasmid transfer rates and segregation rate values, with a positive correlation between level of resistance and plasmid transfer and a negative correlation with the segregation rates (*Figure 28* B,C).

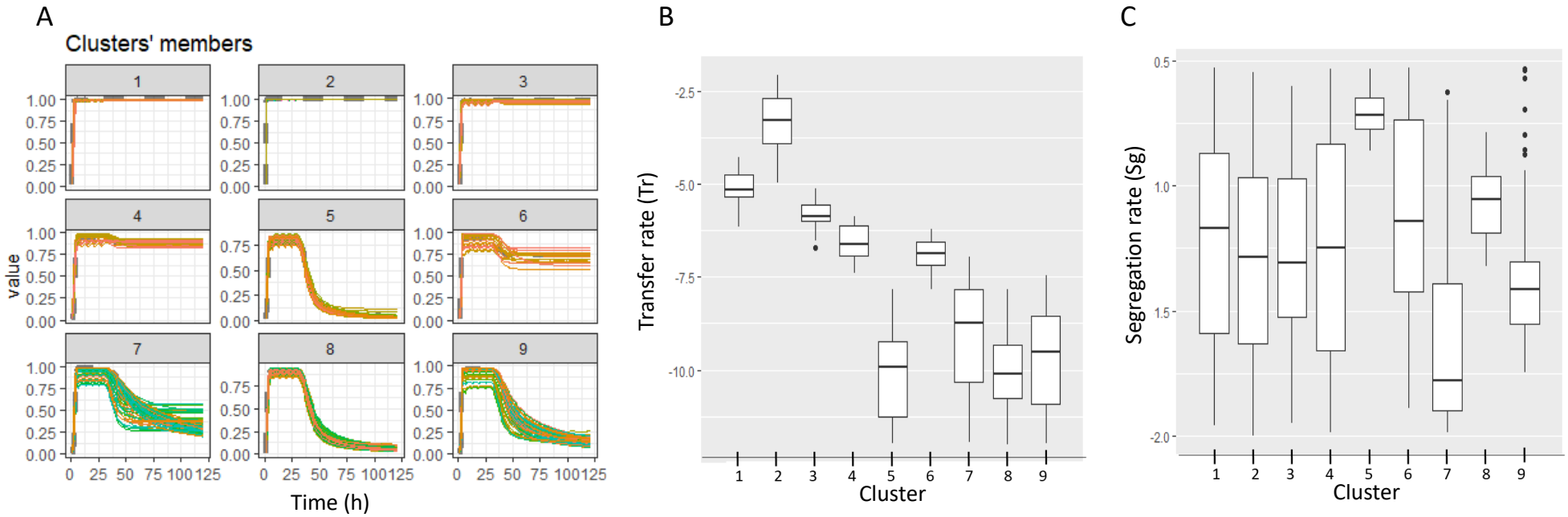

Figure 28 : Clusters' members of antimicrobial resistance evolution (A) and the associated distribution of transfer rate values (B) and segregation rate (C).
A: The cluster were simulated over time (by step of 4 h) with the following treatment: 5 doses of 10 mg/kg/24h, Ka=1, k=0.1, V=1, F=1 mono-compartmental model with absorption. B and C : Boxplot of log of transfer rates and segregation rate (respectively) for the 9 clusters;

According to the PCA analysis, the fitness cost and growth were not correlated with the percentage of resistance at different time points as shown in *Figure 29*.

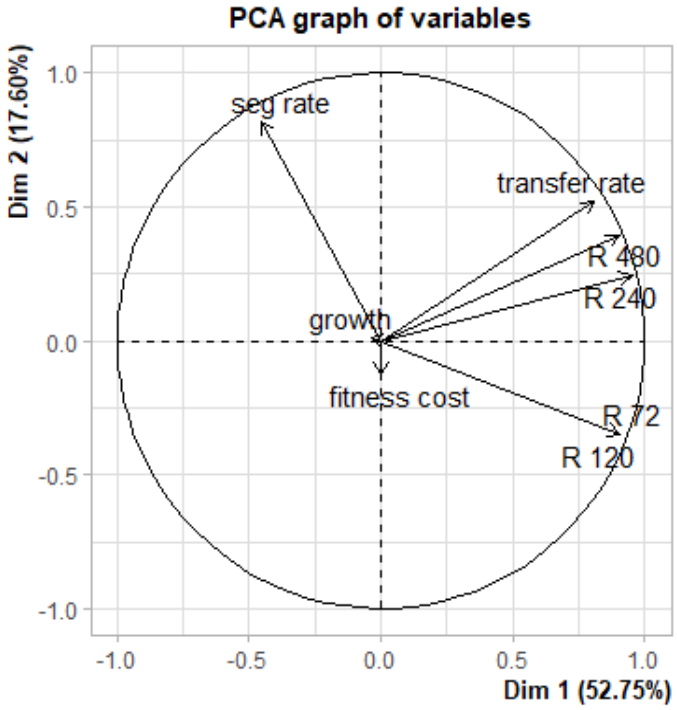

Figure 29 : Partial component analysis of relation between variances and bacterial parameters as explicative variables for the design regimen n°2.
Resistance ratio at 72, 120, 240 and 480 h are reported as observed variables.

4.7.3. Dosing regimen n°3

For the last dosing regimen, three doses of 1 mg/kg at 24 h interval associated to a low clearance value and slow absorption rate (Ka= 0.1, k=0.01) that lead to accumulation of the antibiotic were simulated (*Figure 30*) to show the effect of long term selective pressure on the evolution of the susceptible and resistant populations and development of resistance.

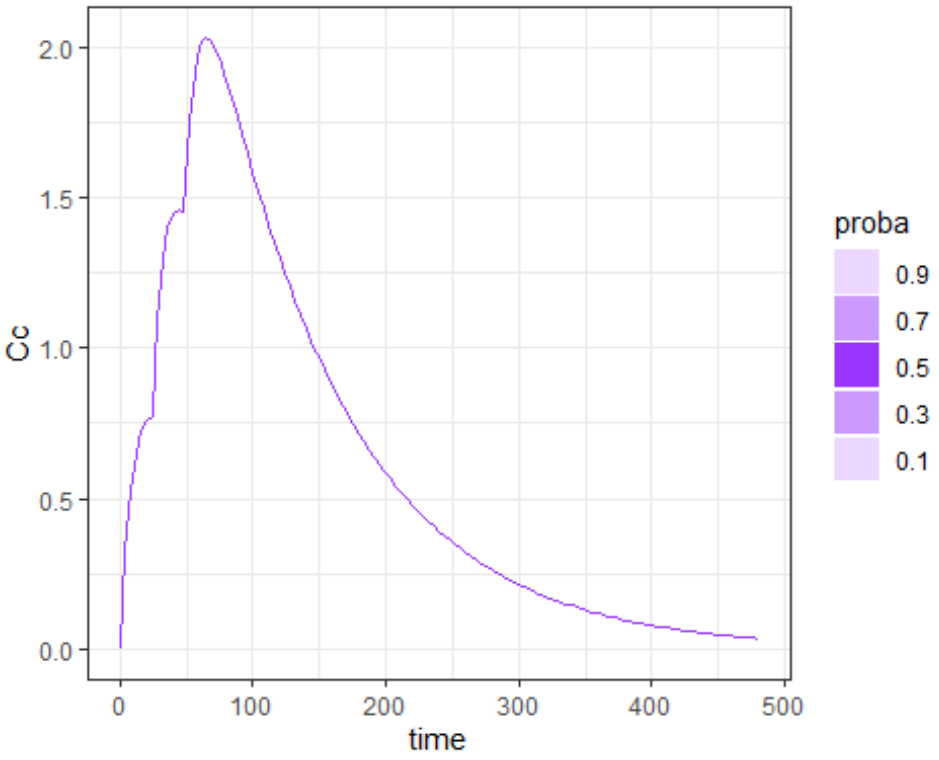

Figure 30 : Antibiotic time-concentration profile with the dosing regimen n°2

Conditions: 3 doses 1 mg/kg/24h, Ka=0.1, k=0.01, V=1, F=1 mono-compartmental model with absorption)

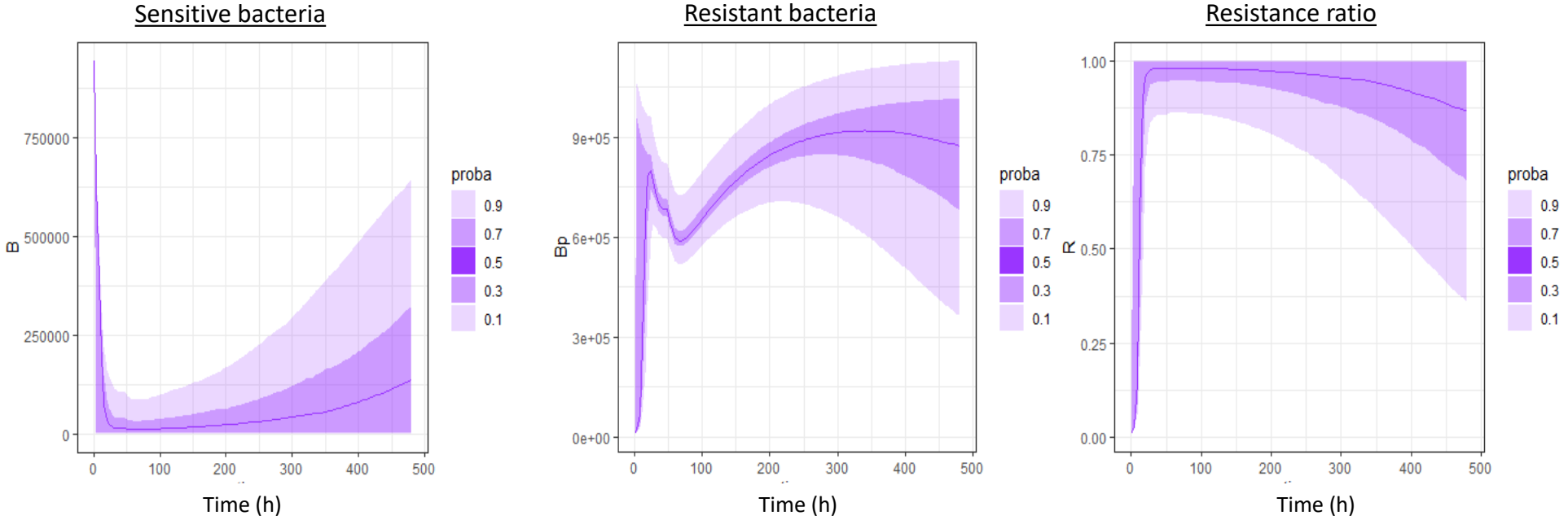

Figure 31 : Percentiles distribution for the Sensitive, Resistant bacteria number and resistance ratio over time with the dosing regimen N°3
Conditions: 3 doses 1 mg/kg/24h, Ka=0.1, k=0.01, V=1, F=1 mono-compartmental model with absorption)

The evolution of resistance follows different patterns but with less diversity than for the other dosing regimens (*Figure 32* A). The clusters lead to 100 % of resistance at 96 h followed by high levels of resistance until 480h (1, 2, 3, 5, 7), high level of resistance (6), medium level (8, 9).

As seen with the other dosing regimens, the clusters were associated to the value of the log transfer rate with high value associated to high level of resistance (*Figure 32* B) while high value of segregation rate were associated to the loss of resistance along time (*Figure 32* BC. According to the PCA analysis, the fitness cost and growth rate are partially correlated with the percentage of resistance at different time points (*Figure 33*).

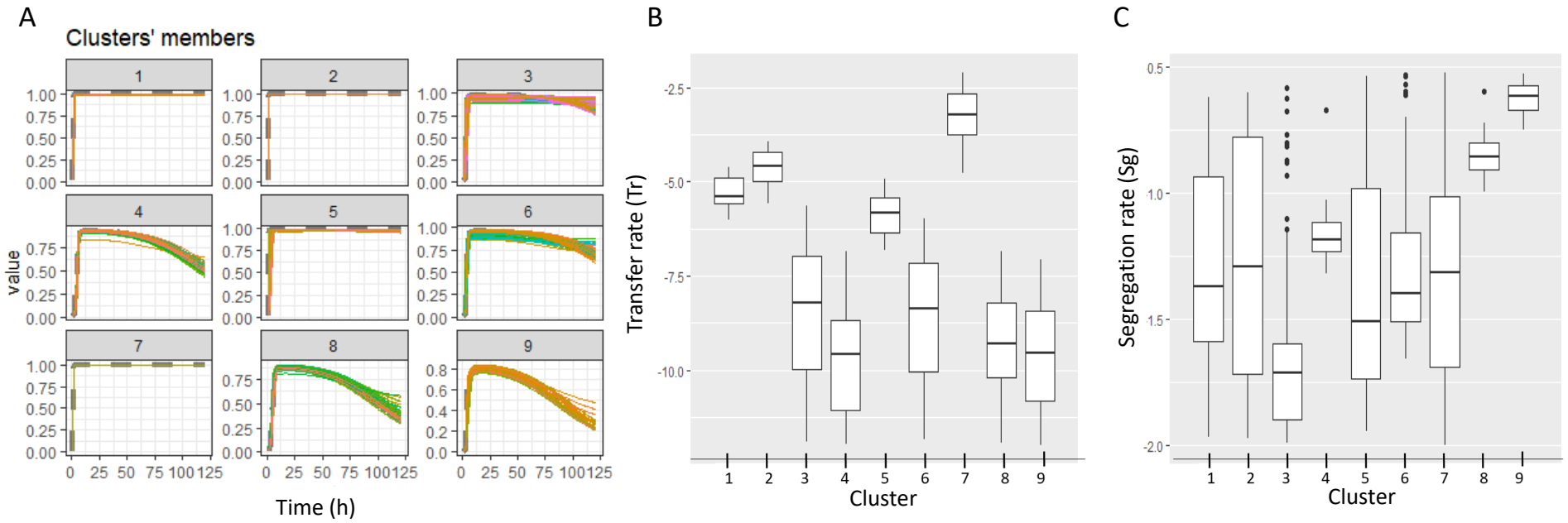

Figure 32 : Clusters' members of antimicrobial resistance evolution (A) and the associated distribution of transfer rate values (B) and segregation rate (C).
A: The cluster were simulated over time (by step of 4 h) with the following treatment: 3 doses 1 mg/kg/24h, Ka=0.1, k=0.01, V=1, F=1 mono-compartmental model with absorption. B and C : Boxplot of log of transfer rates and segregation rate (respectively) for the 9 clusters;

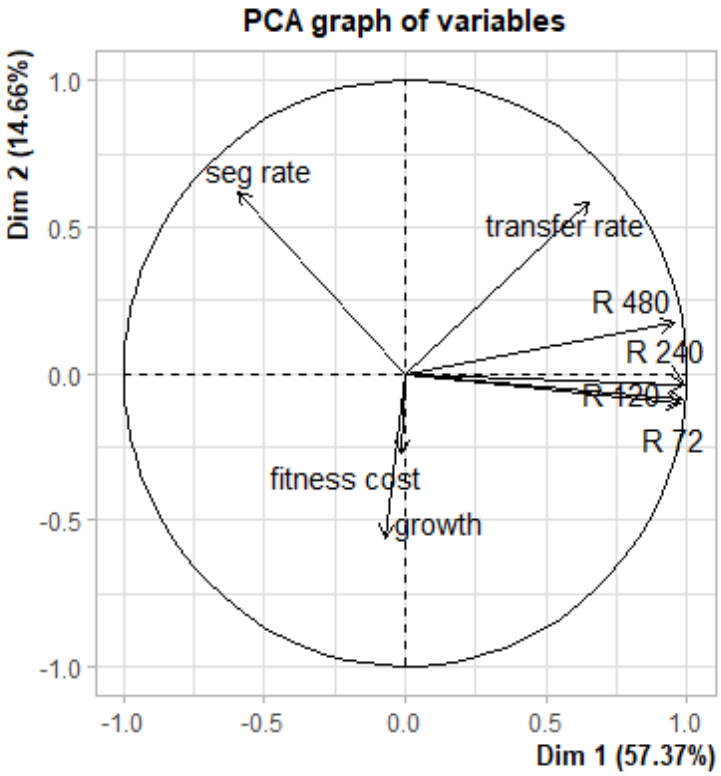

Figure 33 : Partial component analysis of relation between variances and bacterial parameters as explicative variables for the design regimen n°3.
Resistance ratio at 72, 120, 240 and 480 h are reported as observed variables.

4.8. Discussion about the clone dissemination

The modelling approach and analysis workflow were inspired by the work done previously by the team of Volkova (Cazer, Volkova, and Gröhn 2018; 2014). For our study, we limit our analysis on the effect of bacterial parameters describing horizontal gene transfer on the selection of resistance. We choose to test the influence of the combination of parameters on resistance selection by the use of clustering approach adapted to time series and recently provided as R Package (Sardá-Espinosa 2019).

To assess the influence of the bacterial parameters on the different patterns, we analyse the distribution of the log value of the plasmid transfer, growth and plasmid segregation rates and the value of the fitness cost. The range of value tested were closed to those reported in a similar study simulating evolution of antimicrobial resistance in humans (Tepekule et al. 2019). In fixed conditions of antibiotic exposure, the most important parameters were always the plasmid transfer and segregation rates (*Figure 25*, *Figure 29*, *Figure 33*). Their combination explains the type of equilibrium reached after an antimicrobial selective pressure period as well as the equilibrium reached over time after introduction of a resistant population without any selective pressure. Our results are similar to those recently reported about the influence of HGT on the development of resistance in different

conditions of selective pressure (Lopatkin et al. 2017) who had investigated *in vitro* the persistence of plasmids. They developed some models to take into account different hosts with different bacterial properties. Our modelling approach is able to combine three model layers, PK, Bacterial and PD to investigate the effect of variability of the different parameters on the development of resistance. The influence of each layers can be independently simulated as fixed or under random conditions, as seen with the full PKPD model in pigs (see part. 3).

The use of time pattern clustering allow us to classified easily the different patterns leading to different level of resistance (*Figure 24*, *Figure 28*,*Figure 32*) and to analyse their relation with the variance by partial component analysis (*Figure 25*, *Figure 29*, *Figure 33*). Overall this modelling approach combined with a statistical analysis of the patterns of time series offers the opportunity to move forward in the research of synergy between plasmid-curing compounds and conjugation inhibitors as antibiotic adjuvant as suggested by different authors (Lopatkin et al. 2017; Hernando-Amado et al. 2019; Baquero 2011). It offers also the opportunity to develop more complex models able to describe the ecological inter-relation between bacterial species in the microbiota in order to get a better assessment of the impacts of antimicrobial treatments (Ruppé et al. 2019, Burdet et al. 2019).

5. General discussion

5.1. Gaps to develop mechanistic PKPD models

There is a need of a better understanding of the mechanism that contribute to the spread of antimicrobial resistance in farm animals in order to limit and control this risk. Therefore, mechanistic models were developed in order to describe these phenomena and hence, find which relevant policy measure could be taken. The main aim of the generic PKPD model developed in this work was to include a relevant pharmacokinetic part and find which factors are the most important in the selection of resistant bacteria.

Our results explored the influence of the route of administration on the actual exposure of intestinal bacteria, but also highlighted the most influential bacterial parameters that lead to the development of resistance. As outlined in this recent review, there are only few model that take into account the PK at the host level and the bacterial/PD part simultaneously (Birkegård*, et al.*, 2018).

However, we could identify several gaps that prevent the development of robust PKPD models of AMR (Birkegård*, et al.*, 2018; Knight*, et al.*, 2019; Leclerc*, et al.*, 2019; Niewiadomska*, et al.*, 2019) :

- As for many of antimicrobial resistance model previously published, these models are based on parameters values that are either empirically derived or based on a simplification/extrapolation of published values that may not always be relevant (Birkegård*, et al.*, 2018; Knight*, et al.*, 2019). As an example, a recent meta-analysis about conjugation frequencies from *Escherichia coli* highlighted the impact of different factors like the temperature, the type of media (liquid/solid), etc… (Alderliesten*, et al.*, 2020). As a consequence, they reported conjugation frequencies with a variation over 11 orders of magnitude ($4.5.10^{-11}$ – 2.1)(Alderliesten*, et al.*, 2020). Moreover, some experimental conditions are far from the reality and it may be erroneous to derive conclusions based on their results. For instance, bacterial interaction are often studied in liquid culture assays whereas bacteria are very often in dense community on solid media (Frost*, et al.*, 2018). There is a need to further study the bacterial interactions (competition/cooperation with the space dimension), between sensitive and resistant strains of the same species, especially in a complex environment as the gut microbiota. Recent studies showed surprising results : antibiotic treatment may select against antibiotic-resistant strains, by promoting the competition towards sensitive cell because the resistance mechanism, for instance beta-lactamase produced by resistant strains that protect the sensitive ones (Frost, et al., 2018). This is definitively a major limiting factor for the predictive ability of these models because we showed that these parameters are the most influential in the outcome of resistance spread (see part 4.)

- The complexity to develop a realistic digestive PK model: huge variability/heterogeneity between literature data, because of the differences of the study design (different breed of pigs/weight/age/ fasted or not…) (Tan*, et al.*, 2016) but also due to the inherent variability of the transit rate within digestive tract between individuals (Kostewicz*, et al.*, 2014). The impact of the type of food/meal is also important on the variability of the digesta flow, and this has been shown even with indigestible markers (Jacobs*, et al.*, 2017). To get a more precise view of the impact of antimicrobial within microbiota, more mechanistic model could be used that take into account much more physiological parameter (pH, nutriments concentrations, peristaltic flow(Cremer, et al., 2017),…). However, most PBPK models of the digestive tract that were developed for human are focused on the oral absorption processes rather than the local impact of drug on the microbiota.

- The need of (external) observed data to validate the model although it is more difficult to carry-out in vivo experiments, compared to *in vitro* experiments, due to financial and ethical reasons. This is the main limitation to most of all published models which a lack of real validation

(predictions without confronting real data). Again, the methods of measurement/collections of the observed data is fundamental. The best would be to get individual longitudinal data, in order to characterize properly the intra-individual variability. For instance, concerning the resistant bacteria within intestinal/fecal samples, it is often only pooled samples from several animals at few different time points. However, one study showed that the sampling times influence the variability in antimicrobial resistance (expressed in fecal *E. coli*) more than the within-animal diversity in pig faeces (Brun*, et al.*, 2002). The question of the representativeness of the intestinal concentration of antibiotic by assaying faecal sample is also raised. As the colon is the site of water reabsorption all along its tract, it may increase the concentration of antibiotic at the end and therefore we may overestimate the actual exposure of intestinal bacteria to antibiotic. Nevertheless, it remains an easy and non-invasive way of exploring the digestive antimicrobial concentration evolution.

5.2. The persistence of antimicrobial resistance

The use of ATB is known to be a driver of emergence/selection of ATBR but the opposite is not always true. Indeed, the prudent use or the cessation of use of ATB will not always lead to a decrease of antibiotic resistance (Christaki*, et al.*, 2019). Several reasons were given by Christaki et al, in order to explain this phenomena:

- Compensatory mutations which restore the fitness of antibiotic-resistant bacteria and thus which help the se bacteria to compete with sensitive ones.

- Plasmid acquisitions which are fitness cost-free for the resistant bacteria (and sometimes also for chromosomal mutations)

- Co-selection with other resistance gene, especially due to the fact that plasmid often harbour multi-resistance genes

- Plasmid stability mechanisms (Wein*, et al.*, 2019)

Some authors used a modelling approach to outline the importance of bacterial persistence in the evolution of antibiotic resistance (Windels*, et al.*, 2019). However, their main goal was to give a supportive framework of their hypothesis, thus they used parameters values which are not specific for any antibiotic-strain combination. As a consequence, it is quite difficult to re-use this kind of model without the relevant parameters values. Again, the increase of data collection should help the future improvements of these models.

Another interesting phenomena is the collateral sensitivity, a process in which a bacteria strain becomes hypersensitive to an antibiotic A meanwhile she becomes resistant to antibiotic B. This may happen for some particular antibiotic couple due to opposite effect of the mutations associated to the resistance mechanisms for each antibiotic. Therefore, it is hypothesized that alternating between drug A and drug B over time will help to limit the risk of ATB-R. A recent PKPD model was published to explore this feature (Udekwu, Weiss, 2018) but was not validated against experimental observed data. This should be further developed in order to manage the use of antibiotic within farms where the same molecules are frequently used.

5.3. The immune system

Several authors have already included the immune system in their PKPD model (Ankomah, Levin, 2014; Gjini, Brito, 2016). These papers highlight the importance of the immune component to control the bacterial load within infection sites. However, these models only apply to acute infection (with existence of a population of resistant bacteria), a situation where a clear involvement of the immune response is expected. In our case for amoxicillin, the gut microbiota is not the primary site of infection and thus the immune response should not be a major factor affecting the response to the treatment. Moreover, it would be quite difficult to model the immune response within gut due to the complexity of this organ and the importance of the spatial dimension in the different segment. Some model were developed, for instance to describe the infection by *Helicobacter pilori* within gastric mucosa and the associated immune response (Verma*, et al.*, 2019). However, to our knowledge, none of them is a PKPD model which takes into account the effect of antibiotic, immune response and the gut microbiota.

6. CONCLUSION

This work highlighted the different tools and methods that exist but also the numerous gaps to develop a mechanistic PKPD model of antimicrobial resistance within guts. Our work outlined the relative importance of the inherent variability of each PK and PD sub-levels for the understanding of the evolution of bacterial populations toward resistance development/selection after a perturbation due to an AMD. The influence of specific bacterial parameters on the plasmid dynamism and its influence on the selection, maintenance or disappearance of resistance could be independent of the initial exposition.

This work outlined that the mechanistic modelling of the digestive tract is still challenging and should be improved but will probably need additional data. Some very mechanistic models of digestion and food transit have already been published but are sometimes theoretical with parameters values not based on experimental measures (Taghipoor*, et al.*, 2014). The complexity of such model will definitively need inter-disciplinary approach combining mathematicians and pharmacologist/biologists.

For the PD model, our simulations focused only on one bacterial specie, *E. coli*, and the different case scenario outlined the need to get a better understanding of the bacterial interactions within specie (Davies*, et al.*, 2019). Indeed, these interactions/competitions between strains are likely a major key that affects the dynamics of resistance evolution (Knight*, et al.*, 2019). However, the inter-specie transmission of AMR should also be considered (Leclerc*, et al.*, 2019) and the development of more complex model including the whole microbiota is currently an ongoing research topic (Cremer*, et al.*, 2017; Ruppé*, et al.*, 2019) and it will probably be possible within the next years to include ecological models inside the PKPD models.

7. ANNEXES

7.1. ANNEXE 1

Table 4 : Published PKPD models for swine intestinal microbiota

PK model	PD model	Used observed data	Modeling method	Type of validation	References
Digestive tract represented as one Compartment for ciprofloxacin *(compartmental/empirical approach)*	2 populations (R and S). Strains: *E. coli*	Faecal data of ciprofloxacin concentrations and count of R population and total (S+R)	Parameter estimations with NLME model based on observed data	Internal validation	(Nguyen, *et al.*, 2014)
Constant intestinal concentration of tetracycline over the duration of treatment.	Multiple strains of *E. coli* (until 20 per pig), mix of R and S.	No observed data	Pure simulations (MC ?) with parameters distributions/values from literature or author's assumptions	None	(Græsbøll, *et al.*, 2014)
Two-compartmental PK-model for tetracycline. Plasma concentration as surrogate.	12 strains of *E. coli* (between 3 and 12 per pig). 1/3 R and 2/3 S	Published plasma data for PK parameters. *In vitro* data for PD parameter.	No information about PK nor PD parameters estimation method. Pure simulations	None	(Ahmad, *et al.*, 2015)
Two-compartmental PK-model for ampicillin. Plasma concentration as surrogate	Multiple strains of *E. coli* (between 3 and 12 per pig). 1/3 R and 2/3 S	Published plasma data for PK parameters *In vitro* data for PD parameter	No information about PK parameters estimation method. Nonlinear least square algorithm for PD parameter. Pure simulations	None	(Ahmad, *et al.*, 2016b)
Two-compartmental PK-model for ampicillin and tetracycline. Plasma concentration as surrogate	10 strains of *E. coli*	Published plasma data for PK parameters *In vitro* data for PD parameter	- No information about PK parameters estimation method. - nonlinear minimizing routine for growth rates then nonlinear minimizing routine for the other PD parameters	None	(Ahmad, *et al.*, 2016a)

7.2. ANNEXE 2 : Rmarkdown code for clone dissemination

Mathematical Model

The pharmacokinetic model corresponds to a single compartment with an extravascular administration with 3 PK parameters: V, volume of distribution, ka, rate of absorption and k, rate of elimination. The bacterial clone is described by its growth rate (g) and the maximal population size (BM). The plasmid carrying a resistance gene is described by its fitness cost (fc), its transmission factor (ltr) and is segregation rate (sg). The antimicrobial killing rate is described by a hill function with a maximal killing rate corresponding to the double of the growth rate, a concentration to reach 50% of the maximum killing rate and a hill factor (gamma or gammap). The susceptible and resistant bacteria differ only by the difference of potency (EC50 and EC50p) and the fitness cost.

The model is coded in mlxtran for simulation by simulx using R.

```
Mymodel<-inlineModel("<MODEL>
[INDIVIDUAL]
                     input={g_min, g_max,ltr_min,ltr_max,fc_min,fc_max,lsg
_min,lsg_max}

                     DEFINITION:
                     g={distribution=uniform, min=g_min, max=g_max}
                     ltr={distribution=uniform, min=ltr_min, max=ltr_max}
                     fc={distribution=uniform, min=fc_min, max=fc_max}
                     lsg={distribution=uniform, min=lsg_min, max=lsg_max}

  [LONGITUDINAL]
input = {ka, V, k, g, Emax, Ec50, gamma,Emaxp,Ec50p,gammap,ltr,fc,Lb0,Lb0p
,LbM,lsg}

PK:
Cc = pkmodel(ka,V,k)

EQUATION:
t0=0
B_0=10^Lb0-10^Lb0p
Bp_0=10^Lb0p
BM=10^LbM
tr=10^ltr
sg=10^lsg
Cg=(Cc^gamma)
Cgp=(Cc^gammap)
ddt_B=g*B*(1-((B+Bp)/BM)-(2*g*Cg/((Ec50^gamma)+Cg)))-tr*B*Bp+sg*g*Bp
ddt_Bp=g*Bp*(1-fc-sg)*(1-((B+Bp)/BM)-(2*g*Cgp/((Ec50p^gammap)+Cgp)))+tr*B*
Bp
B_sat=max(B,1e-6)
Bp_sat=max(Bp,1e-6)
R=Bp_sat/(B_sat+Bp_sat)
")
```

Conditions for simulation

```
Nind<-500
Tsimulation<-c(480)
IntSim<-c(4)
Amount<-c(10)
Ndose<-c(3)
IntDose<-c(24)
ka<-c(1)
k<-c(.1)
V<-c(1)
gmin<-0.5
gmax<-1
LbM<-c(6)
Lb0<-c(5.98)
Lb0p<-c(4)
Emax<-c(2)
Emaxp<-c(2)
EC50<-c(1)
EC50p<-c(8)
Gamma<-c(1)
Gammap<-c(1)
ltr_min<--12
ltr_max<--2
lsg_min<--2
lsg_max<--0.52
fc_min<-0
fc_max<-.1

## [INFO] The lixoftConnectors package has been successfully initialized:
## lixoftConnectors package version -> 2019.1
## Lixoft softwares suite version   -> 2019R1
```

The output value are the concentration, the size of bacterial populations and the fraction of resistance R. The individual parameters g, ltr, sg and fc are recorded.

Clustering analysis of Resistance time series

The resistance time series have been joined to the table containing individual value for bacteriological parameters. Then they are standardized for further analysis by rejection of time series containing negative value or value above 1.

```
## function (x, ...)
## UseMethod("end")
## <bytecode: 0x0000000011fe9aa8>
## <environment: namespace:stats>
```

Pattern analysis and clustering have been performed using the package dtwclust and the function tclust. The type of clustering is 'partitional'. The number of pattern cluster is set at 10.

Figure : Centroid patterns for resistance by cluster

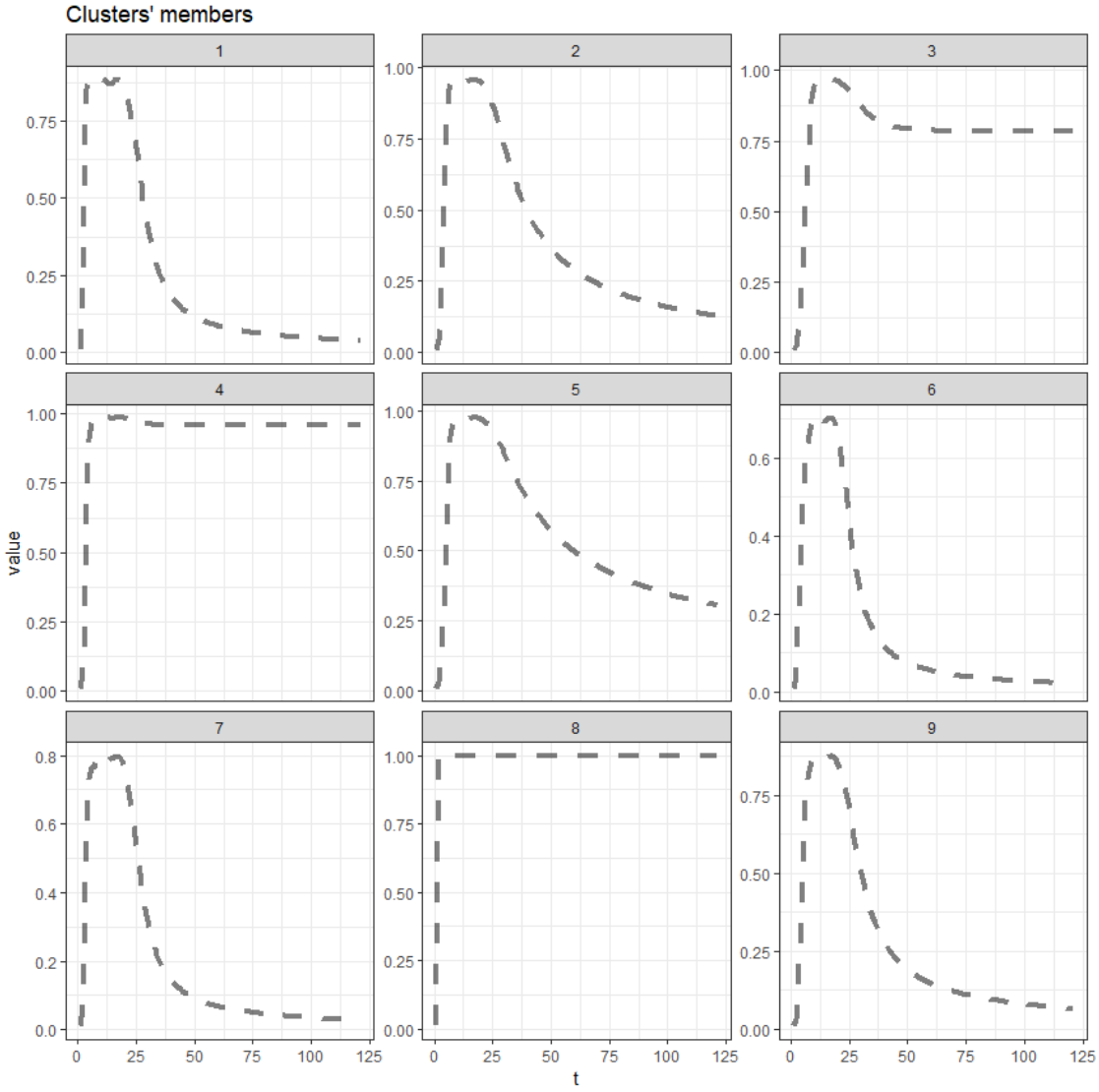

Mean value and standard deviation for the different parameters and resistance levels at 24, 48, 96, 240 and 480 h are summarized in the following tables.

Table : Growth rates (mean, SD) by cluster

cluster	N	moy	sd
1	30	0.88	0.08
2	85	0.76	0.14
3	38	0.75	0.15
4	43	0.71	0.14
5	47	0.74	0.15
6	12	0.69	0.13
7	31	0.77	0.13
8	183	0.75	0.14
9	30	0.70	0.15

Table : Segregation rates (mean, SD) by cluster

cluster	N	moy	sd
1	30	-1.02	0.10
2	85	-1.47	0.25
3	38	-1.27	0.45
4	43	-1.33	0.45
5	47	-1.48	0.42
6	12	-0.62	0.07
7	31	-0.74	0.10
8	183	-1.35	0.42
9	30	-1.13	0.17

Table : Plasmid transfer rates (mean, SD) by cluster

cluster	N	mean	sd
1	30	-10.11	0.91
2	85	-9.82	1.28
3	38	-6.90	0.45
4	43	-6.17	0.52
5	47	-8.52	1.45
6	12	-9.55	0.82
7	31	-10.43	1.11
8	183	-3.89	1.06
9	30	-9.93	1.29

Table : Plasmid costs (Mean, SD) by cluster

cluster	N	Mean	sd
1	30	0.057	0.026
2	85	0.050	0.029
3	38	0.048	0.029
4	43	0.049	0.028
5	47	0.047	0.029
6	12	0.052	0.024
7	31	0.060	0.029
8	183	0.051	0.031
9	30	0.047	0.029

Table : Resistance at 24 h (Mean, SD) by cluster

cluster	N	Mean	sd
1	30	0.877	0.029
2	85	0.908	0.101
3	38	0.898	0.083
4	43	0.957	0.038
5	47	0.890	0.092
6	12	0.615	0.100
7	31	0.737	0.069
8	183	0.998	0.003
9	30	0.806	0.125

Table : Resistance at 48 h (Mean, SD) by cluster

cluster	N	Mean	sd
1	30	0.882	0.026
2	85	0.939	0.052
3	38	0.920	0.060
4	43	0.968	0.019
5	47	0.931	0.063
6	12	0.700	0.035
7	31	0.776	0.028
8	183	0.998	0.003
9	30	0.879	0.048

Table : Resistance at 96 h (Mean, SD) by cluster

cluster	N	Mean	sd
1	30	0.686	0.050
2	85	0.843	0.088
3	38	0.870	0.067
4	43	0.960	0.022
5	47	0.841	0.112
6	12	0.452	0.031
7	31	0.528	0.042
8	183	0.998	0.003
9	30	0.717	0.080

Table : Resistance at 240 h (Mean, SD) by cluster

cluster	N	Mean	sd
1	30	0.094	0.017
2	85	0.268	0.060
3	38	0.775	0.070
4	43	0.949	0.032

5	47	0.443	0.076
6	12	0.060	0.015
7	31	0.066	0.019
8	183	0.999	0.003
9	30	0.149	0.025

Table : Resistance at 480 h (Mean, SD) by cluster

cluster	N	Mean	sd
1	30	0.038	0.008
2	85	0.141	0.040
3	38	0.774	0.071
4	43	0.949	0.032
5	47	0.351	0.119
6	12	0.027	0.010
7	31	0.028	0.011
8	183	0.999	0.003
9	30	0.070	0.014

Factorial analysis

A factorial analysis is performed on the distribution of bacterial parameters.

```
MPCA<-cbind(MPC[,2:5],MR[,19],MR[,31],MR[,61],MR[,121])
vars<-c("growth","transfer rate","seg rate","fitness cost","R 72","R 120",
"R 240","R 480")
colnames(MPCA)<-vars
res.pca<-PCA(MPCA,ncp=5,graph=TRUE)
```

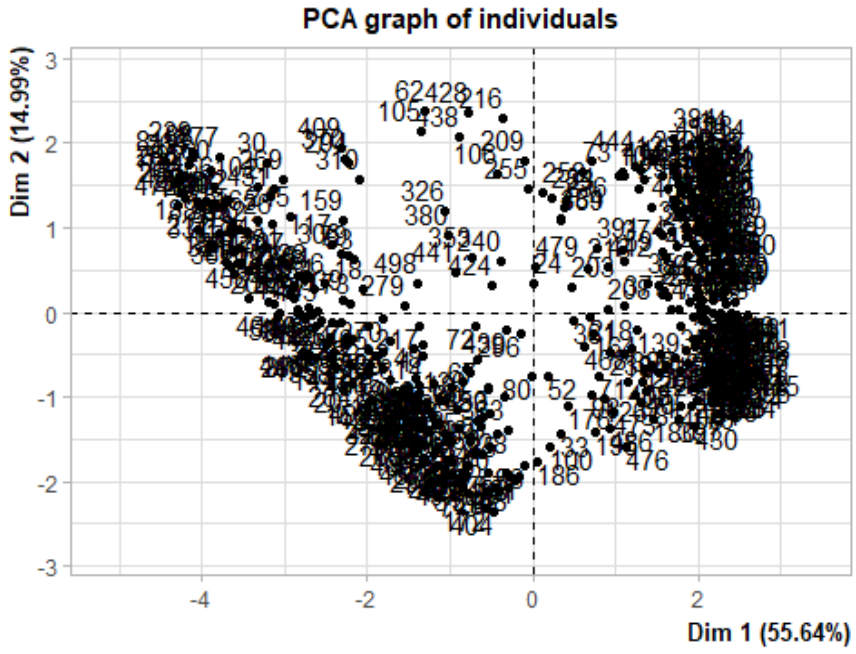
PCA graph of individuals
Dim 2 (14.99%)
Dim 1 (55.64%)

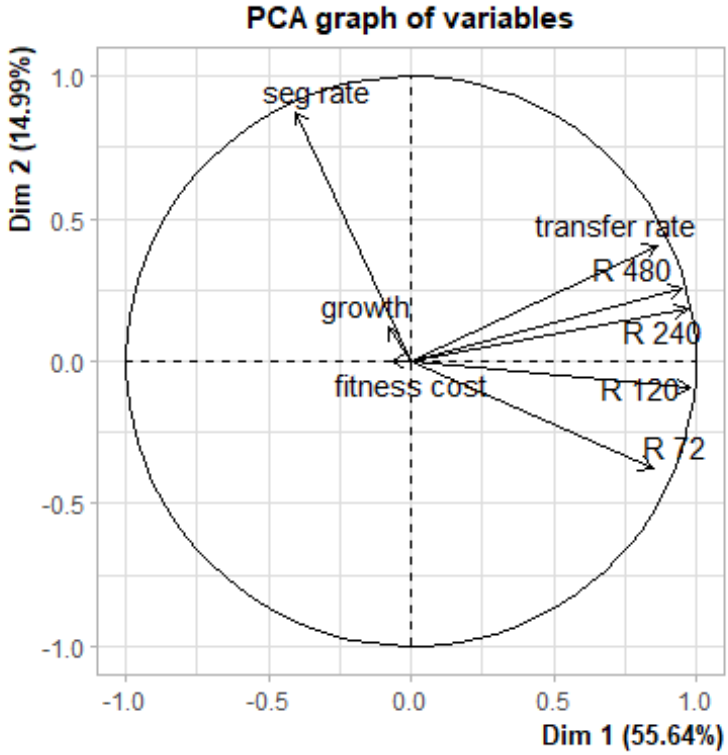
PCA graph of variables
Dim 2 (14.99%)
Dim 1 (55.64%)
seg rate
transfer rate
R 480
growth
R 240
fitness cost
R 120
R 72

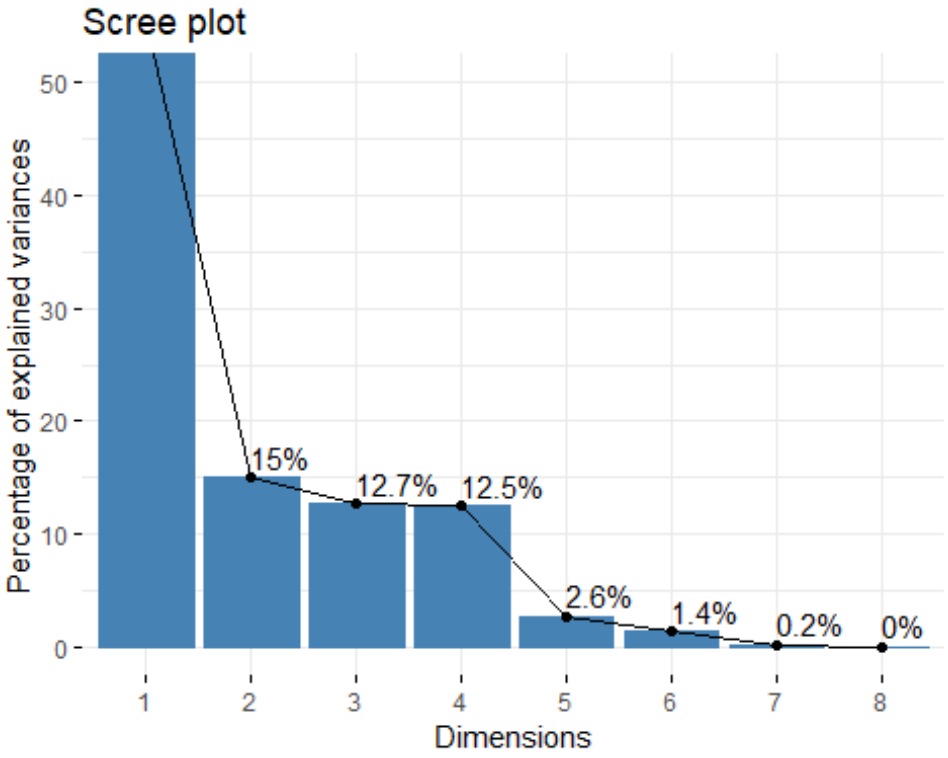
Scree plot
Percentage of explained variances
50
40
30
20
10
0
15%
12.7%
12.5%
2.6%
1.4%
0.2%
0%
1
2
3
4
5
6
7
8
Dimensions

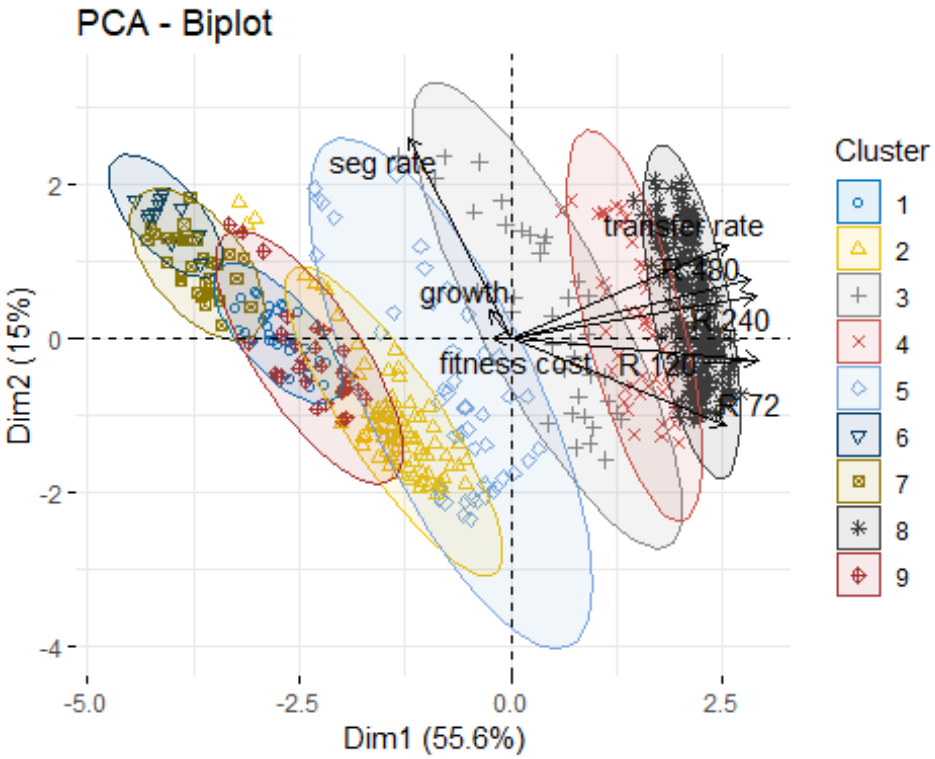
PCA - Biplot
seg rate
transfer rate
R 180
growth
R 240
fitness cost
R 120
R 72
Dim2 (15%)
2
0
-2
-4
-5.0
-2.5
0.0
2.5
Dim1 (55.6%)
Cluster
1
2
3
4
5
6
7
8
9

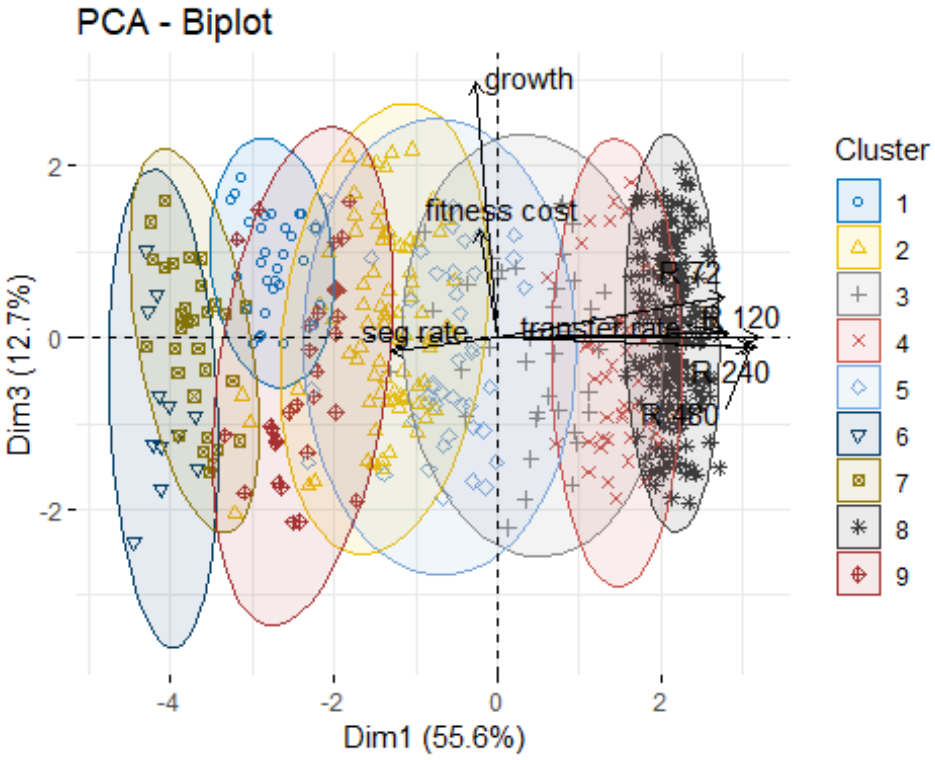
PCA - Biplot
growth
fitness cost
seg rate
transfer rate
R 72
R 120
R 240
R 480
Cluster
1
2
3
4
5
6
7
8
9
Dim3 (12.7%)
Dim1 (55.6%)
2
0
-2
-4
-2
0
2

8. REFERENCES

Agersø, H., Friis, C., 1998a. Penetration of amoxycillin into the respiratory tract tissues and secretions in pigs. Research in veterinary science. 64, 245-250

Agersø, H., Friis, C., 1998b. Bioavailability of amoxycillin in pigs. Journal of veterinary pharmacology and therapeutics. 21, 41-46

Agersø, H., Friis, C., Haugegaard, J., 1998. Water medication of a swine herd with amoxycillin. Journal of veterinary pharmacology and therapeutics. 21, 199-202

Ahmad, A., Græsbøll, K., Christiansen, L.E., Toft, N., Matthews, L., Nielsen, S.S., 2015. Pharmacokinetic-pharmacodynamic model to evaluate intramuscular tetracycline treatment protocols to prevent antimicrobial resistance in pigs. Antimicrobial Agents and Chemotherapy. 59, 1634-1642.10.1128/AAC.03919-14

Ahmad, A., Zachariasen, C., Christiansen, L.E., Græsbøll, K., Toft, N., Matthews, L., Nielsen, S.S., Olsen, J.E., 2016b. Modeling the growth dynamics of multiple Escherichia coli strains in the pig intestine following intramuscular ampicillin treatment. BMC Microbiology. 16.10.1186/s12866-016-0823-3

Ahmad, A., Zachariasen, C., Christiansen, L.E., Græsbøll, K., Toft, N., Matthews, L., Olsen, J.E., Nielsen, S.S., 2016a. Multistrain models predict sequential multidrug treatment strategies to result in less antimicrobial resistance than combination treatment. BMC Microbiology. 16.10.1186/s12866-016-0724-5

Alderliesten, J.B., Duxbury, S.J., Zwart, M.P., de Visser, J.A.G., Stegeman, A., Fischer, E.A., 2020. Effect of donor-recipient relatedness on the plasmid conjugation frequency: a meta-analysis. BMC microbiology. 20, 1-10

Allaire J, Xie Y, McPherson J, Luraschi J, Ushey K, Atkins A, Wickham H, Cheng J, Chang W, Iannone R (2020). *rmarkdown: Dynamic Documents for R*. R package version 2.5, https://github.com/rstudio/rmarkdown.

Anderson, D.L., Bartholomeusz, F.D., Kirkwood, I.D., Chatterton, B.E., Summersides, G., Penglis, S., Kuchel, T., Sansom, L., 2002. Liquid gastric emptying in the pig: effect of concentration of inhaled isoflurane. Journal of Nuclear Medicine. 43, 968-971

Ankomah, P., Levin, B.R., 2014. Exploring the collaboration between antibiotics and the immune response in the treatment of acute, self-limiting infections. Proceedings of the National Academy of Sciences. 111, 8331-8338

Baquero, F. 2011. "The 2010 Garrod Lecture: The Dimensions of Evolution in Antibiotic Resistance: Ex Unibus Plurum et Ex Pluribus Unum." Journal of Antimicrobial Chemotherapy 66 (8): 1659–72. https://doi.org/Export Date 2 August 2013Art. No. dkr214.

Bergšpica, I., Kaprou, G., Alexa, E.A., Prieto, M., Alvarez-Ordóñez, A., 2020. Extended Spectrum β-Lactamase (ESBL) Producing Escherichia coli in Pigs and Pork Meat in the European Union. Antibiotics. 9, 678

Bernier, D., 2010. Étude et modélisation de la cinétique orale de l'amoxicilline chez le porcelet.

Bibbal, D., Dupouy, V., Ferré, J.-P., Toutain, P.-L., Fayet, O., Prère, M.-F., Bousquet-Mélou, A., 2007. Impact of three ampicillin dosage regimens on selection of ampicillin resistance in Enterobacteriaceae and excretion of blaTEM genes in swine feces. Applied and Environmental Microbiology. 73, 4785-4790

Birkegård, A.C., Halasa, T., Toft, N., Folkesson, A., Græsbøll, K., 2018. Send more data: a systematic review of mathematical models of antimicrobial resistance. Antimicrobial Resistance & Infection Control. 7, 117

Blanquart, F., 2019. Evolutionary epidemiology models to predict the dynamics of antibiotic resistance. Evol Appl. 12, 365-383.10.1111/eva.12753

Boëlle, P.-Y., Thomas, G., 2016. Resistance to antibiotics: limit theorems for a stochastic SIS model structured by level of resistance. Journal of mathematical biology. 73, 1353-1378

Brun, E., Holstad, G., Kruse, H., Jarp, J., 2002. Within-sample and between-sample variation of antimicrobial resistance in fecal Escherichia coli isolates from pigs. Microbial Drug Resistance. 8, 385-391

Burch, D., 2007. Pharmacokinetics of antimicrobials at different levels of the intestinal tract and their relationship to Escherichia coli resistance patterns in the pig. The Pig Journal. 59, 91-111

Burch, D., Sperling, D., 2018. Amoxicillin—current use in swine medicine. Journal of veterinary pharmacology and therapeutics. 41, 356-368

Burdet, Charles, Thu Thuy Nguyen, Xavier Duval, Stéphanie Ferreira, Antoine Andremont, Jérémie Guedj, France Mentré, et al. 2019. "Impact of Antibiotic Gut Exposure on the Temporal Changes in Microbiome Diversity." Antimicrobial Agents and Chemotherapy 63 (10). https://doi.org/10.1128/AAC.00820-19.

Carroll, A C, and A Wong. 2018. "Plasmid Persistence: Costs, Benefits, and the Plasmid Paradox." Canadian Journal of Microbiology 64 (5): 293–304. https://doi.org/10.1139/cjm-2017-0609.

Cavaco, L.M., Abatih, E., Aarestrup, F.M., Guardabassi, L., 2008. Selection and Persistence of CTX-M-Producing Escherichia coli in the Intestinal Flora of Pigs Treated with Amoxicillin, Ceftiofur, or Cefquinome. Antimicrobial Agents and Chemotherapy. 52, 3612-3616.10.1128/aac.00354-08

Cazer, C L, V V Volkova, and Y T Gröhn. 2014. "Use of Pharmacokinetic Modeling to Assess Antimicrobial Pressure on Enteric Bacteria of Beef Cattle Fed Chlortetracycline for Growth Promotion, Disease Control, or Treatment." Foodborne Pathogens and Disease 11 (5): 403–11. https://doi.org/10.1089/fpd.2013.1677.

Cazer, C.L., Ducrot, L., Volkova, V.V., Gröhn, Y.T., 2017. Monte Carlo simulations suggest current chlortetracycline drug-residue based withdrawal periods would not control antimicrobial resistance dissemination from feedlot to slaughterhouse. Frontiers in Microbiology. 8.10.3389/fmicb.2017.01753

Cazer, Casey L,Volkova, Victoriya V,Gröhn, Yrjö T. 2018. "Expanding Behavior Pattern Sensitivity Analysis with Model Selection and Survival Analysis." BMC Veterinary Research 14 (1). https://doi.org/10.1186/s12917-018-1674-y.

Chauzy, A., Gaelzer Silva Torres, B., Buyck, J., de Jonge, B., Adier, C., Marchand, S., Couet, W., Grégoire, N., 2019. Semimechanistic Pharmacodynamic Modeling of Aztreonam-Avibactam Combination to Understand Its Antimicrobial Activity Against Multidrug-Resistant Gram-Negative Bacteria. CPT: pharmacometrics & systems pharmacology. 8, 815-824

Chesa-Jiménez, J., Peris, J.E., Torres-Molina, F., Granero, L., 1994. Low bioavailability of amoxicillin in rats as a consequence of presystemic degradation in the intestine. Antimicrobial agents and chemotherapy. 38, 842-847

Christaki, E., Marcou, M., Tofarides, A., 2019. Antimicrobial Resistance in Bacteria: Mechanisms, Evolution, and Persistence. Journal of molecular evolution, 1-15

Coates, J., Park, B.R., Le, D., Şimşek, E., Chaudhry, W., Kim, M., 2018. Antibiotic-induced population fluctuations and stochastic clearance of bacteria. eLife. 7.10.7554/eLife.32976

Cremer, J., Arnoldini, M., Hwa, T., 2017. Effect of water flow and chemical environment on microbiota growth and composition in the human colon. Proceedings of the National Academy of Sciences, 201619598

Davies, N.G., Flasche, S., Jit, M., Atkins, K.E., 2019. Within-host dynamics shape antibiotic resistance in commensal bacteria. Nature Ecology & Evolution, 1

Davis, S., Illum, L., Hinchcliffe, M., 2001. Gastrointestinal transit of dosage forms in the pig. Journal of pharmacy and pharmacology. 53, 33-39

de Muinck, E.J., Stenseth, N.C., Sachse, D., vander Roost, J., Rønningen, K.S., Rudi, K., Trosvik, P., 2013. Context-dependent competition in a model gut bacterial community. PLoS One. 8, e67210

De Smet, J., Boyen, F., Croubels, S., Rasschaert, G., Haesebrouck, F., De Backer, P., Devreese, M., 2018. Similar gastro-intestinal exposure to florfenicol after oral or intramuscular administration in pigs, leading to resistance selection in commensal Escherichia coli. Frontiers in pharmacology. 9, 1265

De Smet, J., Croubels, S., De Backer, P., Devreese, M., 2017. Effect of administration route and dose alteration on sulfadiazine-trimethoprim plasma and intestinal concentrations in pigs. International journal of antimicrobial agents. 50, 707-714

EMA/CVMP/CHMP/, 2019. Categorisation of antibiotics in the European Union EMA/CVMP/CHMP/682198/2017

Erah, P., Goddard, A., Barrett, D., Shaw, P., Spiller, R., 1997. The stability of amoxycillin, clarithromycin and metronidazole in gastric juice: relevance to the treatment of Helicobacter pylori infection. The Journal of antimicrobial chemotherapy. 39, 5-12

European Committee on Antimicrobial Susceptibility Testing. Data from the EUCAST MIC distribution website, last accessed March 2020 ". http://www.eucast.org"

Ferran, A.A., Lacroix, M.Z., Bousquet-Mélou, A., Duhil, I., Roques, B.B., 2020. Levers to Improve Antibiotic Treatment of Lambs via Drinking Water in Sheep Fattening Houses: The Example of the Sulfadimethoxine/Trimethoprim Combination. Antibiotics. 9, 561

Fischer, E.A., Dierikx, C.M., van Essen-Zandbergen, A., van Roermund, H.J., Mevius, D.J., Stegeman, A., Klinkenberg, D., 2014. The IncI1 plasmid carrying the bla CTX-M-1 gene persists in in vitro culture of a Escherichia coli strain from broilers. BMC microbiology. 14, 77

Freire, J., Guerreiro, A., Cunha, L., Aumaitre, A., 2000. Effect of dietary fibre source on total tract digestibility, caecum volatile fatty acids and digestive transit time in the weaned piglet. Animal Feed Science and Technology. 87, 71-83

Frost, I., Smith, W.P., Mitri, S., San Millan, A., Davit, Y., Osborne, J.M., Pitt-Francis, J.M., MacLean, R.C., Foster, K.R., 2018. Cooperation, competition and antibiotic resistance in bacterial colonies. The ISME journal. 12, 1582-1593

Gjini, E., Brito, P.H., 2016. Integrating antimicrobial therapy with host immunity to fight drug-resistant infections: classical vs. adaptive treatment. PLoS computational biology. 12, e1004857

Gjonbalaj, M., Keith, J.W., Do, M.H., Hohl, T.M., Pamer, E.G., Becattini, S., 2020. Antibiotic degradation by commensal microbes shields pathogens. Infection and Immunity. 88

Græsbøll, K., Nielsen, S.S., Toft, N., Christiansen, L.E., 2014. How fitness reduced, antimicrobial resistant bacteria survive and spread: A multiple pig - multiple bacterial strain model. PLoS ONE. 9.10.1371/journal.pone.0100458

Gregory, P., McFadyen, M., Rayner, D., 1990. Pattern of gastric emptying in the pig: relation to feeding. British Journal of Nutrition. 64, 45-58

Gregory, P., McFadyen, M., Rayner, D., 1995. Control of gastric emptying in the pig: influence of cholecystokinin, somatostatin and prokinetic agents. Experimental Physiology: Translation and Integration. 80, 159-165

Hansen, K.H., Damborg, P., Andreasen, M., Nielsen, S.S., Guardabassi, L., 2013. Carriage and fecal counts of cefotaxime M-producing Escherichia coli in pigs: a longitudinal study. Appl Environ Microbiol. 79, 794-798.10.1128/aem.02399-12

Hazenberg, M., Pennock-Schröder, A., Van de Merwe, J., 1986. Reversible binding of polymyxin B and neomycin to the solid part of faeces. Journal of Antimicrobial Chemotherapy. 17, 333-339

Hernando-Amado, S, T M Coque, F Baquero, and J L Martínez. 2019. "Defining and Combating Antibiotic Resistance from One Health and Global Health Perspectives." Nature Microbiology 4 (9): 1432–42. https://doi.org/10.1038/s41564-019-0503-9.

Herrero-Fresno, A., Zachariasen, C., Hansen, M.H., Nielsen, A., Hendriksen, R.S., Nielsen, S.S., Olsen, J.E., 2016. Apramycin treatment affects selection and spread of a multidrug-resistant Escherichia coli strain able to colonize the human gut in the intestinal microbiota of pigs. Veterinary research. 47, 12

Hirte, K., Seiwert, B., Schüürmann, G., Reemtsma, T., 2016. New hydrolysis products of the beta-lactam antibiotic amoxicillin, their pH-dependent formation and search in municipal wastewater. Water research. 88, 880-888

Humphrey, B., Thomson, N.R., Thomas, C.M., Brooks, K., Sanders, M., Delsol, A.A., Roe, J.M., Bennett, P.M., Enne, V.I., 2012. Fitness of Escherichia coli strains carrying expressed and partially silent IncN and IncP1 plasmids. BMC Microbiology. 12, 53.10.1186/1471-2180-12-53

Jacobs, B.M., Patience, J.F., Lindemann, M.D., Stalder, K.J., Kerr, B.J., 2017. Disappearance and appearance of an indigestible marker in feces from growing pigs as affected by previous-and current-diet composition. Journal of animal science and biotechnology. 8, 32

Jacobs, M., Grégoire, N., Couet, W., Bulitta, J.B., 2016. Distinguishing antimicrobial models with different resistance mechanisms via population pharmacodynamic modeling. PLoS computational biology. 12, e1004782

Jansen, G., Weissing, F., de Vries Hospers, H., Tonk, R., Van der Waaij, D., 1992. The non-enzymatic inactivation of thirteen β-lactam antibiotics in human faeces. Infection. 20, 355-359

Jensen, B.B., 1998. The impact of feed additives on the microbial ecology of the gut in young pigs. J. Anim. Feed Sci. 7, 45-64

Jensen, G.M., Lykkesfeldt, J., Frydendahl, K., Møller, K., Svendsen, O., 2006. Pharmacokinetics of amoxicillin administered in drinking water to recently weaned 3-to 4-week-old pigs with diarrhea experimentally induced by Escherichia coli O149: F4. American journal of veterinary research. 67, 648-653

Jensen-Waern, M., Melin, L., Lindberg, R., Johannisson, A., Petersson, L., Wallgren, P., 1998. Dietary zinc oxide in weaned pigs—effects on performance, tissue concentrations, morphology, neutrophil functions and faecal microflora. Research in veterinary science. 64, 225-231

Kaeseberg, T., Zhang, J., Schubert, S., Oertel, R., Krebs, P., 2018. Abiotic, biotic and photolytic degradation affinity of 14 antibiotics and one metabolite–batch experiments and a model framework. Environmental Pollution. 241, 339-350

Knight, G.M., Davies, N.G., Colijn, C., Coll, F., Donker, T., Gifford, D.R., Glover, R.E., Jit, M., Klemm, E., Lehtinen, S., 2019. Mathematical modelling for antibiotic resistance control policy: do we know enough? BMC Infectious Diseases. 19, 1011

Kostewicz, E.S., Aarons, L., Bergstrand, M., Bolger, M.B., Galetin, A., Hatley, O., Jamei, M., Lloyd, R., Pepin, X., Rostami-Hodjegan, A., 2014. PBPK models for the prediction of in vivo performance of oral dosage forms. European Journal of Pharmaceutical Sciences. 57, 300-321

Kristoffersson, A.N., Bissantz, C., Okujava, R., Haldimann, A., Walter, I., Shi, T., Zampaloni, C., Nielsen, E.I., 2020. A novel mechanism-based pharmacokinetic–pharmacodynamic (PKPD) model

describing ceftazidime/avibactam efficacy against β-lactamase-producing Gram-negative bacteria. Journal of Antimicrobial Chemotherapy. 75, 400-408

Lavielle Marc (2020). mlxR: Simulation of Longitudinal Data. R package version 4.1.3. https://CRAN.R-project.org/package=mlxR

Leclerc, Q J, J A Lindsay, and G M Knight. 2019. "Mathematical Modelling to Study the Horizontal Transfer of Antimicrobial Resistance Genes in Bacteria: Current State of the Field and Recommendations." Journal of the Royal Society Interface 16 (157). https://doi.org/10.1098/rsif.2019.0260.

Lee, A.J., Wang, S., Meredith, H.R., Zhuang, B., Dai, Z., You, L., 2018a. Robust, linear correlations between growth rates and β-lactam–mediated lysis rates. Proceedings of the National Academy of Sciences, 201719504

Lenhard, J.R., Smith, N.M., Quach, C.D., Nguyen, T.Q., Doan, L.H., Chau, J., 2019. Bacterial brothers in arms: cooperation of Staphylococcus aureus and Pseudomonas aeruginosa during antimicrobial exposure. Journal of Antimicrobial Chemotherapy. 74, 2657-2665

Levin, B R, F M Stewart, and V A Rice. 1979. "The Kinetics of Conjugative Plasmid Transmission: Fit of a Simple Mass Action Model." Plasmid 2 (2): 247–60. https://doi.org/10.1016/0147-619X(79)90043-X.

Li, J., Petit-Jetté, C., Bi, D.G., Fenneteau, F., del Castillo, J., Nekka, F., 2008. Assessing pharmacokinetic variability directly induced by drug intake behaviour through development of a feeding behaviour–pharmacokinetic model. Journal of theoretical biology. 251, 468-479

Little, S., Crabb, H., Woodward, A., Browning, G., Billman-Jacobe, H., 2019. Water medication of growing pigs: sources of between-animal variability in systemic exposure to antimicrobials. animal. 13, 3031-3040

Liu, Y.-Y., Wang, Y., Walsh, T.R., Yi, L.-X., Zhang, R., Spencer, J., Doi, Y., Tian, G., Dong, B., Huang, X., Yu, L.-F., Gu, D., Ren, H., Chen, X., Lv, L., He, D., Zhou, H., Liang, Z., Liu, J.-H., Shen, J., 2015. Emergence of plasmid-mediated colistin resistance mechanism MCR-1 in animals and human beings in China: a microbiological and molecular biological study. The Lancet Infectious Diseases.10.1016/S1473-3099(15)00424-7

Lopatkin, A J, H R Meredith, J K Srimani, C Pfeiffer, R Durrett, and L You. 2017. "Persistence and Reversal of Plasmid-Mediated Antibiotic Resistance." Nature Communications 8 (1). https://doi.org/10.1038/s41467-017-01532-1.

Lopatkin, A J, T A Sysoeva, and L You. 2016. "Dissecting the Effects of Antibiotics on Horizontal Gene Transfer: Analysis Suggests a Critical Role of Selection Dynamics." BioEssays 38 (12): 1283–92. https://doi.org/10.1002/bies.201600133.

Luise, D., Lauridsen, C., Bosi, P., Trevisi, P., 2019. Methodology and application of Escherichia coli F4 and F18 encoding infection models in post-weaning pigs. Journal of animal science and biotechnology. 10, 53

Madec, J.Y., Haenni, M., Nordmann, P., Poirel, L., 2017. Extended-spectrum β-lactamase/AmpC- and carbapenemase-producing Enterobacteriaceae in animals: a threat for humans? Clin Microbiol Infect. 23, 826-833.10.1016/j.cmi.2017.01.013

Martinez-Larranaga, M., Anadón, A., Martinez, M., Diaz, M., Frejo, M., Castellano, V., Isea, G., De la Cruz, C., 2004. Pharmacokinetics of amoxycillin and the rate of depletion of its residues in pigs. Veterinary record. 154, 627-632

McNally, K., Cotton, R., Loizou, G.D., 2011. A workflow for global sensitivity analysis of PBPK models. Frontiers in pharmacology. 2, 31

Merchant, H.A., McConnell, E.L., Liu, F., Ramaswamy, C., Kulkarni, R.P., Basit, A.W., Murdan, S., 2011. Assessment of gastrointestinal pH, fluid and lymphoid tissue in the guinea pig, rabbit and pig, and implications for their use in drug development. European Journal of Pharmaceutical Sciences. 42, 3-10

Mohamed, A.F., Cars, O., Friberg, L.E., 2014. A pharmacokinetic/pharmacodynamic model developed for the effect of colistin on Pseudomonas aeruginosa in vitro with evaluation of population pharmacokinetic variability on simulated bacterial killing. Journal of Antimicrobial Chemotherapy. 69, 1350-1361

Nadeau, E., Fairbrother, J., Zentek, J., Belanger, L., Tremblay, D., Tremblay, C.-L., Röhe, I., Vahjen, W., Brunelle, M., Hellmann, K., 2017. Efficacy of a single oral dose of a live bivalent E. coli vaccine against post-weaning diarrhea due to F4 and F18-positive enterotoxigenic E. coli. The Veterinary Journal. 226, 32-39

Nguyen, T.T., Guedj, J., Chachaty, E., de Gunzburg, J., Andremont, A., Mentre, F., 2014. Mathematical modeling of bacterial kinetics to predict the impact of antibiotic colonic exposure and treatment duration on the amount of resistant enterobacteria excreted. PLoS Comput Biol. 10, e1003840.10.1371/journal.pcbi.1003840

Nielsen, E.I., Friberg, L.E., 2013. Pharmacokinetic-pharmacodynamic modeling of antibacterial drugs. Pharmacological reviews. 65, 1053-1090

Niewiadomska, A.M., Jayabalasingham, B., Seidman, J.C., Willem, L., Grenfell, B., Spiro, D., Viboud, C., 2019. Population-level mathematical modeling of antimicrobial resistance: a systematic review. BMC medicine. 17, 81

Nordmann, P., Poirel, L., 2016. Plasmid-mediated colistin resistance: an additional antibiotic resistance menace. Clin Microbiol Infect. 22, 398-400.10.1016/j.cmi.2016.03.009

Rey, J.F., Laffont, C.M., Croubels, S., De Backer, P., Zemirline, C., Bousquet, E., Guyonnet, J., Ferran, A.A., Bousquet-Melou, A., Toutain, P.-L., 2014. Use of Monte Carlo simulation to determine pharmacodynamic cutoffs of amoxicillin to establish a breakpoint for antimicrobial susceptibility testing in pigs. American journal of veterinary research. 75, 124-131

Rhouma, M., Beaudry, F., Thériault, W., Bergeron, N., Beauchamp, G., Laurent-Lewandowski, S., Fairbrother, J.M., Letellier, A., 2016. In vivo therapeutic efficacy and pharmacokinetics of colistin sulfate in an experimental model of enterotoxigenic Escherichia coli infection in weaned pigs. Veterinary Research. 47, 58.10.1186/s13567-016-0344-y

Rhouma, M., Beaudry, F., Thériault, W., Bergeron, N., Laurent-Lewandowski, S., Fairbrother, J.M., Letellier, A., 2015. Gastric stability and oral bioavailability of colistin sulfate in pigs challenged or not with Escherichia coli O149: F4 (K88). Research in Veterinary Science. 102, 173-181.http://dx.doi.org/10.1016/j.rvsc.2015.08.005

Rousselière, Y., Hémonic, A., Marcon, M., Monitoring of the individual drinking behavior of healthy weaned piglets and pregnant sows.

Rousseliere, Y., Hemonic, A., Marcon, M., ROCHER, P., LOISEAU, D., RICHARD, R., 2016. Suivi individuel du comportement d'abreuvement du porcelet sevré. Journées Recherche Porcine. 48, 355-356

Royer, E., Moundy, G., Albar, J., Martineau, G., 2004. Analyse descriptive du degre d'hygiene microbiologique de la machine a soupe dans neuf elevages porcins: 1. Revue de médecine vétérinaire. 155, 609-618

Royer, E., Moundy, G., Albar, J., Martineau, G., 2005. Analyse descriptive du degre d'hygiene microbiologique de la machine a soupe dans neuf elevages porcins: 2. Revue de médecine vétérinaire. 156, 23-28

RStudio Team (2018). RStudio: Integrated Development for R. RStudio, Inc., Boston, MA URL. http://www.rstudio.com/.

Ruppé, E., Ghozlane, A., Tap, J., Pons, N., Alvarez, A.-S., Maziers, N., Cuesta, T., Hernando-Amado, S., Clares, I., Martínez, J.L., Coque, T.M., Baquero, F., Lanza, V.F., Máiz, L., Goulenok, T., de Lastours, V., Amor, N., Fantin, B., Wieder, I., Andremont, A., van Schaik, W., Rogers, M., Zhang, X., Willems, R.J.L., de Brevern, A.G., Batto, J.-M., Blottière, H.M., Léonard, P., Léjard, V., Letur, A., Levenez, F., Weiszer, K., Haimet, F., Doré, J., Kennedy, S.P., Ehrlich, S.D., 2019. Prediction of the intestinal resistome by a three-dimensional structure-based method. Nature Microbiology. 4, 112-123.10.1038/s41564-018-0292-6

Santiago, F., Doscher, E., Kim, J., Camps, M., Meza, J., Sindi, S., Barlow, M., 2020. Growth rate assays reveal fitness consequences of β-lactamases. PloS one. 15, e0228240

Sardá-Espinosa, A. 2019. "Time-Series Clustering in R Using the Dtwclust Package." R Journal 11 (1). https://doi.org/10.32614/rj-2019-023.

Sebastien Le, Julie Josse, Francois Husson (2008). FactoMineR: An R Package for Multivariate Analysis. Journal of Statistical Software, 25(1), 1-18. 10.18637/jss.v025.i01

Sheppard, R J, A E Beddis, and T G Barraclough. 2020. "The Role of Hosts, Plasmids and Environment in Determining Plasmid Transfer Rates: A Meta-Analysis." Plasmid 108. https://doi.org/10.1016/j.plasmid.2020.102489.

Shin, J., Ko, K.S., 2015. Effect of plasmids harbouring blaCTX-M on the virulence and fitness of Escherichia coli ST131 isolates. International journal of antimicrobial agents. 46, 214-218

Snoeck, V., Huyghebaert, N., Cox, E., Vermeire, A., Saunders, J., Remon, J.P., Verschooten, F., Goddeeris, B., 2004. Gastrointestinal transit time of nondisintegrating radio-opaque pellets in suckling and recently weaned piglets. Journal of controlled release. 94, 143-153

Soraci, A.L., Amanto, F., Tapia, M.O., de la Torre, E., Toutain, P.-L., 2014. Exposure variability of fosfomycin administered to pigs in food or water: impact of social rank. Research in veterinary science. 96, 153-159

Suenderhauf, C., Parrott, N., 2013. A physiologically based pharmacokinetic model of the minipig: data compilation and model implementation. Pharmaceutical research. 30, 1-15.10.1007/s11095-012-0911-5

Taghipoor, M., Barles, G., Georgelin, C., Licois, J.-R., Lescoat, P., 2014. Digestion modeling in the small intestine: Impact of dietary fiber. Mathematical biosciences. 258, 101-112

Tan, A.Y., Sourial, M., Hutson, J.M., Southwell, B.R., 2016. Non-invasive measures of oral-rectal transit in young pigs. Livestock Science. 188, 13-20

Tepekule, B, P A Z Wiesch, R D Kouyos, and S Bonhoeffer. 2019. "Quantifying the Impact of Treatment History on Plasmid-Mediated Resistance Evolution in Human Gut Microbiota." Proceedings of the National Academy of Sciences of the United States of America 116 (46): 23106–16. https://doi.org/10.1073/pnas.1912188116.

Tetteh, J.N., Matthäus, F., Hernandez-Vargas, E.A., 2020. A survey of within-host and between-hosts modelling for antibiotic resistance. Biosystems, 104182

Trckova, M., Lorencova, A., Hazova, K., Zajacova, Z.S., 2015. Prophylaxis of post-weaning diarrhoea in piglets by zinc oxide and sodium humate. Veterinarni Medicina. 60

Tuomanen, E., Cozens, R., Tosch, W., Zak, O., Tomasz, A., 1986. The rate of killing of Escherichia coli byβ-lactam antibiotics is strictly proportional to the rate of bacterial growth. Microbiology. 132, 1297-1304

Udekwu, K.I., Weiss, H., 2018. Pharmacodynamic considerations of collateral sensitivity in design of antibiotic treatment regimen. Drug design, development and therapy. 12, 2249

Van Saene, J.J., Van Saene, H.K., Stoutenbeek, C.P., Lerk, C.F., 1985. Influence of faeces on the activity of antimicrobial agents used for decontamination of the alimentary canal. Scandinavian journal of infectious diseases. 17, 295-300

Verma, M., Bassaganya-Riera, J., Leber, A., Tubau-Juni, N., Hoops, S., Abedi, V., Chen, X., Hontecillas, R., 2019. High-resolution computational modeling of immune responses in the gut. GigaScience. 8, giz062

Viel, A., Henri, J., Perrin-Guyomard, A., Laroche, J., Couet, W., Grégoire, N., Laurentie, M., 2018. Lack of experimental evidence to support mcr-1-positive Escherichia coli strain selection during oral administration of colistin at recommended and higher dose given by gavage in weaned piglets. International journal of antimicrobial agents. 51, 128-131

Volkova, V V, Z Lu, C Lanzas, H M Scott, and Y T Gröhn. 2013. "Modelling Dynamics of Plasmid-Gene Mediated Antimicrobial Resistance in Enteric Bacteria Using Stochastic Differential Equations." Scientific Reports 3. https://doi.org/10.1038/srep02463.

Volkova, V. V., C. L. Cazer, and Y. T. Gröhn. 2017. "Models of Antimicrobial Pressure on Intestinal Bacteria of the Treated Host Populations." Epidemiology and Infection 145 (10): 2081–94. https://doi.org/10.1017/S095026881700084X.

Volkova, V.V., Kukanich, B., Riviere, J.E., 2016. Exploring Post-Treatment Reversion of Antimicrobial Resistance in Enteric Bacteria of Food Animals as a Resistance Mitigation Strategy. Foodborne Pathogens and Disease. 13, 610-617.10.1089/fpd.2016.2152

Volkova, V.V., Lanzas, C., Lu, Z., Grohn, Y.T., 2012. Mathematical model of plasmid-mediated resistance to ceftiofur in commensal enteric Escherichia coli of cattle. PLoS One. 7, e36738.10.1371/journal.pone.0036738

Wein, T., Hülter, N.F., Mizrahi, I., Dagan, T., 2019. Emergence of plasmid stability under non-selective conditions maintains antibiotic resistance. Nature communications. 10, 1-13

Wickham et al., (2019). Welcome to the tidyverse. Journal of Open Source Software, 4(43), 1686, https://doi.org/10.21105/joss.01686

Wilfart, A., Montagne, L., Simmins, H., Noblet, J., van Milgen, J., 2007. Digesta transit in different segments of the gastrointestinal tract of pigs as affected by insoluble fibre supplied by wheat bran. British Journal of Nutrition. 98, 54-62

Windels, E.M., Michiels, J.E., Fauvart, M., Wenseleers, T., Van den Bergh, B., Michiels, J., 2019. Bacterial persistence promotes the evolution of antibiotic resistance by increasing survival and mutation rates. The ISME journal. 13, 1239-1251

Zhou, D., Zhu, Y.-H., Zhang, W., Wang, M.-L., Fan, W.-Y., Song, D., Yang, G.-Y., Jensen, B.B., Wang, J.-F., 2015. Oral administration of a select mixture of Bacillus probiotics generates Tr1 cells in weaned F4ab/acR− pigs challenged with an F4+ ETEC/VTEC/EPEC strain. Veterinary research. 46, 95

Zimmermann, M., Zimmermann-Kogadeeva, M., Wegmann, R., Goodman, A.L., 2019. Separating host and microbiome contributions to drug pharmacokinetics and toxicity. Science. 363

Zwanzig, M., Harrison, E., Brockhurst, M.A., Hall, J.P., Berendonk, T.U., Berger, U., 2019. Mobile compensatory mutations promote plasmid survival. MSystems. 4, e00186-00118